VOLUME 36, NUMBER 5, OCTOBER 2013

HADRONIC JOURNAL

HADRONIC JOURNAL Volume 36, Number 5, October 2013

Founded in 1978 by Prof. R. M. Santilli at Harvard University. Some of the past Editors include Professors S. L. Adler, A. 0. Barut, L. C. Biedenharn, N. N. Bogoliubov, M. Froissart, J.Lohmus, S. Okubo, Nobel Laureate Ilya Prigogine, M. L. Tomber, J. P.Vigier, J. Wess, Nobel Laureate Chen Ning Yang.

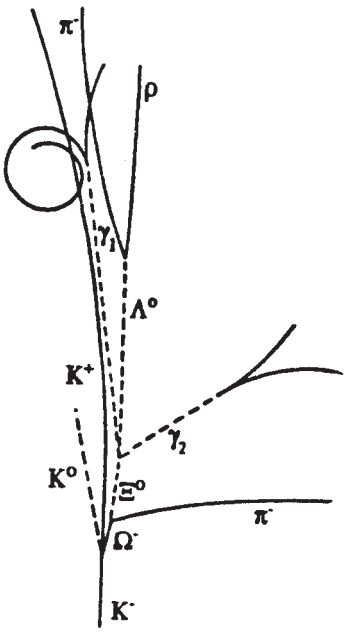

EDITORIAL BOARD
A.O.Animalu
D. P. Bhattacharyya
G.-C. Cavalleri
V. De Sabbata
T. L. Gill
L. P. Horwitz
H. Hurst
S. L. Kalla
S. I. Kruglov
S. S. Moskaliuk
M. Nishioka
R. F. O'Connell
Z. Oziewicz
E. Recami
M. Saleem
D. V. Shirkov
S. Silvestrov
D.S. Sourlas
H. M. Srivastava
A. I. Studenikin
R.I. Tsonchev
QI-Ren Zhang
C.A.Wolf
YI-Zhong Zhuo

FOUNDER:
RUGGERO M. SANTILLI

EDITOR IN CHIEF
CHRISTIAN CORDA

HADRONIC PRESS, INC.

HADRONIC JOURNAL

VOLUME 36, NUMBER 5, OCTOBER 2013

SANTILLI'S NEW FUELS AS SOURCES OF CLEAN COMBUSTION, 507
Indrani B. Das Sarma
Department of Applied Chemistry
Jhulelal Institute of Technology
Lonara, Nagpur – 441 111, India

AN INTRODUCTORY ACCOUNT OF SANTILLI'S IRS, IBS AND NIS, 529
Ritesh L. Kohale
Department of Physics
R.T.M. Nagpur University
Nagpur – 440033, India

MADELBROT ISO-SETS: ISO-UNIT IMPACT ASSESSMENT, 541
Reza Katebi
Department of Physics, California State University
800 North State College Boulevard
Fullerton, CA 92831, USA
Nathan O. Schmidt
Department of Mathematics, Boise State University
1910 University Drive
Boise, ID 83725, USA

THE GRAVITATIONAL ENERGY OF THE UNIVERSE, 555
Kenneth Dalton
General Delivery
Bang Saphan Yai 77140
Prachuap Kiri Khan, Thailand

THE MAGNEHYDROGEN™ IN HYDRONIC CHEMISTRY, 565
Sangesh P. Zodape
Department of Chemistry
Visvesvaraya National Institute of Technology
Nagpur – 440 010, India
Anil A. Bhalekar[2]
Department of Chemistry
R.T.M. Nagpur Univ., Amravati Rd. Campus, Nagpur – 440 033, India
And Thunder Fusion Corporation, U.S.A.
And Institute for Theoretical Physics and Advanced Mathematics, Italy

INTRODUCTION TO THE NEW SPECIES OF THE MAGNECULES OF HADRONIC CHEMISTRY, 593
Chandrashekhar P. Pandhurnekar
Department of Applied Chemistry
Ramdeobaba College of Engineering and Management
Nagpur – 440 013, India

HADRONIC JOURNAL 36, 507 - 528 (2013)

SANTILLI'S NEW FUELS AS SOURCES OF CLEAN COMBUSTION

Indrani B. Das Sarma
Department of Applied Chemistry
Jhulelal Institute of Technology
Lonara, Nagpur – 441 111, India
dassarmaindrani@rediffmail.com

Received February 24, 2014

Abstract

Molecular combustion or nuclear fission is the conventional source of energy, which are not clean as they generate large amount of green house gas or nuclear waste. Clean energy can be obtained by harnessing renewable energy sources like solar, wind, etc. However, each of these sources has their own limitations and is dependent on geographical locations. The modern day demand of clean, cheap and abundant energy gets fulfilled by the novel fuels that have been developed through hadronic mechanics/chemistry by Professor R. M. Santilli. In the present paper, a short review on such novel fuels like Hadronic energy of non-nuclear type (combustion of MagneGas) has been presented.

Keywords: Magnecules, alternative energy sources, hadronic chemistry, magnecular combustion.

Copyright © 2013 by Hadronic Press, Inc., Palm Harbor, FL 34684, USA

1 Introduction

The technological advancement of the modern society has created a dearth for energy as due the technological advances demand of energy has tremendously increased over its generation. The conventional sources of energy are molecular combustion of fossil fuels and hydrogen or nuclear fission. However, combustion of fossil fuel generates large amount of green house gas like CO_2 and hydrogen combustion depletes atmospheric O_2 by forming H_2O. Apart from depleting substantial amount of breathable oxygen, the exhaust gases are generally rich in green house gases that have high global warming potential [1]. Some of them are listed in Table-1.

These green house gases are responsible for global warming which has various cataclysmic effects. The sudden increase in cyclones, tornadoes, flash floods across the globe is some of the effect of impending threats of global warming. Similarly, nuclear fission generates large amount of nuclear waste risking ecosystem. These energy sources are supported by the 20th century sciences.

Clean energy can be obtained by harnessing renewable energy sources like solar, wind, geothermal, tidal, etc. Nevertheless; each of these sources has their own drawbacks and is generally dependent on geographical locations and the power generated cannot be stored efficiently and effectively due to the development of battery technology has yet not reached the desired level.

The demand of energy is constantly changing with progress of technology. The eighteenth century saw change in energy scenario from combustion of wood to coal. This subsequently changed to hydrocarbon based fuel to reduce the NO_X and SO_X emissions of coal as well as to obtain cleaner combustion. Now-a-days, the demand is to obtain still cleaner energy source that is cheap and abundant. The fuels developed should be such, which can be used in existing engines without any or major modifications. This requirement has been fulfilled by changing the approach from quantum mechanics to hadronic mechanics to hadronic chemistry. Italian-American physicist Ruggero Maria Santilli developed various new fuels of non-nuclear type (such as MagneGas) and nuclear type (such as controlled fusion) characterized by hadronic mechanics/chemistry [2-6], which shows

Table 1: Various green house gases and their corresponding global warming potential in different time horizons

Species	**Chemical Formula**	**Lifetime (years)**	**Global Warming Potential (Time Horizon)**		
			20 years	**100 years**	**500 years**
Carbon dioxide	CO_2	variable[1]	1	1	1
Methane[2]	CH_4	12±3	56	21	6.5
Nitrous oxide	N_2O	120	280	310	170
HFC-23	CHF_3	264	9100	11700	9800
HFC-32	CH_2F_2	5.6	2100	650	200
HFC-41	CH_3F	3.7	490	150	45
HFC-43-10mee	$C_5H_2F_{10}$	17.1	3000	1300	400
HFC-125	C_2HF_5	32.6	4600	2800	920
HFC-134	$C_2H_2F_4$	10.6	2900	1000	310
HFC-134a	CH_2FCF_3	14.6	3400	1300	420
HFC-152a	$C_2H_4F_2$	1.5	460	140	42
HFC-143	$C_2H_3F_3$	3.8	1000	300	94
HFC-143a	$C_2H_3F_3$	48.3	5000	3800	1400
HFC-227ea	C_3HF_7	36.5	4300	2900	950
HFC-236fa	$C_3H_2F_6$	209	5100	6300	4700
HFC-245ca	$C_3H_3F_5$	6.6	1800	560	170
Sulphur hexafluoride	SF_6	3200	16300	23900	34900
Per-fluoro-methane	CF_4	50000	4400	6500	10000
Per-fluoro-ethane	C_2F_6	10000	6200	9200	14000
Per-fluoro-propane	C_3F_8	2600	4800	7000	10100
Per-fluoro-butane	C_4F_{10}	2600	4800	7000	10100
Per-fluoro-cyclobutane	c-C_4F_8	3200	6000	8700	12700
Per-fluoro-pentane	C_5F_{12}	4100	5100	7500	11000
Per-fluoro-hexane	C_6F_{14}	3200	5000	7400	10700

[1]Derived from the Bern carbon cycle model.
[2]The GWP for methane includes indirect effects of tropospheric ozone production and stratospheric water vapor production.

better efficiency than existing fossil based fuels. The present paper is a short review on Hadronic fuels of non-nuclear type.

2 Conventional Molecular Combustion

The molecular combustion of fossil fuels or petroleum products is still not completely understood. The lower thermal efficiency, incomplete combustion despite using excess air and production of soot, unburnt hydrocarbons clogging the fuel lines and causing air pollution are some of the problems. The incomplete combustion of the hydrocarbons is due to formation of molecular clusters in the flame at high temperature. The interior of such cluster is lean in oxygen content, even on supplying excess air and hence it leads to the formation of uncombusted carbon or carbon monoxide in the flue gas. The lower thermal efficiency could be due to the non-polar nature of both oxygen molecule as well as the hydrocarbon molecules. This results in weaker Van der Waal's interaction prior to formation of free radicals of oxygen and/or hydrocarbons during combustion. Thus, it can be assumed that if there is comparatively stronger interaction between the oxidant and the fuel molecule prior to the formation of the free radicals then the thermal efficiency would be higher. This is evident from the fact that when ozone is used as an oxidant or when the hydrogen is atomized prior to the combustion [7,8], the thermal efficiency is found to be higher. Ozone being an unstable molecule as compared to oxygen it is a better oxidant. Enhancing thermal efficiency/flame temperature of the existing fuels by changing the oxidant is well-known and is commonly used in Atomic Absorption Spectroscopy or Flame Emission Spectroscopy [9]. Thus, pretreatment of the existing fuels whether hydrogen or hydrocarbon based fuel is necessary for enhancing the thermal output. Prof. R. M. Santilli proposed a novel chemical species, magnecules that has high thermal output resulting in cleaner combustion.

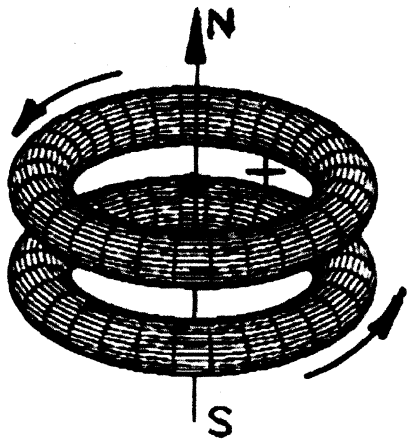

Figure 1: A conceptual depiction of an elementary magnecule comprising two identical or different atoms whose bond is entirely of magnecular character, namely, originating from opposing polarities North-South-North-South of the toroidal distributions of orbitals, as well as the polarization of nuclear and electron magnetic moments.

3 Magnecules

Magnecules have at least one magnecular bond between two atoms or radicals or molecules. The atoms are held together by magnetic fields originating due to toroidal polarization of the atomic electron orbits. The rotation of the electrons within the toroid creates the fifth field force, the magnetic field, which cannot originate for the same atom if the conventional spherical electron distribution in orbitals is a physical reality. When two such polarized atoms are sufficiently close to each other and in north-south north-south alignment, the resulting total force between the two atoms is attractive as shown in Fig.1.

Thus, the simple principle of synthesizing magnecules is similar to the magnetization of a ferromagnet where the orbits of unbounded electrons are polarized. Hence, in principle any matter whether solid, liquid or gas can

be converted to magnecules provided it is subjected to sufficiently strong external magnetic field.

The magnecules which are clusters comprising individual atoms, such as H, C, O, etc or radicals, such as H-O, C-H, etc and ordinary molecules, such as CO, CO_2, etc bonded together by opposing magnetic polarities of toroidal polarizations of atomic orbitals plus opposing nuclear and electron magnetic polarizations.

The industrial production of new fuels with Santilli magnecular structure takes place by submerged electric arcs due to the need for very strong magnetic fields that are indeed provided by electric arcs at atomic distances. In particular, the arc:

1. Polarizes atomic orbitals into toroids with symmetry axis tangent to the local magnetic force given by a circle perpendicular to the arc direction.

2. Couples different atoms with opposing magnetic polarities North-South-North-South etc and

3. Compresses magnetically polarized and coupled atoms toward the arc due to still unknown effects. The schematic representation of the arc causing polarization due to high magnetic field of high voltage DC arc is shown in Fig. 2.

4 Hadronic Refinery and its efficiency

Electric arcs between carbon electrodes efficiently separates water molecules by producing plasma of mostly ionized H, O and C atoms around the electrode tips. However, H and O atoms recombine forming H_2O in the arc, thus lowering efficiency and increasing the cost for the production of combustible gas. The stationary submerged electric arcs between carbon electrodes produces high amount of CO_2 and CO in the plasma, due to the high temperature initiating combustion of C of electrodes. Santilli developed a new method called Plasma Arc Flow (PAF), consisting of continuously flowing liquid feedstock through the arc and controlling the cooling of the plasma by

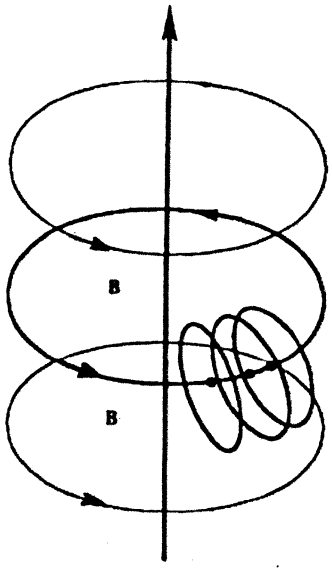

Figure 2: A schematic view of the main mechanism underlying the creation of magnecules, here illustrated for the case of the hydrogen molecule.

the surrounding liquid resulting in controlled formation of the combustible gas with magnecular structure. Plasma Arc Flow moves the plasma away from the electrodes and controls the formation of MagneGas that rises to the surface for collection. The latter is cleaned by bubbling through the liquid. This new PAF process allows the production of a clean burning, cost competitive magnecular gas ready for combustion at the time of its production without any additional refining.

Plasma Arc Flow Refineries are known as Santilli hadronic refineries because of their conception and engineering realization via the use of hadronic mechanics and chemistry. A schematic representation of hadronic refinery is shown in Fig. 3.

The pump for Magne Arc Flow facilitates removal of ionized atoms/radicals from within the arc. This facilitates their magnetization and cooling of the magnecules formed. The six characteristic temperature ranges and associ-

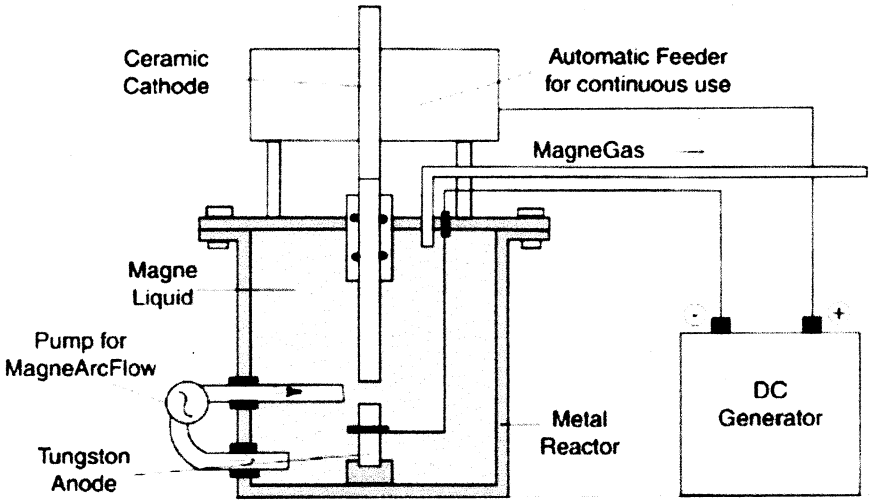

Figure 3: Santilli hadronic refinery for converting liquid waste into a clean burning, cost competitive gaseous fuel with magnecular structure. The pressure-metal vessel; the submerged electrodes; the recirculation of the feedstock through the arc; the external AC-DC converter; the external automatic controls of the arc and the collection of the produced magnecular fuel.

ated regions are tabulated in Table 2. A main feature of Santilli hadronic reactors is their high efficiency with an energy output that is a multiple of the used electric energy. This important feature is due to the fact that the primary source of energy of hadronic reactors is not the electric energy of the arc, but carbon combustion in the plasma. As a matter of fact, Santilli conceived his reactors for the primary purpose of developing new, cleaner and more efficient carbon combustion. In the plasma of an electric arc between carbon electrodes submerged in water we have all chemical reactions of the conventional combustion of carbon in air, such as the synthesis of CO with the release of 288 kcal/mole, the synthesis of CO_2 with the release of 87 kcal/mol, and others. Additionally, in the plasma of hadronic reactors we have the synthesis of H_2 with the release of 110 kcal/mol energy, which is not the case in conventional carbon combustion in air, thus showing that Santilli's combustion of carbon in the plasma of an arc has a large amount

Table 2: The characteristic temperature ranges and associated regions near the submerged DC electric arc.

Regions	Temperature Range	Processes or Reactions taking place
Underwater arc (30 to 40V DC, 500 to 1000A)	T>1500^{0}C	Dissociation of H_2O ($\sim$ 110 kcal/mol), association of CO ($\sim$ 255 kcal/mol) and CO_2 molecules
Region close to arc	800^{0}C to1500^{0}C	Association of H_2 ($\sim$104 kcal/mol) and H_2O
Region close to arc	700^{0}C to 800^{0}C	Very small bubbles of CO, H_2, CO_2, and H_2O gases
Region close to arc	150^{0}C to 700^{0}C	Very small bubbles of CO, H_2, CO_2, and H_2O gases
Region close to arc	100^{0}C to 150^{0}C	Association of O_2 molecules and complexes ($\sim$30 kcal/mol), small and big bubbles of CO, H_2, CO_2, O_2 and H_2O gases
Region far from the arc	70^{0}C to 100^{0}C	Association of complexes ($\sim$30 kcal/mol), water condensation, big bubbles of CO, H_2, CO_2 and O_2 gases leaving the liquid

of energy output than the combustion of the same carbon in air.

The efficiency of Hadronic reactor is expressed in two ways namely scientific efficiency, E_S and commercial efficiency, E_C as shown by expressions 1 and 2 respectively.

$$E_S = \frac{W}{e_e + e_c} \ll 1 \tag{1}$$

where W is the total energy output; e_e is the electric energy and e_c is energy from the carbon combustion

$$E_C = \frac{W}{e_e} \gg 1 \tag{2}$$

It is noticed that the scientific efficiency is always less than 1 as per the Carnot theorem. However, the Hadronic reactors do not produce energy

sufficient for the entire regeneration of the used electric energy for various reasons, such as dispersion, very low efficiency of current electric generators etc. Regardless of this limitation, the production of MagneGas (MH) in an electric power plant (to whom the cost of electricity is zilch) is very advantageous from an energy viewpoint because-

1. For every kW of used energy, they produce at least the equivalent of 3 kW of thermal energy in MagneGas (MH);

2. When MH is used as an additive to coal or petroleum combustion, the H-content of MagneGas can burn at least half of the combustible components in the plant exhaust that now constitute environmental problems; and

3. There are additional savings (of the order of several millions of dollars per year) in scrubbing and other means to clean the exhaust.

In summary, Magnegas Corporation has documented evidence that an electric power plant, by producing MagneGas locally and injecting it into the flame of the used fossil fuel, can increase the production of electricity by at least 30% with the use of the same fossil fuel.
The credibility of this statement is evident due to the fact that about 60% of the energy of fossil fuels is wasted due to formation of combustible CO, hydrocarbons and other contaminants in flue gas. These combustible exhausts are burnt off when combined with the H_2 in MagneGas as is well known to chemists. Hence the indicated 30% gain in the production of electricity from a given fossil fuel volume is about half of the lost energy.
MH in fossil fuel decreases its volatility [3] probably due to their anomalous adsorption, consequently attaining higher temperature which results in a cleaner combustion. Thus the consideration of commercial efficiency becomes evident for all practical purposes.

5 Types of magnecules

Magnecules are classified depending on their composition and chemistry. The schematic representation of magnecules based on composition is given

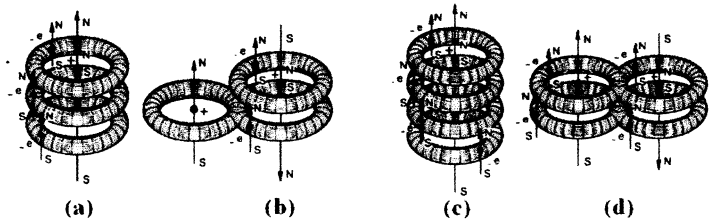

Figure 4: Various magnecules: a) H_3 (elementary magnecule: comprising of three H-atoms), b) H_3 (magneplex: comprising of one hydrogen molecule and one hydrogen atom, c) H_4 (elementary magnecule: comprising of four H-atoms), d) H_4 (elementary magnecule: comprising of two hydrogen molecules)

in Fig.4. The magnecules are classified as follows-

1. Elementary when composed only of two molecules,
   e.g.:{H-H}×{H-H}; and so on.
   where '−' denotes conventional valence bond and '×' denotes magnecular bond.

2. Magneplexes when entirely composed of several identical molecules
   e.g.: {H-O-H}×{H-O-H}×{H-O-H}×{H-O-H}×{H-O-H}×...; and so on.

3. Magneclusters when composed of several different molecules
   e.g.: {H-H}×{C-O}×{O-C-O}×{C=O}×{H-H}×...; and so on.

Magnecules are also classified depending on their chemistry as-

1. Isomagnecules when having all single-valued characteristics and being reversible in time, namely, when they are characterized by isochemistry,

2. Genomagnecules when having all single-valued characteristics and being irreversible in time, namely, when they are characterized by genochemistry; and

3. Hypermagnecules when having at least one multi-valued characteristic and being irreversible in time, namely, when they are characterized by hyperchemistry.

The magnecules differ from their molecular counterparts predominantly due to their magnetic bond originating due to toroidal polarization of the peripheral electron orbital. This gives rise to many anomalous characteristic properties of the magnecules.
Santilli magnecules are characterized [4, 5] by-

1. Large atomic weights which are ten times or more than the conventional molecules.

2. Large peaks in macroscopic percentages in mass spectra, which do not belong to conventional molecules.

3. These peaks show same infra-red and ultra-violet signature as expected from the conventional molecules and/or dimers constituting the magnecule.

4. Said infrared and ultraviolet signatures are generally altered with respect to the conventional versions.

5. Magnecules have an anomalous adhesion to other substances.

6. They can break down into fragments under high energetic collisions, with subsequent recombination with other fragments and/or conventional molecules.

7. They can build up or lose individual atoms, diatomic radicals or molecules during collision.

8. They have an anomalous penetration through other substances indicating a reduction of the average size of conventional molecules as expected under magnetic polarizations.

9. Gas magnecules show an anomalous solubility in liquids due to new magnetic bonds between gas and liquid molecules caused by magnetic induction.

10. Magnecules can be formed by molecules of immiscible liquids.

11. A gas with magnecular structure does not follow the perfect gas law.

12. Substances with magnecular structure have anomalous physical characteristics, as compared to the conventional molecules.

13. Magnecules release more energy in thermochemical reactions than that is released by the same reaction among the unpolarized molecular constituents.

14. All the above characteristic features disappear when the magnecules are brought to a sufficiently high temperature (Curie Magnecular Temperature), which varies from species to species.

The property of magnecules to undergo magnecular combustion with high energy output which is attributed to weak magnecular bond [10]. This is exploited for the industrial development of novel clean fuels such as magnegas.

6 Hadronic Energy of Non-nuclear Type: Magnecular Combustion

Hydrogen molecule is thermally stable and does not dissociate at normal temperature as the dissociation reaction is highly endothermic.

$$H_2\ (molecules) \longrightarrow 2H\ (atomic) \quad \Delta H = 436\ kJ/mol \tag{3}$$

However, at high temperature as in case of electric arc they do atomize to elemental/atomic hydrogen as shown by reaction 3. Atomic hydrogen is highly reactive species having life time of less than a second and readily recombine to form hydrogen molecule releasing large amount of thermal energy. This property is used for atomic hydrogen welding. (It is an arc welding process, invented by Irving Langmuir that uses an arc between two tungsten electrodes in shielding hydrogen atmosphere. Hydrogen dissociates into atomic form, simultaneously absorbing a large amount of heat from the

arc. When the atomic hydrogen strikes a relatively cold surface (weld zone), it recombines into its diatomic form releasing the energy associated with the formation of molecular bond. The temperature obtained in this case ranges from 3400 to 4000^0C whereas without the arc, an oxy-hydrogen flame can only reach 2800^0C).

It is known that atomic hydrogen does have high thermal content but the major drawback is its high reactivity and hence cannot be stored. This problem can be overcome by converting the atomic hydrogen into magnehydrogen using Plasma Arc Flow technology in hadronic refinery. In other words, magnehydrogen can be considered as magnetically stabilized atomic hydrogen.

The magnetic bonds are weaker than molecular bonds, but still correspondingly a high energy output occurs during the combustion of magnecules without breaking of molecular covalent bonds. The stored magnetostatic energy could also be responsible in anomalous heat output. This property is exploited for the industrial development of novel clean fuels such as MagneGas.

6.1 Combustion of molecular hydrogen and oxygen

$$H - H + \frac{1}{2}O_2 \longrightarrow H_2O \tag{4}$$

Consider the case of combustion of molecular hydrogen and oxygen to produce H_2O as given in equation 4. The dissociation of H_2 and O_2 molecules consume 163.7 kcal/mol and thereafter the atom recombines to produce H_2O releasing 221.25 kcal/mol, hence the net release of energy is 57 kcal/mol [5]. In case of magnecular hydrogen $\{H\times H\}$ and atomic oxygen O combustion, as given in equation 5, the energy output is predicted to be approximately three times the value predicted by molecular structures with the same atomic constituents and combustion temperature [5].

$$\{H \times H\} + O \longrightarrow H_2O \tag{5}$$

Considering H×H bond dissociation energy arbitrarily zero (as magnetic bond is weaker in nature), the energy output is predicted to be approx-

imately three times the value predicted by molecular structures with the same atomic constituents and combustion temperature.

6.2 Combustion of magnecules

The energy content of magnecules depends on the structural bonding of the magnecules. Considering the common molecular combustion reactions given by equations 4 and 6

$$CO + \frac{1}{2}O_2 \longrightarrow CO_2 \tag{6}$$

would be replaced by the reaction as shown in equation 7

$$Magnecule + nO_2 \longrightarrow mH_2O + kO_2 + lCO_2 + \cdots + \Delta E \text{ kcal} \tag{7}$$

where n, m, k, l, ... are integers and Magnecule is assumed to consist of both H_2 and CO.

This give increased energy released per H_2 or per CO molecule. The energy balance for the magnecular combustion is given by equation 8

$$E[\text{combustion}] = mE[H_2O] + kE[O_2] + lE[CO_2] + \cdots\cdots - E[\text{magnecule}] \tag{8}$$

where $E[H_2O]$, $E[O_2]$, $E[CO_2]$, $\cdots\cdots$ are ground state energies of the molecular constituents and E[magnecule] is ground state energy of the original magnecule.

Energy balance is calculated using dissociation energy of the magnecule, D[magnecule]. However, D[magnecule] should be different for magnecules of different mass and composition. In case of chemical reactions, reaction equilibrium constant K is considered. For example in equation 4 ΔH = -57.5 kcal/mol and $K = 10^{40}$ at $T = 25^0$C. This value is for the total combustion of H_2 gas at $T = 25^0$C.

Generally, for all highly exothermic reactions (say $\Delta H < -15$ kcal/mol), the reaction equilibrium constant is high. The opposite reaction of equation 4 given by equation 9

$$H_2O \longrightarrow H_2 + \frac{1}{2}O \tag{9}$$

occurs only at very high temperatures, at which $K < 1$.

$K = 1$ indicates equilibrium at stoichiometric composition, while $K < 1$ indicates backward shifted equilibrium.

The relation between the heat of reaction, ΔH and the reaction equilibrium constant, K, is given by equation 10,

$$-2.303RT \log K = \Delta G \tag{10}$$

where,

$$\Delta G = \Delta H - T\Delta S \tag{11}$$

with $R = 1.986\,\text{cal K}^{-1}\text{mol}^{-1}$; T is the temperature in Kelvin; and ΔS is the entropy of the reaction. This shows that the equilibrium constant is not solely determined by the endothermicity or exothermicity of the reaction but also the ΔS of reaction also vitally contributes to it.

The above outline of the reaction equilibrium constant's dependence on the Gibbs free energy, the enthalpy and entropy of reaction helps us to conclude that the combustion of MagneGas is characterized by a very high value of the reaction equilibrium constant (perhaps even bigger than $K = 10^{40}$ at $T = 25^0$C).

6.3 Factors favoring Magnecular Combustion

Combustion of MagneGas is a highly exothermic reaction [11]. Magnecules have more ordered structure than its combustion products. So, during the combustion there is large increase of the entropy $\Delta S > 0$, eventually very high value of the reaction constant K.

For most elements, ΔG of oxidation reactions increases linearly with the temperature, indicating that the resulting oxides are less stable at high temperatures than at low temperatures such as H_2O dissociates at high temperature ($\sim 1000^0$C). However, in case of oxidation of carbon to carbon monoxide, as given by equation 12

$$\text{C} + \text{CO}_2 \longrightarrow 2\text{CO} \tag{12}$$

ΔG decreases with the increase of the temperature. The number of moles of gaseous product increases about twice during the reaction, increasing the entropy, $\Delta S > 0$. Thus, indicating the greater stability of CO molecule at high temperatures than at low temperatures consequently, a better quality of the exhaust is obtained at lower original temperatures of MagneGas.

6.4 High reaction rate

The rate of reaction between magneH_2 and magneO_2 is substantially higher than the thermal reaction between the conventional H_2 and O_2 molecules. This can be understood as follows. In the latter case the initiation step is the O-O covalent bond cleavage and the entire energy required for this is derived from the thermal energy of the system. Whereas in the former case the magneO_2 possesses additional energy of magnetostatic origin and hence the thermal energy required to break O-O bond of magneO_2 is considerably less. Moreover, the toroidal configuration of orbitals of H_2 and O_2 in magnecular state further facilitates the meeting of the steric requirements of the chemical reaction to produce a water molecule in much better way than in the reaction between conventional H_2 and O_2 molecules. Consequently, bigger reaction rate releases bigger power. Also, the combustion of a magnecule consisting of H_2 and CO, does not require the necessary previous dissociation of the O_2 molecule (-119.1 kcal), as each O-atom in a magnetically polarized O_2 molecule is ready for the combustion. So, the magnecular structure acts as a catalyst where both O-atoms of the O_2 molecule start to react with the nearest pair of $H_2 \times H_2$ or $H_2 \times CO$ or $CO \times CO$ almost simultaneously. This also implies requirement of less amount of external energy to activate the reaction, resulting, in an anomalous energy release in combustion. (Activation energy is supplied by heat). So, the combustion of magnegas can be initiated at smaller temperature, in comparison to that of the simple mixture of H_2 and CO gases.

6.5 MagneGas: MagneHydrogen^{TM} and MagneOxygen^{TM}

The Plasma Arc Flow technology converts most liquid waste into a clean fuel called MagneGas. MagneGas is a cost competitive synthetic gas made from many liquid wastes such as sewage, sludge, animal manure, glycerin, used antifreeze, some oil based liquids and waste water. MagneGas is a hydrogen based fuel that has a combination of hydrogen, carbon monoxide and inert trace gases. If resulting MagneGas is richer in magnecular hydrogen concentration then it is termed as MagneHydrogen. Conventional

H_2 and O_2 gases can also be turned into their respective magnecular structure called MagneHydrogen^{TM} (MH) and MagneOxygen^{TM} (MO) by subjecting them to strong external magnetic field generally carried out in a Hadronic refinery. H_2 is diamagnetic and cannot acquire a total net magnetic polarity. However, the orbit of each H atom acquires a toroidal polarization under sufficiently strong external magnetic field. The opposite magnetic moments of the two H atoms explain the diamagnetic character of the hydrogen molecule. Also the intrinsic magnetic moments of nuclei and electrons of H_2 molecule are polarized which creates new chemical species having higher specific weight due to formation of new bonds between pairs of individual H atoms.

The MO is formed comparatively easily as oxygen is paramagnetic, so electrons acquire an overall magnetic polarity. However, significant increase of the specific weight of the oxygen requires the toroidal polarization of at least some of the peripheral atomic electrons, along with total magnetic polarization.

6.6 HHO: Magnecular Water

HHO gas has distinctly different chemical composition than *Brown gas*, even though both gases have many similarities. HHO gas is magnecular water having general structure as $\{H{\times}H{-}O\}$ whereas Brown gas is a mixture of conventional molecular hydrogen and oxygen in 2:1 ratio. Since HHO is a MagneGas it has all the characteristics of magnecules. It also does not require atmospheric oxygen unlike MH thereby overcoming the problem of depletion of atmospheric oxygen due to combustion. The oxygen present in HHO is sufficient to bring about complete combustion of the gas. The important aspect of this gas is its anomalous adsorption to liquids, solids and gases and widely varying thermal content.

7 Applications : Fuel additive

The anomalous adsorption makes it a perfect additive to other fuels. The flash point of diesel was found to increase from 75^0C to 79^0C on purging

the same with HHO [2]. This anomalous rise was not of just 4^0C but of 42^0C as addition of gas to liquid reduces its flash point by half. This could be attributed to the magnecular structure of the HHO which influences to form magnecluster HHO and diesel molecules, thereby drastically increasing its flash point. If HHO existed as gas then the flash point would not have increased. The adsorption of the HHO to the diesel molecules is also expected to significantly reduce the harmful emission of the original fuel (due to inherent O content) and increases the thermal output of the fuel in case of combustion. Thus, MagneGas is a good additive for clean combustion [12] because:

1. When produced from the recycling of water-base liquid wastes, magnegas contains about 65% hydrogen, thus qualifying as an effective additive to improve fossil fuel combustion;

2. The cost of magnegas is competitive over that of fossil fuel, particularly when produced by the electric power plants, because of the reduced cost of electricity and the possibility of producing magnegas from the recycling of city sewage, with a consequential income that covers most of the operating costs of PlasmaArcFlow Recyclers.

3. MagneGas fuel has a very high combustion flame temperature of $3{,}800^0$C (verified by the City College of New York). The higher the temperature, the more complete the combustion of the fuel and the cleaner the emissions.

4. Each fuel tested resulted in a reduction of CO_2 by 30-40%, an increase in heat output and significant reductions in CO and other pollutants.

8 Applications : Thermal Output

HHO exhibits a wide range of thermal output. It ranges from relatively cold flame in open air (150^0C) to large releases of thermal energy depending on the substance to which the flame is applied (instantaneous melting of W or bricks requiring $\sim 9000^0$C). This capability can be explained by the presence of polarized H-atom in the HHO gas. Instantaneous melting of bricks

is only possible due to the polarized hydrogen contained in the HHO gas which rapidly penetrates into the deep layers of the brick. Besides due to smaller sectional area, penetration is fast. Polarized H-atoms induces polarization of the brick's atomic orbitals, leading to attraction of the polarized H atoms. This leads to faster penetration within the solid lattice causing higher reactivity and consequently higher melting temperature.

9 Conclusions

Hadronic Chemistry has one of its applications in the development of novel magnecular fuel which shows clean combustion as compared to its molecular counterparts. It can be considered superior to molecular combustion due to:

1. Comparatively weak bond of magnecules.
2. Its stored magnetostatic energy, and
3. Highly ordered structure.

They also have promising application as fuel additive for improving combustion of existing fossil fuel due to their high miscibility, higher combustion/co-combustion rate and thermal output. The magnecules might be acting as detonator to the conventional fuel molecules resulting in near complete combustion of the latter like the volatile matter detonating the fixed carbon of pulverized coal. Thus, they hold promising applications as sustainable energy requirements.

Acknowledgments

The financial support for this work from The R. M. Santilli Foundation is gratefully acknowledged. The author expresses her deep gratitude to Professor R. M. Santilli for his personal interest and suggestions. The author is also thankful to Professor C. Corda, Professor R. Anderson and Professor A. A. Bhalekar for constant encouragements and valuable guidance in preparing this manuscript.

References

[1] Website of United Nations Framework Convention on Climate Change *http : //unfccc.int/ghg$_d$ata/items/*3825.*php* downloaded on 02/01/2014.© 2014 United Nations Framework Convention on Climate Change.

[2] R. M. Santilli and A. K. Aringazin, Structure and combustion of MagneGases, Hadronic Journal, 27, (2004), 299-330; arXiv:physics/ 0112066 [physics.gen-ph].

[3] R. M. Santilli, The new fuels with magnecular structure; International Academic Press, (2005).

[4] R. M. Santilli, "Theoretical Prediction and Experimental Verifications of New Chemical Species of Magnecules", Hadronic J., 21, (1998), 789 - 894.

[5] I. Gandzha and J. Kadeisvily; New Sciences For A New Era: Mathematical, Physical and Chemical Discoveries of Ruggero Maria Santilli; Sankata Printing Press, Kathmandu, Nepal, (2011).

[6] R. M. Santilli, Experimental confirmation of Nitrogen synthesis from Deuterium and Carbon without harmful radiations, New Advances in Physics, 5, (2011), 29-36.

[7] N. Saksono, Magnetizing Kerosene For Increasing Combustion Efficiency, Jurnal Teknologi, Edisi No. 2, Tahun XIX, (2005), 155-162. (ISSN 0215-1685).

[8] M. Wilk and A. Magdziarz, Ozone Effects on the Emissions of Pollutants Coming from Natural Gas Combustion Polish J. of Environ. Stud., 19(6), (2010), 1331-1336.

[9] G. H. Jeffery, J. Bassett, J. Mendham, R. C. Denney, Vogel's Textbook of Quantitative Chemical Analysis, published by Longman Scientific & Technical and co-published by John Wiley & Sons, Inc., New York, pp. 784.

[10] Y. Yang, J. V. Kadeisvili and S. Marton, Experimental confirmations of the new chemical species of Santilli magnecules; Submitted to the Analytical Chemistry on December 30, 2012.

[11] R. M. Santilli, The New Fuels With Magnecular Structure, International Academic Press, Palm Harbor, FL 34684, USA, (2005). http://www.i-b-r.org/docs/Fuels-Magnecular-Structure.pdf

[12] Website of MagneGas Corporation http://magnegas.com/ downloaded on 18.01.2014. Copyright 2014 MagneGas Corporation, 150 Rainville Rd., Tarpon Springs, FL 34689, U.S.A.

AN INTRODUCTORY ACCOUNT OF SANTILLI'S IRS, IBS AND NIS

Ritesh L. Kohale
Department of Physics
R.T.M. Nagpur University
Nagpur – 440033, India
riteshkohale@gmail.com

Received February 5, 2014

Abstract

This paper summarizes the physical and mathematical basis of the 1991 hypothesis by R. M. Santilli concerning of IsoRedShift (IRS) and IsoBlueShift (IBS).This particular hypothesis reveals that light losses its energy to a cold medium without any relative motion in between the source, the medium and the observed and frequency shift of light takes place towards red named as Santilli's IsoRedShift (IRS) ; also the light gains from a hot medium without any relative motion and frequency shift of light takes place towards blue named as Santilli's IsoBlueShift (IBS).In this work we have concentrated on concurrence of Santilli's IRS and IBS with the adages of special relativity beneath their appropriate mathematical interpretations. Besides we focused on the innovative experimental verifications of IRS by Santilli in 2010 for a blue laser light in a tube containing air pressure up to 2,000 psi ≈ 1137 bars. Also we have focused on G. West and G. Amato's 2011 experimental confirmations on IRS and IBS and the assenting measurements by Santilli, West and Amato in 2012 on the west coast of Florida on the origin of IRS related to the redness of the Sun in the transition from the zenith to the horizon. It has been also noticed that the further positive extents of IRS of Sunlight from the Zenith to Sunset the island of Kos, Greece, studied on September 20, 2012. Identification and truthful confirmations that gives the differences in origins of the redshift by Santilli's 1991 IRS hypothesis with particular reference to Zwicky's 1929 hypothesis of Tired Light has also been studied in this paper. Cosmological and other suggestions of Santilli IRS, IBS and NIS are taken in consideration for study in these proceedings.

Keywords: *IsoRedShift, IsoBlueShift, NoIsoShift*

Copyright © 2013 by Hadronic Press, Inc., Palm Harbor, FL 34684, USA

1. Introduction

The determinate achievements of the spectroscopic measurements presented in this paper is centered on a comprehensive mathematics established by the Italian-American scientist Ruggero Maria Santilli when he was at MIT (from 1974 to 1978), at Harvard University (from 1978 to 1981) and at the Institute for Basic Research (from 1982 on) for the time invariant illustration of interior dynamical systems. For this particular study Santilli embark on conventional applied mathematics employed in 20th century as being precisely valid for exterior dynamical systems referred to point like particles and electromagnetic waves transmitting in the homogeneous and isotropic vacuum [1]. In general, electromagnetic waves and particles propagate inside the anisotropic and inhomogeneous physical media. A prime difference in between interior and exterior systems is appearance in the form of interaction, non-linear, non-local and non-potential interactions that cannot be persistently characterized using a Hamiltonian or a Lagrangian formulation. In addition, the literature survey reveals that Lorentz symmetry is not exactly appropriate inside a physical media and it prerequisites consistent generalization for exterior dynamical problems.

Santilli's studies have presented a significant reconsideration of the special theory of relativity. In his 1991 hypothesis Santilli established the requirement to realize the light as electromagnetic waves propagating within a universal substratum. In 2012 Santilli completed [2] the efficient measurements and established that while light traverses from Zenith to the Horizon, the entire spectrum of Sunlight experiences an *IRS* of about 100 nm. With his mathematical, theoretical and to some extent his experimental evidences [3] he contested the ideas like expansion of universe, the acceleration of the expansion, the expansion of space itself, dark matter, the big bang, and dark energy. The present review is an attempt to present professor Santilli's view point on Isoredshift (IRS) and Isoblueshift (IBS) by considering his step by step mathematical and experimental justifications [4].

2. Preceding Theoretical and Physical Conventions.

The previous astrophysical discoveries , such as those by E. Hubble [5] ,V. Sllipher [6] presented the predictable law which reveals that the cosmological redshift of galactic light is proportional to the distance of galaxies in "all" radial directions from Earth, and the redshift essentially occurs for "all" frequencies of galactic light. Immediately after above discovery, F. Zwisky [7] submitted the hypothesis according to which the cosmological redshift is due to light losing energy because of scattering with the intergalactic medium. It is known that the only quantitative representation of all experimental evidence for all frequencies is given by the Maxwell's concept of light. The transverse electromagnetic waves propagating in the universal substratum is given by historical expression for its speed within transparent physical media as, $C = c / n\ (x, v, \omega, \delta...,)$, where c is the velocity of light in vacuum and n is the index of refraction. This expression depends on all local variables, such as coordinates x, speed v, frequency ω, density δ, temperature T, etc. However Lorentz first attempted to establish the universal symmetry of local speeds $C = c / n\ (x, v, \omega, \delta, T...,)$ and came across the major technical difficulties by considering the simpler case of constant speed c which sets aside the foundations of special relativity [8]. Afterward Prof. R. M. Santilli came to conclusion that the problem considered in Lorentz's theory is generally nonlinear, nonlocal-integral and non-Hamiltonian. Consequently, in 1996

Prof. R. M. Santilli had constructed a new mathematics applicable within physical media known as *Santilli isomathematics* which is specifically built for interior dynamical problems. This *isomathematics* is based on the locally varying speed of light $C = c / n (x, v, \omega, \delta, T...,)$, which is today known as the *Lorentz-Poincare-Santilli (LPS) isosymmetry* and the isotopeis of this special relativity known as *Santilli isorelativity* [2].

A central prediction of special relativity is based on the Doppler Red shift which states that, when the light source travels away from the observer, the frequency of light f is shifted toward the red. But this Doppler redshift is not applicable for the propagation of light within transparent physical medium. Santilli has carried out a step-by step isotopic lifting of the physical laws of special relativity resulting in a new theory i.e. *Santilli isorelativity*. Santilli's new measurements confirmed that, while traversing from the Zenith to the horizon, Sunlight experiences a shift of about 100 nm toward the red for the entire frequencies without any appreciable relative motion between the Sun, the atmosphere and the observer [9]. Therefore, light loses energy $E = h\nu$ to cold media and experiences a decrease of its frequency ν. This process takes place at atomic level and independent from molecular processes, such as scattering or absorption. It is claimed that Santilli's IRS is similar to the cosmological redshift that has been described in ref. [10, 11].

3. Santilli's Experimental Confirmations of IsoRedShift

Almost after two consequent decades of refusals Santilli decided to conduct the needed experimental measurements since he had no other choice to demonstrate these fundamental implications. Consequently, with the assistance of the technicians at the Institute for Basic Research in Florida, as well as the support of external laser experts, Santilli constructed the IsoShift Testing Station consisting an initial air-conditioned cabin containing a blue laser; a second air-conditioned cabin containing wavelength analyzers; the laser and analyzer being interconnected by a 60 ft $\approx$ 18 m long steel pressure pipe containing air at the maximal pressures up to 2000 psi $\approx$ 137 bars. After several months of successful measurements, Santilli released the results for publication [12] and put the accent on the main scope of the measurements which was establish to confirm the existence of the IRS, without any possibility of conducting statistical averages with the available experimental set up.

3.1 First Experimental Confirmation of Santilli IsoRedShift

In his first experimental confirmation of isoredshift he obtained chromatogram of the entire Sunlight spectrum at the Zenith and the main part of the resulting spectrum over background at the horizon using the Yokogawa wavelength analyzer model AQ6373 which has range from 400 to 1100 nm by Santilli, West, and Amato [2] on March 16, 2012.Figure 1 indicates spectrograms of typical wavelengths of the Sun at the Zenith (left) and at about 60^0 elevation on the horizon (right) forming an IRS of the order of 0:06 nm. The significance of these measurements is that, at said elevation, no redshift of the Sun is visible to the naked eye. With the decrease of the elevation, the IRS of individual wavelengths increases to such a value that the originally detected spectral lines obtain the characteristics of consequent spectral lines with no apparent IRS; accordingly it requires the analysis of the entire sunlight.

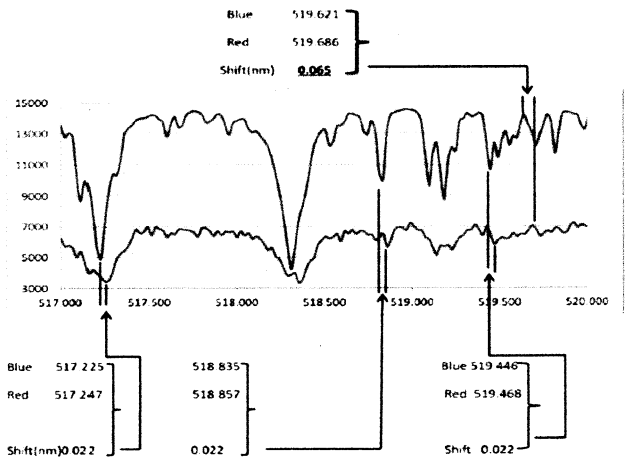

Figure 1: Spectrograms of demonstrative wavelengths of the Sun at the Zenith (left) and at about 60^0 elevation on the horizon (right) forming an IRS of the order of 0:06 nm.

3.2 Second Experimental Confirmation of Santilli IsoRedShift

With the subsequent measurements [12], G.West and G. Amato [13] delivered precise experimental confirmations of the existence of Santilli IRS,as well as the first experimental confirmation on the existence of the IBS , the NIS and the dependence of the IsoShift on the temperature via the same IsoShift Testing Station used for measurements .West and Amato carried out their measurements using the Avantes wavelength analyzer model AvaSpec 3648 which is proficient to detect frequencies of Sunlight from 400 to 1100 nm. Figure 2 indicates the chromatographs visibly showing the shift toward the red of the entire spectrum of Sunlight, together with the predictable lack of frequency shift of absorption lines, thus confirming the earlier measurements by the use of the Yokogawa wavelength analyzer model AQ6373.

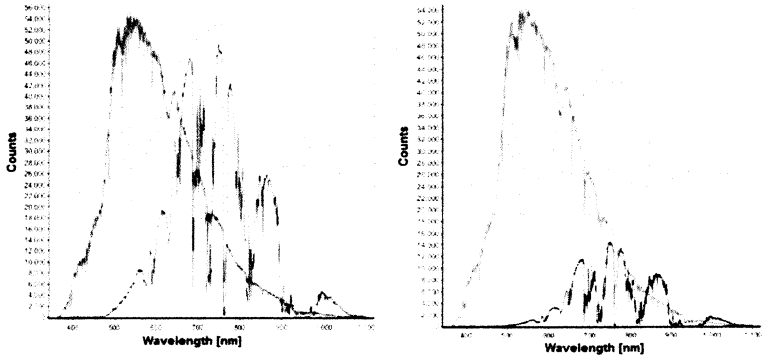

Figure 2: Representative chromatographs of Sunlight from the Zenith to the horizon obtained on April 22, 2012, via the use of the Avantes wavelength analyzer

Correspondingly these chromatographs provided the experimental confirmation of the absence of an appreciable frequency shift for the reflection of the blue laser light on a polished metal mirror under increased temperature, all the way to near the melting value .The further measurements were done to approve the elastic scattering produces no frequency shift. Moreover these confirmations also reveals that the measurements taken by G. West and G. Amato [13] were firmly referred to direct blue laser light by avoiding significant contributions from the portion of said light which is scattered in all directions inside the tube via the use of collimators, slits and other means. This leads to sole reasonable occurrence of loss of energy by light to the air inside the tube, and the underlying local mutation of the Minkowski spacetime. The latter measurements were performed to confirm that elastic scattering that produces no frequency shift.

3.3 Third Experimental Confirmation of Santilli IsoRedShift

For the experimental confirmations of IRS and IBS Santilli constructed the IsoShift Testing Station and conducted measurements [12] on Sunlight from the Zenith to the horizon. Santilli et al. [2] first established the existence of small IRS values of individual spectral lines of the Sun in the transition from the Zenith to 60^0 elevations over the horizon (Figure 1). Nevertheless, with the decrease of the elevation, the IRS gradually increases to such values that the original spectral lines acquires the characteristics of subsequent spectral lines resulting in no apparent IRS. To overcome and clarify the said discrepancy Santilli et al. performed the spectrographic measurements of Sunlight from the Zenith to the horizon via an Avantes, wavelength analyzer model Avaspec-3648- USB2-FCPC which is capable of detecting frequencies from 450 to 570 nm (from green to red). Figure 3 indicates the Illustrative scans at the Zenith and at the horizon (the top view of Fig.3) showing no apparent IRS, except for the evident decrease of intensity for Sunlight at the horizon.

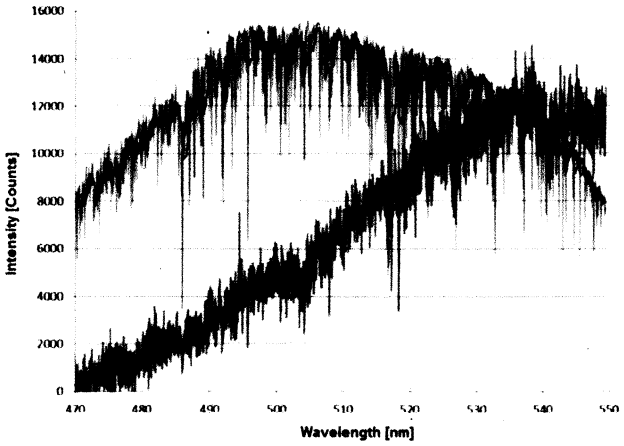

Figure 3: The Illustrative scans at the Zenith and at the horizon

The measurements in this particular confirmation recognized that the entire spectrum of Sunlight experiences a shift toward the red for about 100 nm, plus there is the appearance of about 100 nm in the infrared at the horizon that was not present at the Zenith. The measurements were conducted at the St. Petersburg Beach, Florida West Coast, also from the Zenith to the horizon, and at the same sequence of elevation over the horizon as done for the Yokogawa

analyzer. Analysis of the new raw data was also done with the same methods as those used for the preceding measurements. Furthermore clear confirmation of the chromatographic analyses conducted in Florida using the Avantes wavelength analyzer model AvaSpec-ULS2048 .

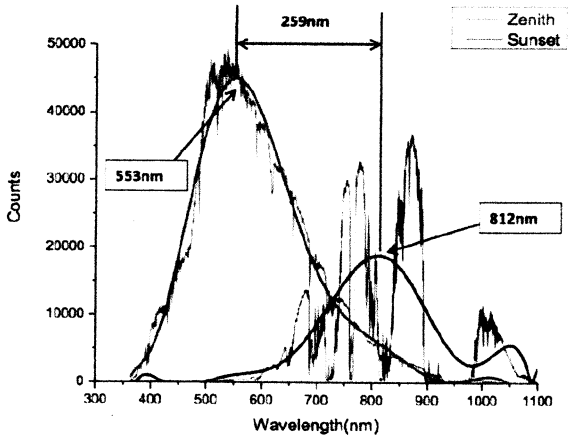

Figure 4: Representative chromatographs of Sunlight from the Zenith to the horizon obtained on September 20, 2012, at the island of Kos, Greece.

The another experimental observations that gives confirmation of Santilli's IRS was carried out on October 20, 2012, at Cocoa beach .The scans presented this measurement suggests that the Sun at the horizon with numerical values essentially the same as those of the preceding scans for the Sunset. These scans also represent Sunlight at the Zenith in the left and that at lower elevation in the right. However, their order is inverted with respect to the scans for Sunset because the first detection for Sunrise is the redness of the Sun that progressively shifts toward the white for the Zenith shown in figure 5.

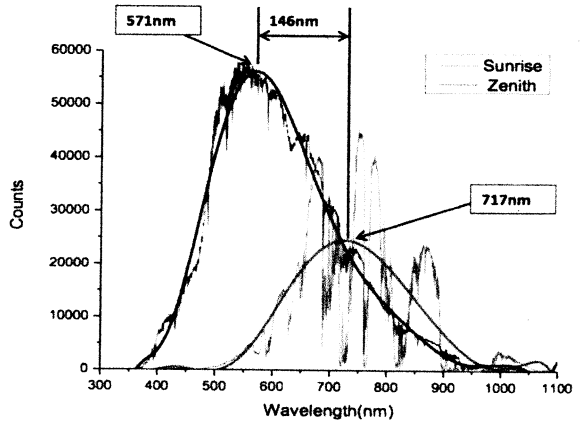

Figure 5: Chromatographs of Sunlight from Sunrise to the Zenith obtained for the first time by the authors on October 20, 2012, at Cocoa beach in the East Coast of Florida.

3.4 Fourth Experimental Confirmation of Santilli IsoRedShift

The measurements on the island of Kos, Greece, provide a clear experimental confirmation that the redness of the Sun at Sunset is dominated by Santilli's IRS, except for a small contribution of the order of 10^{-6} for the conventional Doppler's effect due to the motion of the observer away from the Sun at Sunset caused by Earth's rotation .One of the most important consequences of this measurements is to provide an additional experimental confirmation of the mutation of the Minkowski spacetime for the vacuum into the covering Minkowski-Santilli isospacetime for our atmosphere, with consequential applicability of the covering LPS isosymmetry and related isorelativity.This fourth verification of Santilli's IRS origin of the redness of the Sun at the horizon was conducted by the authors on September 20, 2012, on the southwest beach side of the island of Kos in the Kefalos town, Greece, for the first time in the transition of the Sun from the Zenith to the horizon (Sunset).

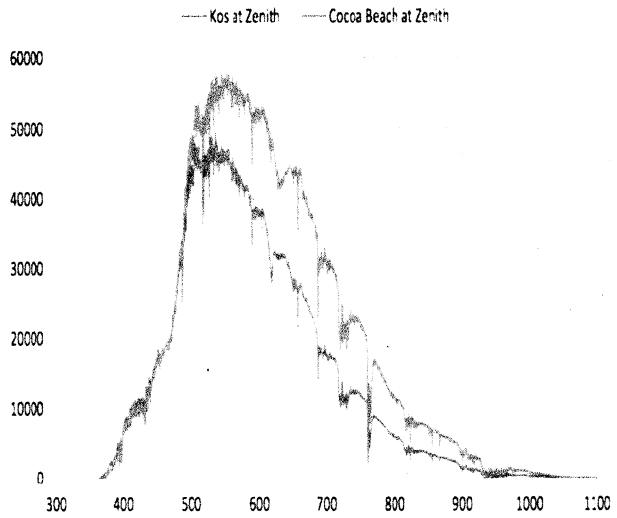

Figure 6: The Sun at the Zenith in two different locations, at Kos, Greece and at Cocoa Beach Florida.

Comparison of results with the previous ones [2,13] establishes the achievement of the same numerical values of Santilli's IRS, namely, about 100 nm frequency shift of the blue to the red, plus the appearance of about 100 nm in the infrared at the horizon that was not detectable at the Zenith. The small difference in the intensity (Figure 6) is due to the manual orientation of the telescope and it is fully within the range of accurate measurement of frequencies by the Avantes analyzer. Even assuming that such a variation of intensity may affect frequencies, the related numerical value would be ignorable over the large IRS from the Zenith to the horizon.

4. Mathematical Background.

Santilli's fundamental idea is the representation of supposed interactions with a isotopic lifting to $\hat{I}$ of the fundamental unit I of conventional theories, under the exclusive condition that $\hat{I}$ is positive-definite, thus admitting the inverse $\hat{I} = 1/\hat{T}$ and with the arbitrary functional dependence on local quantities, such as time t, coordinates r, velocities v , energy e, density d, frequency ω, temperature T , and other variables

$$I \to \hat{I} = \hat{I}(t,r,v,e,d,\omega,\tau,...) = 1/\hat{T}(t,r,v,d,\omega,\tau,...) > 0. \tag{1}$$

Today the isotopically lifted unit is called *Santilli isounit*; its inverse $\hat{T}$ is called the isotopic element, where $\hat{T}$ remains fixed, under which $\hat{I}$ indeed is to the right and left multiplying unit of the theory.

In 1983 Santilli [10] presented the isotopies of the Minkowski spacetime with his generalized symmetric (non-singular) spacetime given by,

$$x^2 = x_1^1 b_1^2 + x_2^1 b_2^2 + x_3^1 b_3^1 - t^2 c^2 b_4^2 = x_1^2/n_1^2 + x_2^2/n_2^2 + x_3^2/n_3^2 - t^2 c^2/n_4^2 \tag{2}$$

that today it is known as the *Minkowski-Santilli isospacetime*. In the above equation, the terms $b_\mu = 1/n_\mu$ are the characteristic quantities considered for the medium; which are explicitly positive functions of all probable local variables, for example distance traveled by light d, temperature τ, frequency of light ν, density ρ, etc., $b_\mu = b_\mu(d,\rho,\tau,\nu,\ldots) = 1/n_\mu = 1/n_\mu(d,\rho,\tau,\nu,\ldots)$; they are normalized for the vacuum as $b_\mu = 1/n_\mu = 1$, $\mu = 1, 2, 3, 4$; the quantity $1/b_4 = n_4$ is time characteristic and familiar to the index of refraction corresponding to speed of electromagnetic waves $C = cb_4 = c/n_4$; the characteristics space quantities $b_k = 1/n_k$, $k = 1, 2, 3$, stands for the anisotropy and inhomogeneity of the medium; and their values are set by physical verification. The new *Doppler-Santilli IsoShift* referred to a frequency shift partially due to relative motion between the source and the observer, and partially due to the medium in which the electromagnetic waves propagates and is given by

$$\omega \approx \omega_0 \left(1 \pm \frac{v_s^2}{c^2} \frac{n_4^2}{n_s^2} + \cdots \right), \tag{3}$$

The effect depends on the anisotropic and inhomogeneous character of the medium. Subsequently, Santilli has re-established the velocity of light as the local variable $C = c/n$. Next Santilli provided an evidence that, when the speed of light within a physical medium is no longer c, the universal *Lorentz- Poincare-Santilli isosymmetry (LPS)* for all possible local speeds $C = c/n$ characterizes the Doppler-Santilli isoredshift [14]. Santilli evidently recognized the fact that the characteristic quantities n_μ are velocity dependent. Therefore, isolaw (3) reveals an exact case, in which a frequency shift occurs without any relative motion between the source, the medium and the observer,

$$\omega_e = \omega_0 (1 \pm Kd + \cdots) \ , \ kd = \left[\frac{v^2}{c^2} \frac{n_4^2}{n_3^2} \right]_{v=0} \neq 0 \tag{4}$$

where ω_e (ω_0) is the frequency measured (at the origin) and d represents the distance traveled by light in the medium. In the above Santilli's formulation the relative motion is null and this formulation is termed as *Santilli Isoshift* [15, 16].

Santilli IsoShift (IS), is a shift of the frequency of light when propagating within a physical medium without any relative motion between the source, the medium and the observer.

Thus Santilli's classification of Isoshift is as follows

IsoRedShift (IRS), occurs for the minus sign in (4) when the medium is at a adequately low temperature when atoms are in their ground state, in such case light loses energy $E = h\nu$ to the medium that produces significant anomalous redshift.

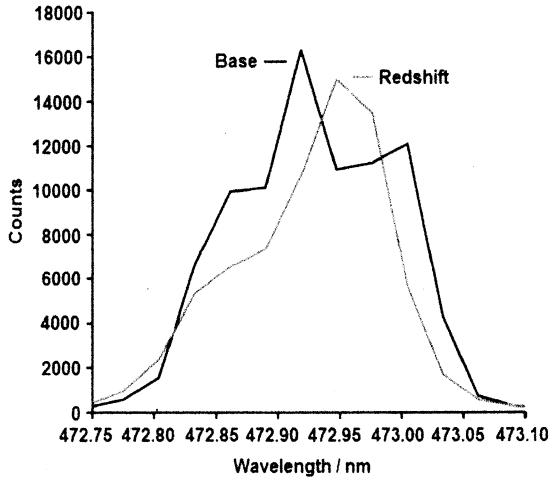

Figure 7: One of the systematic experimental confirmations obtained by G. West and G. Amato [17] on the existence of Santilli's IRS via the same IsoShift Testing Station used in Ref. [16], (adapted from Fig. 6 of Ref.[11])

IsoBlueShift (IBS), occurs for the plus sign in (4) when the medium is at adequately high temperature when most of its atoms are in excited states, in such case light acquires energy $E = h\nu$ from the medium by means of significant anomalous blueshift.

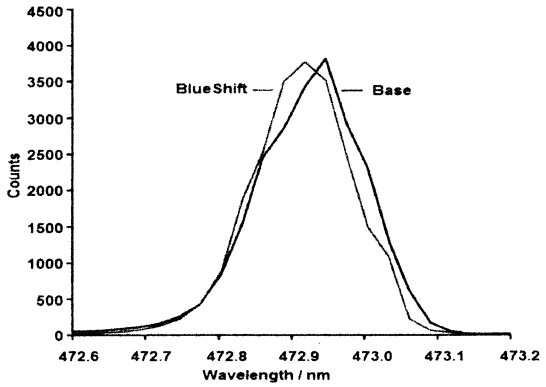

Figure 8 :One of the systematic experimental confirmations obtained by G. West and G. Amato [16] on the existence of Santilli's IBS via the same IsoShift Testing Station used in Ref. [17],(adapted from Fig. 8 of Ref .[16])

NoIsoShift (NIS), occurs when the energy lost by light to the medium is equal to the energy released by the medium to light with no anomalous shift in which case $K = 0$ in (4).

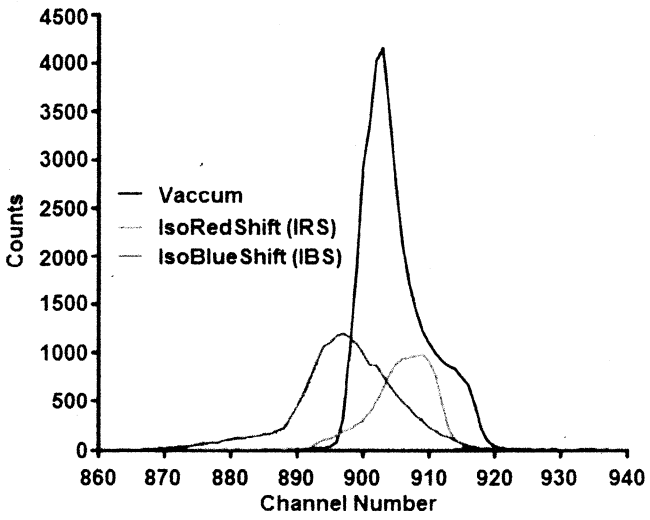

Figure 9: The first of systematic experimental confirmations obtained by G. West and G. Amato [16] on the existence of Santilli's IBS via the same IsoShift Testing Station used in Ref. [17].The central peak indicates the blue laser light under vacuum; the peak to the right indicates IRS obtained at night; and the peak to the left presents the first measured IBS (adapted from Fig. 7 of Ref. [16]).

5. Concluding Remarks

Santilli's fifty years of research and his experimental confirmations presented in this review confirm the inapplicability of special relativity for all interior dynamical problems of extended particles and electromagnetic waves propagating within physical media. According to Santilli the most significant cosmological inference is that it gives an opportunity to reconsider the status of the current proposal of the expansion of universe. Santilli's Iso-redshift could have important cosmological implications and on this issue the further investigations are in progress. Prof. R. M. Santilli conducted his mathematical, theoretical and experimental studies for *interior dynamical problems* and confirmed that light propagating within the physical media admits *IsoRedShift (IRS)* and *IsoBlueShift (IBS)*. His discoveries regarding *(IRS)* and *(IBS)* deal with excitation and de-excitation of atomic electrons, and independent from known molecular processes, such as scattering or absorption and various measurements confirms the existence of Santilli's hypothesis of anomalous redshift (blueshift) of light propagating within a gaseous medium atsufficiently low temperature without any relative motion between the source, the medium and the observer.

Acknowledgments

The author expresses his deepest gratitude to Prof. R. M. Santilli for providing an opportunity to get initiated in this field of research and his guidance and valuable suggestions during ICNAAM -2013, Rhodes, Greece workshop. Additionally, the author would like to thank Prof. A. A. Bhalekar for his guidance during the one day motivational workshop held at Smt. Bhagwati Chaturvedi College of Engineering, Nagpur-09 (INDIA) on April 6, 2013 and for providing valuable suggestions during the preparation of this paper. The financial support from the R. M. Santilli Foundation is gratefully acknowledged.

References

1. R. M. Santilli. *Hadronic J.* **1**, 223 (1978). http://www.santilli-foundation.org/docs/Santilli-58.pdf
2. R. M. Santilli, G. West and G. Amato. "Experimental Confirmation of the IsoRedShift at Sun at Sunset and Sunrise with Consequential Absence of Universe Expansion and Related Conjectures," *J. Comput. Methods Sci. Eng.* **12,** 165 (2012). http://www.santilli-foundation.org/docs/Confirmation-sun-IRS.pdf
3. R. M. Santilli, "Iso-Minkowskian Geometry For Interior Dynamical Problems," Contributed paper in Cosmology, Quantum Vacuum, and Zeta Functions, Diego Saez-Gomez, Sergei Odintsov Sebastia Xambo Editors, *Springer*, Berlin, 2011. http://www.santilli-foundation.org/docs/Isominkowskian-Geom.
4. R.M. Santilli, Experimental Verification of IsoRedShift and its Cosmological Implications, contributed paper to the *Proceedings of the International Conference on Numerical Analysis and Applied Mathematics,* Rhodes, Greece, September 19–25, 2010, T. E. Simos, ed., *American Institute of Physics Conference Proceedings,* **1281**, 882 (2010). http://www.santilli-foundation.org/docs/Isoredshift-Letter.pdf
5. E. Hubble, *Proc. Nat. Acad. Sci. USA*, **15**, 168 (1929).
6. V. Slipher, *Popular Astronomy*, **23,** 21 (1915).

7. F. Zwicky, *Proc. Nat. Acad. Sci. USA*, **15,** 773 (1929).
8. I. Gandzha and J. Kadeisvily, "New Sciences for a New Era", Sankata Printing Press, Kathmandu, Nepal, 2011.
http://www.santilli-foundation.org/docs/RMS.pdf
9. R. M. Santilli. *Foundation of Theoretical Mechanics*, Volume I (1978) , and Volume II (1982), Springer-Verlag, Heidelberg, Germany,
http://www.santilli-foundation.org/docs/Santilli-209.pdf ,
10. R. M. Santilli, "Lie-isotopic Lifting of Special Relativity for Extended Deformable Particles," *Lettere Nuovo Cimento*, **37**, 545 (1983).
http://www.santilli-foundation.org/docs/Santilli-50.pdf
11. H. Ahmar, G. Amato, J. V. Kadeisvili, J. Manuel, G. West, and O. Zogorodnia, "Additional experimental confirmations of Santilli's IsoRedShift and the consequential expected absence of universe expansion," *J. Comp. Methods Sci. Eng.*, **13,** 321 (2013).
http://www.santilli-foundation.org/docs/Confirmation-sun-IRS.pdf
12. R.M. Santilli, G. West and G. Amato, Documentation of IRS in the Sun.
http://www.santilli-foundation.org/docs/IRSsun.zip.
13. G. West and G. Amato, "Experimental Confirmation of Santilli's IsoRedShift and IsoBlueShift," contributed paper to the Proceedings of the San Marino Workshop on Astrophysics and Cosmology for Matter and Antimatter, Republic of San Marino, September 5 to 9, 2011, in press (2012).
http://www.santillifoundation.org/docs/Confirmation-sun-IRS.pdf
14. R. Mignani, Quasar redshift in iso-Minkowski space, *Physics Essays*, **5,** 531 (1992).
15. R. M. Santilli, *Isotopic Generalizations of Galilei and Einstein Relativities*, Vols. I and II (1991), International Academic Press, Palm Harbor, USA.
http://www.santilli-foundation.org/docs/Santilli-01.pdf.
http://www.santillifoundation.org/docs/Santilli-61.pdf.
16. R. M. Santilli, Experimental Verifications of IsoRedShift with Possible Absence of Universe Expansion, Big Bang, DarkMatter, and Dark Energy, *The Open Astronomy Journal*, **3,** (2010)124.
http://www.santilli-foundation.org/docs/Santilliisoredshift.pdf.
17. G. West and G. Amato, "Experimental Confoirmation of Santilli's IsoRedShift and IsoBlueShift," *Journal of Computational Methods in Sciences and Engineering*, **12,** 169 (2012).
http://www.santilli-foundation.org/docs/Confirmation-IRS-IBS.pdf.

HADRONIC JOURNAL 36, 541 - 554 (2013)

MADELBROT ISO-SETS: ISO-UNIT IMPACT ASSESSMENT

Reza Katebi
Department of Physics, California State University
800 North State College Boulevard
Fullerton, CA 92831, USA
rkatebi.gravity@gmail.com

Nathan O. Schmidt
Department of Mathematics, Boise State University
1910 University Drive
Boise, ID 83725, USA
nathanschmidt@u.boisestate.edu

Received February 9, 2014

Abstract

In this introductory work, we use Santilli's iso-topic lifting as a cutting-edge platform to explore Mandelbrot's set. The objective is to upgrade Mandelbrot's complex quadratic polynomial with iso-multiplication and then computationally probe the effects on this revolutionary fractal. For this, we define the "iso-complex quadratic polynomial" and engage it to generate a locally iso-morphic array of "Mandelbrot iso-sets" by varying the iso-unit, where the connectedness property is topologically preserved in each case. The iso-unit broadens and strengthens the chaotic analysis, and authorizes an enhanced classification and demystification such complex systems because it equips us with an additional degree of freedom: the new Mandelbrot iso-set array is an improvement over the traditional Mandelbrot set because it is significantly more general. In total, the experimental results exemplify dynamic iso-spaces and indicate two modes of topological effects: scale-deformation and boundary-deformation. Ultimately, these new and preliminary developments spark further insight into the emerging realm of iso-fractals.

Keywords: Geometry and topology; Chaos theory; Complex systems; Santilli iso-number; Fractal; Iso-fractal; Mandelbrot set; Mandelbrot iso-set.

Copyright © 2013 by Hadronic Press, Inc., Palm Harbor, FL 34684, USA

1 Introduction

The Mandelbrot set is often considered to be the most famous fractal. It is a mathematical set of points in a Euclidean complex space $\mathbb{C}$, with a distinctive boundary that characterizes a fractal structure with self-similarity [1, 2]. The set is closely related to Julia sets [3] and is named after the French mathematician Benoit Mandelbrot, the pioneer who analyzed and popularized it [1, 2]. Images of Mandelbrot's set are created by iteratively sampling complex numbers and determining, for each one, if the result tends towards infinity when a particular mathematical operation is iterated on it [1, 2]. For each complex number, the real and imaginary components serve as 2D image coordinates in $\mathbb{C}$ [4], where the pixels are colored to encode the sequence divergence rate [1, 2]. In particular, the Mandelbrot set is the set of values of $c \in \mathbb{C}$ for which the orbit of 0 under iteration of Mandelbrot's complex quadratic polynomial [1, 2]

$$z_{n+1} = z_n^2 + c, \tag{1}$$

remains bounded, where $z_n, z_{n+1}, c \in \mathbb{C}$ are complex numbers. That is, c is part of the Mandelbrot set if, when starting with $z_0 = 0$ and applying the iteration repeatedly, the absolute value of z_n remains bounded however large n gets [1, 2]. Mandelbrot initially hypothesized that the connectedness property is not preserved for his set, but after further experimentation he later revised his conjecture and claimed that the set is connected [5]. Subsequently, Douady and Hubbard proved that indeed Mandelbrot's set is connected [5, 6]. Beyond the discipline of mathematics, the Mandelbrot set has become prominent in various art forms due to its aesthetic appeal [7, 8, 9] and, moreover, because it is an emergent complex structure that arises from the application of *simple* rules [1, 2].

So why are the Mandelbrot set and other such fractals important subjects to study in science and mathematics? Well, it turns out that *fractal geometry* is the language of chaos theory [4, 10], and fractal/chaotic patterns are *abundant* in the physical, chemical, and biological expressions of nature [8, 11, 12]. Moreover, fractal geometry and chaos theory are a relatively new discipline [4]. Chaos theory examines the behavior of dynamical systems that are *highly sensitive* to initial conditions [11, 13]. In a chaotic dynamical system, *miniscule* differences in initial conditions yield *widely*

diverging outcomes, thereby generally rendering long-term predictions impossible [11, 13]. For this, additional examples of chaos and fractals are also observed in lightning discharges [14, 15, 16, 17], weather patterns [18, 19, 20], aquatic ecosystems [21, 22], population biology [23], the biological allometric scaling laws [24, 25, 26, 27, 28], cancers and genetics [29, 30], viruses and pathogens [31, 32], the human brain [33, 34, 35], earthquakes [36, 37, 38], volcanoes [39, 40, 41], the global stock market [42, 43], and more. Certainly, fractals such as the Mandelbrot set must play a fundamental role in classifying and demystifying such *complex* systems—but how?

In this paper, we resume the iso-fractal developments of [4] and attack this complex problem by utilizing the power of Santilli's new iso-topic lifting [44, 45, 46, 47, 48, 49] to probe Mandelbrot's set [1, 2]. For this, we launch with Section 2, where we deploy Santilli's iso-numbers [44, 45, 46, 47, 48, 49] to upgrade Mandelbrot's complex quadratic polynomial—eq. (1)—with iso-multiplication to construct the *iso-complex quadratic polynomial*, which is used to construct a *Mandelbrot iso-set*. For this, we identify the procedure and results for the *main* computational experiment that assesses the impact of Santilli's iso-unit [44, 45, 46, 47, 48, 49] for various Mandelbrot iso-sets, where the connectedness property is preserved. Afterwards, in the *extended* experiment of Section 3, we expand the examination and outcomes to include a Mandelbrot iso-complex polynomial of degree k along with a version based on the tangent trigonometric function. Finally, we conclude with Section 4, where we briefly recapitulate this mode of research and suggest future actions to take.

2 Main Experiment

Here, motivated by the iso-fractal initiation of [4], we engage Santilli's iso-numbers [44, 45, 46, 47, 48, 49] to explore Mandelbrot's set [1, 2] in Euclidean complex space. In the procedure of Section 2.1, we attack our objective by upgrading Mandelbrot's complex quadratic polynomial—eq. (1)—with Santilli's iso-multiplication [44, 45, 46, 47, 48, 49] to construct the iso-complex quadratic polynomial, which is used to construct a Mandelbrot iso-set. Afterwards, in Section 2.2, we examine the computational results for an array of Mandelbrot iso-sets with distinct iso-topic liftings to assess the impact of varying the iso-units.

2.1 Main Procedure

In this section, the iso-complex quadratic polynomial for the experiment is assembled as follows:

1. First, in accordance to Santilli's iso-number methodology [44, 45, 46, 47, 48, 49], we select the positive-definite iso-unit $\hat{r} > 0$ with the corresponding inverse $\hat{\kappa} = \frac{1}{\hat{r}} > 0$.

2. Second, given that $\mathbb{C}$ is the set of all complex numbers, then we demonstrate that $\mathbb{C}$ is iso-topically lifted via $\mathbb{C} \to \mathbb{C}_{\hat{r}}$ to establish $\mathbb{C}_{\hat{r}}$, which is the set of all iso-complex numbers [4, 44, 45, 46, 47, 48, 49]. Thus, if $z_1, z_2 \in \mathbb{C}$ are complex numbers, then the corresponding iso-complex numbers $\hat{z}_1, \hat{z}_2 \in \mathbb{C}_{\hat{r}}$ are directly related via [4, 44, 45, 46, 47, 48, 49]

$$\begin{array}{rcl} \hat{z}_1 & = & z_1 \times \hat{r} \\ & & , \ \forall z_1, z_2 \in \mathbb{C} \to \forall \hat{z}_1, \hat{z}_2 \in \mathbb{C}_{\hat{r}}, \\ \hat{z}_2 & = & z_2 \times \hat{r} \end{array} \tag{2}$$

   where the conventional complex multiplication $\hat{z}_1 \times \hat{z}_2$ is upgraded with the iso-multiplication [4, 44, 45, 46, 47, 48, 49]

$$\hat{z}_1 \ \hat{\times} \ \hat{z}_2 = \hat{z}_1 \times \hat{\kappa} \times \hat{z}_2 = \hat{z}_1 \times \frac{1}{\hat{r}} \times \hat{z}_2. \tag{3}$$

3. Third, given the iso-multiplication of eq. (3), we deduce the iso-square via the expansion

$$\begin{array}{rcl} \hat{z}_n^2 & = & \hat{z}_n \ \hat{\times} \ \hat{z}_n \\ & = & (z_n \times \hat{r}) \times \hat{\kappa} \times (z_n \times \hat{r}) \\ & = & (z_n \times \hat{r}) \times \frac{1}{\hat{r}} \times (z_n \times \hat{r}) \\ & = & z_n \times z_n \times \hat{r}. \end{array} \tag{4}$$

4. Fourth, we prove that the axiom of the multiplicative units of eqs. (2–4) is confirmed by the expressions [4, 44, 45, 46, 47, 48, 49]

$$1 \ \hat{\times} \ \hat{z}_n = 1 \times \hat{\kappa} \times \hat{z}_n = \hat{z}_n \times \frac{1}{\hat{r}} \times 1 = \hat{z}_n \ \hat{\times} \ 1, \ \forall \hat{z}_n \in \mathbb{C}_{\hat{r}}. \tag{5}$$

5. Fifth, we establish that eqs. (2–5) are characterized by the iso-topic lifting and its inverse [4, 44, 45, 46, 47, 48, 49]

$$\begin{aligned} f(\hat{r}): \quad \mathbb{C} &\rightarrow \mathbb{C}_{\hat{r}} \\ f^{-1}(\hat{r}): \quad \mathbb{C}_{\hat{r}} &\rightarrow \mathbb{C}, \end{aligned} \tag{6}$$

respectively, where indeed $\mathbb{C}$ and $\mathbb{C}_{\hat{r}}$ are *locally iso-morphic.*

6. Finally, we engage eqs. (2–6) to upgrade eq. (1) to define the iso-complex quadratic polynomial as

$$\hat{z}_{n+1} \equiv \hat{z}_n^2 + \hat{c} \equiv (\hat{z}_n \,\hat{\times}\, \hat{z}_n) + \hat{c} \equiv (z_n \times z_n \times \hat{r}) + (c \times \hat{r}) \equiv z_{n+1} \times \hat{r}, \tag{7}$$

where $\hat{z}_n, \hat{z}_{n+1}, \hat{c} \in \mathbb{C}_{\hat{r}}$ are iso-complex numbers and $z_n, z_{n+1}, c \in \mathbb{C}$ are the corresponding complex numbers. Hence, we can computationally generate a Mandelbrot iso-set by systematically iterating eq. (7)! Here, we note that the restricted iso-unit case of $\hat{r} = 1$ for eq. (7) yields the conventional Mandelbrot set of eq. (1) with the standard multiplicative unit, therefore the Mandelbrot iso-set array includes the Mandelbrot set as an element so they are connected.

Thus, given that the Mandelbrot set generated by eq. (1) has been proven to have the connectedness property by Douady and Hubbard [5, 6], and given that the iso-topic lifting of eqs. (2–6) is topologically-preserving to the Mandelbrot set, then we deduce that a Mandelbrot iso-set generated by eq. (7)—which is locally iso-morphic—*must inherit the connectedness property.* Here, we *hypothesize* that the Julia set for a given point in a Mandelbrot iso-set is connected, but this notion of "Julia iso-sets" is beyond the limited scope of this paper and will thus be a subject for future research.

At this point, we've successfully upgraded Mandelbrot's complex quadratic polynomial [1, 2] of eq. (1) with Santilli's iso-multiplication [4, 44, 45, 46, 47, 48, 49] to synthesize the iso-complex quadratic polynomial of eq. (7), which is used to generate Mandelbrot iso-sets.

2.2 Main Results

In total, we computationally experimented with the 5 distinct iso-units:

$$\hat{r} \in \{\frac{1}{2}, \frac{3}{4}, 1, \frac{4}{3}, 2\}. \tag{8}$$

In eq. (8), we observe that $\frac{1}{2}$ is the inverse of 2, 1 is the inverse of 1, and $\frac{3}{4}$ is the inverse of $\frac{4}{3}$, so these iso-unit values are in fact *dual*. Our objective is to insert the various iso-units of eq. (8) into the iso-complex quadratic polynomial of eq. (7) to observe the effect of Santilli's iso-topic lifting [4, 44, 45, 46, 47, 48, 49] on Mandelbrot's set [1, 2].

For our experimental control case, we started with $\hat{r} = 1$ and generated the Mandelbrot set—see the *middle* graphic in Figure 1. Afterwards, we varied the iso-unit for $\hat{r} \neq 1$, such that $\hat{r} = \frac{1}{2}, \frac{3}{4}, \frac{4}{3}, 2$, to generate the Mandelbrot iso-sets—see the *non-middle* graphics in Figure 1. In this preliminary assessment, we observe that the iso-unit variation impact results of Figure 1 indicate that Santilli's iso-topic lifting [4, 44, 45, 46, 47, 48, 49] yields—at minimum—*two* general topological effects:

1. **scale-deformation**, where the fractal is magnified ("zoom-in") or de-magnified ("zoom-out"); and

2. **boundary-deformation**, where the relative position of the fractal boundaries and sequence divergence rates are restructured.

Effects 1 and 2 prove the iso-mathematical existence of the proposed Mandelbrot iso-sets, which are indeed *locally iso-morphic* to the Mandelbrot set. Moreover, these computational results are an experimental implementation of the discrete dynamic iso-spaces in [50], where the iso-unit is treated as a dynamic iso-unit function of a parameter that varies by taking on discrete values.

3 Extended Experiment: Procedure and Results

Here, inspired by the procedure and outcomes of Section 2, we further probe the Mandelbrot iso-set array by experimenting with two alternative variations of the iso-complex polynomial of eq. (7) to open up additional iso-fractal cases for investigation.

First, for the *degree-k Mandelbrot iso-set* experimental case, we replace the $\hat{z}_n^2$ of eq. (7) with the generalization $\hat{z}_n^k$ to define the *degree-k Mandelbrot iso-complex polynomial*

$$\hat{z}_{n+1} \equiv \hat{z}_n^k + \hat{c}, \tag{9}$$

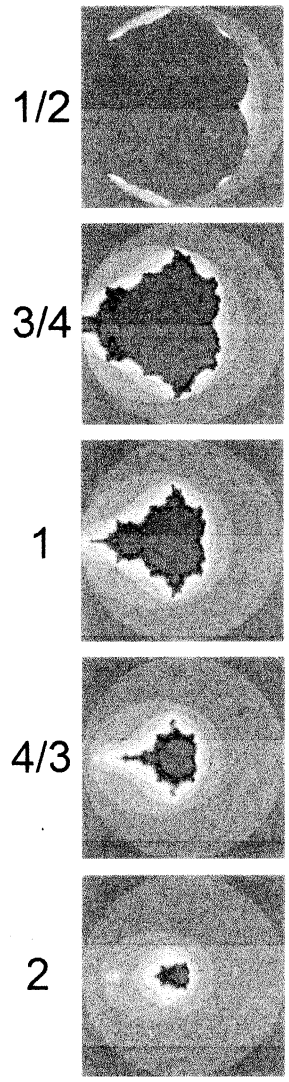

Fig. 1: A depiction of the iso-unit impact variation for the *main* computational experiment. In the *left* column, the varying iso-units of eq. (8) are listed. In the *right* column, the middle graphic is the Mandelbrot set and the non-middle graphics are the Mandelbrot iso-sets that are generated by eq. (7). Observe that Santilli's iso-topic lifting [44, 45, 46, 47, 48, 49] yields two general topological effects: scale-deformation and boundary-deformation.

such that $k > 0$ is a positive-definite natural number. Subsequently, for eq. (9), we set $k = 3$ and re-execute the computational experiment with the same 5 distinct iso-unit parameters of eq. (8): the resulting degree-3 Mandelbrot iso-sets are displayed in the *left* column of Figure 2, which are indeed *locally iso-morphic* to each other. Here, similar to the computational results of Section 2.2, we observe the two general topological effects: scale-deformation and boundary-deformation.

Second, for the *tangent Mandelbrot iso-set* experimental case, we replace the $\hat{z}_n^2$ of eq. (7) with the variation $\tan(\hat{z}_n^2)$ to define the *tangent Mandelbrot iso-complex polynomial*

$$\hat{z}_{n+1} \equiv \tan(\hat{z}_n^2) + \hat{c}. \tag{10}$$

Subsequently, for eq. (10), we re-execute the computations with the same 5 distinct iso-unit parameters of eq. (8): the resulting tangent Mandelbrot iso-sets are displayed in the *right* column of Figure 2, which are indeed *locally iso-morphic* to each other. Here, similar to the computational results of the degree-3 Mandelbrot iso-set case, we observe the two general topological effects: scale-deformation and boundary-deformation.

Thus, in total, the extended outcomes of eqs. (9–10) and Figure 2 indicate that it is possible to develop theoretical and experimental computations for generating such Mandelbrot iso-set variations.

4 Conclusion

The outcomes of this investigation reveal and assess the preliminary impact of Santilli's iso-unit [44, 45, 46, 47, 48, 49] on Mandelbrot's set [1, 2]. More precisely, we were inspired by the iso-fractal developments of [4] and deployed iso-topic liftings [44, 45, 46, 47, 48, 49] to transform Mandelbrot's complex quadratic polynomial into an iso-complex quadratic polynomial, which thereby enabled us to forge the new Mandelbrot iso-set—the Mandelbrot set and a given Mandelbrot iso-set are locally iso-morphic. Subsequently, the initial results of the computational experiments revealed that varying the iso-units causes two general topological effects: scale-deformation and boundary-deformation. For this, we noted that this experiment is an implementation of discrete dynamic iso-spaces [50].

The main results of Section 2.2 clearly indicate that the Mandelbrot set is a specific type of Mandelbrot iso-set when the iso-unit $\hat{r}$ is *not* iso-topically

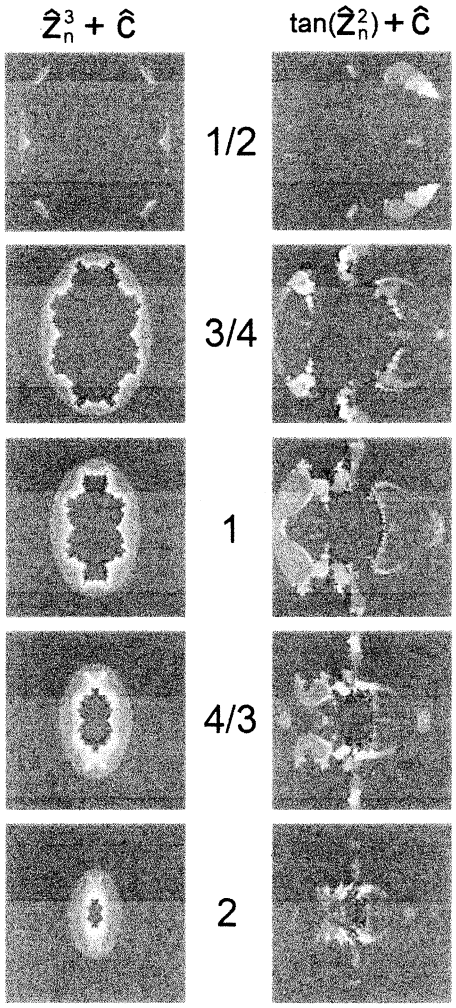

Fig. 2: A depiction of the iso-unit impact variation for the *extended* computational experiment. In the *left* column, the *degree-k Mandelbrot iso-sets* generated by $\hat{z}_n^k + \hat{c}$ in eq. (9) for $k = 3$ are listed. In the *middle* column, the varying iso-units of eq. (8) are listed. In the *right* column, the *tangent Mandelbrot iso-sets* generated by $\tan(\hat{z}_n^2) + \hat{c}$ in eq. (10) are listed. Again, in both experimental cases, observe that Santilli's iso-topic lifting [44, 45, 46, 47, 48, 49] yields two general topological effects: scale-deformation and boundary-deformation.

lifted and thus restricted to the conventional case $\hat{r} = 1$; one could classify the Mandelbrot set as the "base case" of the Mandelbrot iso-set array. Thus, the iso-topic liftings [44, 45, 46, 47, 48, 49] preserve *all* of the Mandelbrot set's characteristics and extend them. For this, the iso-topic liftings [44, 45, 46, 47, 48, 49] enable us to vary $\hat{r}$, which serves as an additional degree of freedom for iso-fractal construction and analysis, and therefore authorizes an enhanced classification and demystification methodology for such chaotic systems because we can take into further account the iso-unit impact of the scale-deformations and boundary-deformations. Hence, we recapitulate these outcomes and implications by pointing out that: *the Mandelbrot iso-set is an improvement over the Mandelbrot set* because the iso-topic liftings [44, 45, 46, 47, 48, 49] render it to be *significantly more general.*

The extended results of Section 3 further probed the Mandelbrot iso-set array by experimenting with two alternative variations of the iso-complex polynomial: the degree-k Mandelbrot iso-set and the tangent Mandelbrot iso-set. Here, the two experimental cases proved the existence of such iso-fractals, which are indeed locally iso-morphic to each other under the topological-preservations of the iso-topic liftings [44, 45, 46, 47, 48, 49], where again, we observed the two said modes of topological deformation effects.

In our opinion, the examination and results indicate an exciting and promising future for this mode of cutting-edge research: the territory of iso-fractals is a vast, uncharted frontier. Ultimately, the implications of this venture are significant because they advance the borderland of iso-mathematics to new trajectories of thought, inquiry, and experimentation. Hence, for future research, we plan to conduct additional related surveys of iso-mathematics that investigate novel patterns for advancement, with the intent to simplify and classify these emerging, developing iso-fractals. More precisely, in future work, we plan to identify the area and Hausdorff dimension [51] of the Mandelbrot iso-set and develop Julia iso-sets to test our connectedness hypothesis in a more generalized iso-fractal framework.

5 Acknowledgment

We wish to thank the anonymous referees for the constructive criticisms and comments that enhanced the quality and application of this paper.

References

[1] B. B. Mandelbrot. *The fractal geometry of nature.* Times Books, 1982.

[2] B. B. Mandelbrot. *Fractals and chaos: the Mandelbrot set and beyond*, volume 3. Springer, 2004.

[3] I. D. Entwistle. Julia set art and fractals in the complex plane. *Computers & Graphics*, 13(3):389–392, 1989.

[4] N. O. Schmidt and R. Katebi. Initiating Santilli's iso-mathematics to triplex numbers, fractals, and Inopin's holographic ring: preliminary assessment and new lemmas. *Hadronic Journal (in press)*, 36, 2013.

[5] O. Knill. Harvard mathematics archive - the Mandelbrot set, 2005.

[6] A. Douady and J. H. Hubbard. Exploring the Mandelbrot set. The Orsay notes.

[7] B. B. Mandelbrot. Fractals and an art for the sake of science. *Leonardo. Supplemental Issue*, pages 21–24, 1989.

[8] J. Briggs. *Fractals: The patterns of chaos: A new aesthetic of art, science, and nature.* Simon and Schuster, 1992.

[9] J. J. Ventrella. Evolving the Mandelbrot set to imitate figurative art. In *Design by Evolution*, pages 145–167. Springer, 2008.

[10] H. O. Peitgen, H. Jürgens, and D. Saupe. *Chaos and fractals: new frontiers of science.* Springer, 2004.

[11] E. N. Lorenz. *The essence of chaos.* Routledge, 1995.

[12] G. W. Flake. *The computational beauty of nature: Computer explorations of fractals, chaos, complex systems and adaption.* The MIT Press, 1998.

[13] S. H. Kellert. *In the wake of chaos: Unpredictable order in dynamical systems.* University of Chicago Press, 1993.

[14] A. A. Tsonis and J. B. Elsner. Fractal characterization and simulation of lightning. *Beiträge zur Physik der Atmosphäre*, 60:187–192, 1987.

[15] J. Sanudo, J. B. Gómez, F. Castano, A. F. Pacheco, and et al. Fractal dimension of lightning discharge. *Nonlinear Processes in Geophysics*, 2(2):101–106, 1995.

[16] G. Milikh and J. A. Valdivia. Model of gamma ray flashes due to fractal lightning. *Geophysical Research Letters*, 26(4):525–528, 1999.

[17] J. A. Riousset, V. P. Pasko, P. R. Krehbiel, R. J. Thomas, and W. Rison. Three-dimensional fractal modeling of intracloud lightning dis-

charge in a New Mexico thunderstorm and comparison with lightning mapping observations. *Journal of Geophysical Research: Atmospheres (1984–2012)*, 112(D15), 2007.

[18] A. A. Tsonis and J. B. Elsner. Chaos, strange attractors, and weather. *Bulletin of the American Meteorological Society*, 70:14–23, 1989.

[19] R. F. Cahalan and J. H. Joseph. Fractal statistics of cloud fields. *Monthly Weather Review*, 117(2):261–272, 1989.

[20] J. B. Elsner and K. P. Georgakakos. Estimating the dimension of weather and climate attractors: important issues about the procedure and interpretation. *Journal of the Atmospheric Sciences*, 50(15), 1993.

[21] S. B. Grant, C. Poor, and S. Relle. Scaling theory and solutions for the steady-state coagulation and settling of fractal aggregates in aquatic systems. *Colloids and Surfaces A: Physicochemical and Engineering Aspects*, 107:155–174, 1996.

[22] J. Huisman and F. J. Weissing. Biodiversity of plankton by species oscillations and chaos. *Nature*, 402(6760):407–410, 1999.

[23] P. Philippe. Chaos, population biology, and epidemiology: some research implications. *Human Biology*, 65(4):525, 1993.

[24] G. B. West, J. H. Brown, and B. J. Enquist. A general model for the origin of allometric scaling laws in biology. *Science*, 276(5309):122–126, 1997.

[25] G. B. West, J. H. Brown, and B. J. Enquist. The fourth dimension of life: fractal geometry and allometric scaling of organisms. *Science*, 284(5420):1677–1679, 1999.

[26] R. Wu, C. X. Ma, R. C. Littell, and G. Casella. A statistical model for the genetic origin of allometric scaling laws in biology. *Journal of Theoretical Biology*, 219(1):121–135, 2002.

[27] G. B. West and J. H. Brown. The origin of allometric scaling laws in biology from genomes to ecosystems: towards a quantitative unifying theory of biological structure and organization. *Journal of Experimental Biology*, 208(9):1575–1592, 2005.

[28] L. Demetrius. The origin of allometric scaling laws in biology. *Journal of Theoretical Biology*, 243(4):455–467, 2006.

[29] P. Duesberg. Chromosomal chaos and cancer. *Scientific American Magazine*, 296(5):52–59, 2007.

[30] G. A. Calin, C. Vasilescu, M. Negrini, and G. Barbanti-Brodano. Genetic chaos and antichaos in human cancers. *Medical Hypotheses*, 60(2):258–262, 2003.

[31] P. Yam. Noisy nucleotides. DNA sequences show fractal correlations. *Scientific American*, 267(3):23–4, 1992.

[32] L. Bos and et al. *Plant viruses, unique and intriguing pathogens: a textbook of plant virology.* Backhuys Publishers, 1999.

[33] X. Nan and X. Jinghua. The fractal dimension of EEG as a physical measure of conscious human brain activities. *Bulletin of Mathematical Biology*, 50(5):559–565, 1988.

[34] S. L. Free, S. M. Sisodiya, M. J. Cook, D. R. Fish, and S. D. Shorvon. Three-dimensional fractal analysis of the white matter surface from magnetic resonance images of the human brain. *Cerebral Cortex*, 6(6):830–836, 1996.

[35] D. S. Bassett, A. Meyer-Lindenberg, S. Achard, T. Duke, and E. Bullmore. Adaptive reconfiguration of fractal small-world human brain functional networks. *Proceedings of the National Academy of Sciences*, 103(51):19518–19523, 2006.

[36] H. J. Xu and L. Knopoff. Periodicity and chaos in a one-dimensional dynamical model of earthquakes. *Physical Review E*, 50(5):3577, 1994.

[37] C. H. Scholz. Earthquakes as chaos. *Nature*, 348(6298):197–198, 1990.

[38] M. Sahimi, M. C. Robertson, and C. G. Sammis. Fractal distribution of earthquake hypocenters and its relation to fault patterns and percolation. *Physical Review Letters*, 70(14):2186, 1993.

[39] S. L. Harris. *Agents of chaos: earthquakes, volcanoes, and other natural disasters.* Mountain Press Publishing Company, 1990.

[40] D. L. Turcotte. *Fractals and chaos in geology and geophysics.* Cambridge University Press, 1997.

[41] U. Kueppers, D. Perugini, and D. B. Dingwell. Explosive energy during volcanic eruptions from fractal analysis of pyroclasts. *Earth and Planetary Science Letters*, 248(3):800–807, 2006.

[42] B. LeBaron. Chaos and nonlinear forecastability in economics and finance. *Philosophical Transactions of the Royal Society of London. Series A: Physical and Engineering Sciences*, 348(1688):397–404, 1994.

[43] E. E. Peters and et al. *Fractal market analysis: applying chaos theory*

to investment and economics, volume 24. Wiley New York, 1994.

[44] R. M. Santilli. Isonumbers and genonumbers of dimensions 1, 2, 4, 8, their isoduals and pseudoduals, and "hidden numbers" of dimension 3, 5, 6, 7. *Algebras, Groups and Geometries*, 10:273, 1993.

[45] R. M. Santilli. Rendiconti circolo matematico di palermo. *Supplemento*, 42:7, 1996.

[46] C. X. Jiang. Fundaments of the theory of Santillian numbers. *International Academic Presss, America-Europe-Asia*, 2002.

[47] R. M. Santilli. Hadronic mathematics, mechanics and chemistry. *Volume I, II, III, IV, and V, International Academic Press, New York*, 2008.

[48] C. Corda. Introduction to Santilli iso-numbers. In *AIP Conference Proceedings-American Institute of Physics*, volume 1479, page 1013, 2012.

[49] C. Corda. Introduction to Santilli iso-mathematics. In *AIP Conference Proceedings-American Institute of Physics*, 2013.

[50] N. O. Schmidt. Dynamic iso-topic lifting with application to Fibonacci's sequence and Mandelbrot's set. *Hadronic Journal (in press)*, 36, 2013.

[51] Mitsuhiro Shishikura. The Hausdorff dimension of the boundary of the Mandelbrot set and Julia sets. *Annals of Mathematics*, pages 225–267, 1998.

HADRONIC JOURNAL 36, 555 - 563 (2013)

THE GRAVITATIONAL ENERGY OF THE UNIVERSE

Kenneth Dalton
General Delivery
Bang Saphan Yai 77140
Prachuap Kiri Khan, Thailand
kxdalton@yahoo.com

Received January 3, 2014
Revised February 2, 2014

Abstract

The gravitational energy, momentum, and stress are calculated for the Robertson-Walker metric. The principle of energy conservation is applied, in conjunction with the Friedmann equations. Together, they show that the cosmological constant Λ is non-zero, the curvature index $k = 0$, and the acceleration $\ddot{R}$ is positive. It is shown that the gravitational field accounts for two-thirds of the energy in the Universe.

Copyright © 2013 by Hadronic Press, Inc., Palm Harbor, FL 34684, USA

1. Introduction

In the standard treatment of cosmology, no attempt is made to directly calculate the energy, momentum, and stress of the gravitational field. The following calculation derives from the scalar, three-vector theory of gravitation.[1,2] In this theory, displacements in time and space are expressed in the form

$$c\,dt = e_0(x)dx^0 \qquad\qquad d\mathbf{r} = \mathbf{e}_i(x)dx^i \tag{1}$$

where $e_\mu = (e_0,\, \mathbf{e}_i)$ is a scalar, 3-vector basis. The fundamental interval[1] is given by

$$\begin{aligned} ds^2 &= c^2dt^2 - d\mathbf{r}^2 = (e_0dx^0)^2 - \mathbf{e}_i \cdot \mathbf{e}_j\, dx^i dx^j \\ &= g_{\mu\nu}dx^\mu dx^\nu \end{aligned} \tag{2}$$

where

$$g_{\mu\nu} = \begin{pmatrix} g_{00} & 0 & 0 & 0 \\ 0 & & & \\ 0 & & g_{ij} & \\ 0 & & & \end{pmatrix} \tag{3}$$

is the scalar, 3-vector metric.

The basis $e_\mu(x)$ varies from point to point according to the formula

$$\nabla_\nu e_\mu = e_\lambda Q^\lambda_{\mu\nu} \tag{4}$$

This separates into scalar and 3-vector parts

$$\nabla_\nu e_0 = e_0 Q^0_{0\nu} \tag{5}$$

$$\nabla_\nu \mathbf{e}_i = \mathbf{e}_k Q^k_{i\nu} \tag{6}$$

By definition $Q^k_{0\nu} = Q^0_{i\nu} \equiv 0$. The $Q^\mu_{\nu\lambda}$ are related to the Christofel coefficients as follows:

[1]This interval is invariant under a Lorentz transformation. At any point P, the vector $d\mathbf{r}$ may be projected onto an orthonormal 3-frame: $\mathbf{i} \cdot d\mathbf{r}$, $\mathbf{j} \cdot d\mathbf{r}$, $\mathbf{k} \cdot d\mathbf{r}$. These projections, together with the time interval dt, are then transformed into new values, which are observed in a relatively moving 3-frame. No coordinates are involved with this procedure.

$$Q^0_{0\lambda} = \Gamma^0_{0\lambda} = \frac{1}{2} g^{00} \partial_\lambda g_{00} \tag{7}$$

$$Q^i_{j0} = \Gamma^i_{j0} = \frac{1}{2} g^{in} \partial_0 g_{nj} \tag{8}$$

$$Q^i_{jk} = \Gamma^i_{jk} = \frac{1}{2} g^{in} \left(\partial_k g_{jn} + \partial_j g_{nk} - \partial_n g_{jk} \right) \tag{9}$$

They comprise the formula

$$Q^\mu_{\nu\lambda} = \Gamma^\mu_{\nu\lambda} + g^{\mu\rho} g_{\lambda\eta} Q^\eta_{[\nu\rho]} \tag{10}$$

where

$$Q^\mu_{[\nu\lambda]} \equiv Q^\mu_{\nu\lambda} - Q^\mu_{\lambda\nu} \tag{11}$$

An observer is free to introduce new coordinates $\{x^{\mu'}\}$. The new coordinates must be *at rest* with respect to the old. Displacements (1) will then be invariant, so that the scalar, 3-vector character is preserved. The coordinate transformations are of the form $x^{0'} = x^{0'}(x^0)$ and $x^{i'} = x^{i'}(x^j)$. In particular, $g_{\mu\nu}$ (3) transforms as a tensor

$$g_{0'0'} = \frac{\partial x^0}{\partial x^{0'}} \frac{\partial x^0}{\partial x^{0'}} g_{00} \qquad\qquad g_{i'j'} = \frac{\partial x^m}{\partial x^{i'}} \frac{\partial x^n}{\partial x^{j'}} g_{mn} \tag{12}$$

The non-zero components of $Q^\mu_{[\nu\lambda]}$ (11) are

$$Q^0_{[0i]} = Q^0_{0i} = \frac{1}{2} g^{00} \partial_i g_{00} \qquad\qquad Q^i_{[j0]} = Q^i_{j0} = \frac{1}{2} g^{in} \partial_0 g_{nj} \tag{13}$$

They transform as tensor components

$$Q^{0'}_{0'i'} = \frac{\partial x^n}{\partial x^{i'}} Q^0_{0n} \qquad\qquad Q^{i'}_{j'0'} = \frac{\partial x^{i'}}{\partial x^m} \frac{\partial x^n}{\partial x^{j'}} \frac{\partial x^0}{\partial x^{0'}} Q^m_{n0} \tag{14}$$

This field strength tensor plays a central role in dynamics. It serves to define the gravitational energy tensor

$$T^{(g)}_{\mu\nu} = \frac{c^4}{8\pi G} \left\{ Q^\rho_{[\lambda\mu]} Q^\lambda_{[\rho\nu]} + Q_\mu Q_\nu - \frac{1}{2} g_{\mu\nu} g^{\eta\tau} \left(Q^\rho_{[\lambda\eta]} Q^\lambda_{[\rho\tau]} + Q_\eta Q_\tau \right) \right\} \tag{15}$$

where $Q_\mu = Q^\rho_{[\rho\mu]}$. The coefficient is chosen such that $T^{(g)}_{\mu\nu}$ reduces to the Newtonian stress-energy tensor

$$T^{(g)}_{00} = \frac{1}{8\pi G}(\nabla\psi)^2 \tag{16}$$

$$T^{(g)}_{0i} = 0 \tag{17}$$

$$T^{(g)}_{ij} = \frac{1}{4\pi G}\Big\{\partial_i\psi\,\partial_j\psi - \frac{1}{2}\delta_{ij}(\nabla\psi)^2\Big\} \tag{18}$$

when

$$g_{00} = 1 + \frac{2}{c^2}\psi \tag{19}$$

2. Gravitational energy, momentum, and stress

The Robertson-Walker metric is given by [3]

$$ds^2 = (dx^0)^2 - \frac{R^2(t)}{r_0^2(1 + kr^2/4r_0^2)^2}\left(dr^2 + r^2 d\theta^2 + r^2\sin^2\theta\, d\phi^2\right) \tag{20}$$

where $k = -1, 0$, or $+1$. Since $g_{00} = 1$, all $Q^0_{0i} = 0$. This leaves only energy and stress components in (15)

$$T^{(g)}_{00} = \frac{c^4}{16\pi G}\left(Q^m_{n0}Q^n_{m0} + Q_0Q_0\right) \tag{21}$$

$$T^{(g)}_{0i} = 0 \tag{22}$$

$$T^{(g)}_{ij} = -\frac{c^4}{16\pi G}\,g_{ij}\left(Q^m_{n0}Q^n_{m0} + Q_0Q_0\right) = -g_{ij}T^{(g)}_{00} \tag{23}$$

A straightforward calculation yields

$$Q^m_{n0}Q^n_{m0} = 3\,\frac{\dot{R}^2}{R^2} \qquad\qquad Q_0Q_0 = 9\,\frac{\dot{R}^2}{R^2} \tag{24}$$

where $\dot{R}$ is the derivative with respect to $x^0 = ct$. Therefore, the non-zero components of the mixed energy tensor are

$$T_0^{(g)0} = \frac{3c^4}{4\pi G}\frac{\dot{R}^2}{R^2} \qquad T_i^{(g)j} = -\delta_i^{\ j}\frac{3c^4}{4\pi G}\frac{\dot{R}^2}{R^2} \tag{25}$$

The stresses are compressive and correspond to an equation of state

$$p_g = \rho_g c^2 \tag{26}$$

According to (25), the gravitational energy and pressure are functions of time alone.

3. Field equations

The gravitational field equations are derived by variation of the action

$$\delta \int \left\{\frac{c^4}{16\pi G}\left(g^{\mu\nu}R_{\mu\nu} - 2\Lambda\right) + L^{(m)}\right\}\sqrt{-g}\, d^4x = 0 \tag{27}$$

There are seven field equations, corresponding to the seven variations $\delta g^{\mu\nu} = (\delta g^{00}, \delta g^{ij})$

$$R_\mu^{\ \nu} - \frac{1}{2}\delta_\mu^{\ \nu}R + \Lambda\delta_\mu^{\ \nu} = -\frac{8\pi G}{c^4}T_\mu^{(m)\nu} \tag{28}$$

Components $R_0^{\ i}$ and $T_0^{(m)i}$ do not appear. Substitute the Robertson-Walker metric (20) and the material energy tensor

$$T_\mu^{(m)\nu} = \begin{pmatrix} \rho_m c^2 & & & \\ & -p_m & & 0 \\ & & -p_m & \\ & 0 & & -p_m \end{pmatrix} \tag{29}$$

in order to obtain the Friedmann equations [3]

$$\frac{3\dot{R}^2}{R^2} + \frac{3k}{R^2} - \Lambda = \frac{8\pi G}{c^4}\rho_m c^2 \tag{30}$$

$$\frac{2\ddot{R}}{R} + \frac{\dot{R}^2}{R^2} + \frac{k}{R^2} - \Lambda = -\frac{8\pi G}{c^4}p_m \tag{31}$$

At the present time, the material pressure $p_m \ll \rho_m c^2$. It will be ignored for the remainder of the paper ($p_m = 0$). Equation (31) then becomes

$$\frac{2\ddot{R}}{R} + \frac{\dot{R}^2}{R^2} + \frac{k}{R^2} - \Lambda = 0 \tag{32}$$

Eliminate k and $\dot{R}^2$ from (30) and (32) to find

$$\frac{\ddot{R}}{R} = \frac{\Lambda}{3} - \frac{4\pi G}{3c^2}\rho_m \tag{33}$$

It follows that a positive cosmological constant is required, if $\ddot{R} > 0$.

4. Energy conservation

The differential law of energy and momentum conservation is (appendix)

$$\text{div}\, T_\mu{}^\nu = T_{\mu\ ;\nu}^{\ \nu} + Q^\beta_{[\alpha\mu]} T^\alpha_\beta = 0 \tag{34}$$

where $T_{\mu\ ;\nu}^{\ \nu}$ is the covariant derivative. The total density of energy, momentum, and stress is given by

$$T_\mu{}^\nu = T_\mu^{(g)\nu} + T_\mu^{(m)\nu} + T_\mu^{(\Lambda)\nu} \tag{35}$$

The final term is implied by the cosmological constant in the field equations. It is yet to be determined, but it must have the form $T_\mu^{(\Lambda)\nu} = C\delta_\mu{}^\nu$ where C is a constant. The material equations of motion give

$$T_{\mu\ ;\nu}^{(m)\nu} = 0 \tag{36}$$

so that energy conservation is expressed by

$$\begin{aligned} \text{div}\, T_0{}^\nu &= T_{0\ ;\nu}^{(g)\nu} + T_{0\ ;\nu}^{(\Lambda)\nu} + Q^j_{[i0]}(T^{(g)} + T^{(m)} + T^{(\Lambda)})^i_j \\ &= \partial_0 T_0^{(g)0} + \Gamma^n_{n0} T_0^{(g)0} + \Gamma^n_{n0} T_0^{(\Lambda)0} = 0 \end{aligned} \tag{37}$$

Substitute (25) to find

$$\frac{2\ddot{R}}{R} + \frac{\dot{R}^2}{R^2} + \frac{4\pi G}{c^4} T_0^{(\Lambda)0} = 0 \tag{38}$$

Comparison with (32) shows that $k = 0$ and

$$T_{\mu}^{(\Lambda)\nu} = -\frac{c^4}{4\pi G}\Lambda\delta_{\mu}{}^{\nu} \tag{39}$$

This energy tensor corresponds to an equation of state

$$p_{\Lambda} = -\rho_{\Lambda}c^2 \tag{40}$$

In equation (30), set $k = 0$ and rearrange to find

$$\Lambda = \frac{3\dot{R}^2}{R^2} - \frac{8\pi G}{c^2}\rho_m \tag{41}$$

Substitution into (35) gives

$$\begin{aligned} T_0^{\,0} &= \frac{3c^4}{4\pi G}\frac{\dot{R}^2}{R^2} + \rho_m c^2 - \frac{c^4}{4\pi G}\Lambda \\ &= 3\rho_m c^2 \end{aligned} \tag{42}$$

Therefore, the gravitational field (with the cosmological term) accounts for two-thirds of the energy in the Universe.

5. Concluding remarks

Formula (41) makes possible an evaluation of the constant Λ, in terms of the mass density and the Hubble ratio

$$\frac{H}{c} = \frac{\dot{R}}{R} \tag{43}$$

The experimental value of the Hubble constant is stated to be

$$H_0 = 71\,\frac{\text{km-s}^{-1}}{\text{Mpc}} = 2.3 \times 10^{-18}\ \text{s}^{-1} \tag{44}$$

For historical reasons, the mass density is expressed in terms of a "critical density"

$$\rho_{cr} = \frac{3H_0^2}{8\pi G} = 9.5 \times 10^{-30}\,\text{g-cm}^{-3} \tag{45}$$

The mass density, including the missing mass, is estimated to be

$$\rho_0 = 0.27\,\rho_{cr} = 2.6 \times 10^{-30}\,\text{g-cm}^{-3} \tag{46}$$

Substitution into (41) yields a positive cosmological constant

$$\begin{aligned} \Lambda &= \frac{8\pi G}{c^2}\left(\frac{3H_0^2}{8\pi G} - \rho_0\right) \\ &= \frac{8\pi G}{c^2}(0.73\,\rho_{cr}) = 1.3 \times 10^{-56}\,\text{cm}^{-2} \end{aligned} \tag{47}$$

According to formula (33), the acceleration will be positive, if

$$\rho_m < \frac{c^2}{4\pi G}\,\Lambda = 1.46\,\rho_{cr} = 1.4 \times 10^{-29}\,\text{g-cm}^{-3} \tag{48}$$

Therefore, the acceleration $\ddot{R}$ is now positive and will remain so in the future. It was apparently negative at times in the distant past. The total pressure is

$$p = p_g + p_\Lambda = \frac{3H^2c^2}{4\pi G} + \frac{c^4}{4\pi G}\,\Lambda \tag{49}$$

which is positive.

Appendix: Conservation of energy and momentum

The differential law of conservation is derived by summing the invariant expression $e_\mu T^{\mu\nu}\,dV_\nu$

$$\sum_{\delta R} e_\mu T^{\mu\nu}\,dV_\nu = \left\{e_\mu\,\partial_\nu(\sqrt{-g}\,T^{\mu\nu}) + (\nabla_\nu e_\mu)\sqrt{-g}\,T^{\mu\nu}\right\}d^4x \tag{50}$$

The region δR is closed and infinitesimal, while dV_ν is the vector

$$dV_\nu = \sqrt{-g}\,(dx^1dx^2dx^3,\ dx^0dx^2dx^3,\ \ldots) \tag{51}$$

By definition, $\nabla_\nu e_\mu = e_\lambda Q^\lambda_{\mu\nu}$, so that

$$\sum_{\delta R} e_\mu T^{\mu\nu}\,dV_\nu = e_\mu\left\{\frac{1}{\sqrt{-g}}\partial_\nu(\sqrt{-g}\,T^{\mu\nu}) + Q^\mu_{\lambda\nu}T^{\lambda\nu}\right\}\sqrt{-g}\,d^4x \tag{52}$$

Energy and momentum are conserved, if

$$\mathrm{div}\, T^{\mu\nu} = \frac{1}{\sqrt{-g}}\partial_\nu(\sqrt{-g}\, T^{\mu\nu}) + Q^\mu_{\lambda\nu} T^{\lambda\nu} = 0 \tag{53}$$

The $Q^\mu_{\lambda\nu}$ are related to the Christofel coefficients $\Gamma^\mu_{\lambda\nu}$ by the formula

$$Q^\mu_{\lambda\nu} = \Gamma^\mu_{\lambda\nu} + g^{\mu\alpha} g_{\nu\beta} Q^\beta_{[\lambda\alpha]} \tag{54}$$

Therefore, the divergence may be written in the form

$$\mathrm{div}\, T^{\mu\nu} = T^{\mu\nu}_{\ \ ;\nu} + g^{\mu\alpha} Q^\beta_{[\lambda\alpha]} T_\beta{}^\lambda \tag{55}$$

where $T^{\mu\nu}_{\ \ ;\nu}$ is the (contracted) covariant derivative. Similarly, the divergence of the mixed energy tensor is

$$\mathrm{div}\, T_\mu{}^\nu = T_\mu{}^\nu_{\ \ ;\nu} + Q^\beta_{[\alpha\mu]} T_\beta{}^\alpha \tag{56}$$

References

1. K. Dalton, "Gravitational Waves", *Hadronic J.* 35(2012)209.
2. K. Dalton, "Gravity and the Fermion Mass", *Nuovo Cim.* 124B(2009)1175.
3. R. Adler, M. Bazin, M. Schiffer, *Introduction to General Relativity*, (McGraw-Hill, New York, 2nd ed., 1975) chap. 12, 13.

THE MAGNEHYDROGEN™ IN HYDRONIC CHEMISTRY[1]

Sangesh P. Zodape
Department of Chemistry
Visvesvaraya National Institute of Technology
Nagpur – 440 010, India
sangesh02@gmail.com

Anil A. Bhalekar[2]
Department of Chemistry
R.T.M. Nagpur Univ., Amravati Rd. Campus, Nagpur – 440 033, India
anabha@hotmail.com
And Thunder Fusion Corporation, U.S.A.
And Institute for Theoretical Physics and Advanced Mathematics, Italy

Received February 10, 2014

Abstract

In this paper we have reviewed in brief one of the great achievements accomplished by the Italian-American scientist Ruggero Maria Santilli [1], namely the isochemical model and magnehydrogen that form the subject matter of the hadronic chemistry. This new chemical species of magnehydrogen consist of individual hydrogen atoms bonded together and form stable clusters under a new internal attractive forces originating from the toroidal polarization of orbitals of atomic electrons when placed in strong magnetic fields. These magnecules are used as pollution free fuel and for other applications because there is no cracking involved while using the stored magnetic energy.

Keywords: Hadronic chemistry, Quantum chemistry, Magnecules, MagneHydrogen.

[1]This work was presented at 11th International Conference of Numerical Analysis and Applied Mathematics 2013 (11th ICNAAM 2013), Rhodes, Greece, 21-27 September 2013 and also at the 2013 International Workshop on Hadronic Chemistry, Mathematics and Physics held at the Department of Chemistry, R. T. M. Nagpur University, Nagpur, India during October 21-26, 2013.

[2]Residential Address: 1 - Shantiniketan Colony, Pallavi Apartments, Rana Pratap Nagar, NAGPUR - 440 022, India

Copyright © 2013 by Hadronic Press, Inc., Palm Harbor, FL 34684, USA

1 Introduction

In the late seventeenth century, Issac Newton discovered classical mechanics, the laws of motion of macroscopic objects. In the early twentieth century, physicists found that classical mechanics does not correctly describe the behavior of very small particles. Such particles are described by a set of laws called quantum mechanics [2–5]. Quantum mechanics is the science of motion of micro (atomic and subatomic) particles. Its study is of great importance in chemistry because physicochemical properties of atoms and molecules, their structures, spectral behavior and even reactions may be interpreted in terms of the motion of micro particles like electron and protons [2–5]. The dynamical properties (position, momentum, energy, etc.) of a particle are determined by laws of mechanics. Classical mechanics does not put any restrictions on the values, large or small, of a dynamical property of a particle. However, experimental measurement for atomic and molecular systems shows that an electron moving around the nucleus of an atom has only discrete set of values of energy. The discreteness, termed quantization, cannot be explained on the basis of classical laws of mechanics and to understand new system of mechanics, called quantum chemistry. Quantum chemistry applies quantum mechanics to problems in chemistry. The influence of quantum chemistry is evident in all branches of chemistry. Physical chemist uses quantum mechanics to calculate thermodynamic properties (for examples, entropy, heat capacity) of gases; to interpret molecular spectra, thereby allowing experimental determination of molecular properties (for examples, molecular geometries, dipole moments, barriers to internal rotation, energy differences between conformational isomers); to calculate molecular properties theoretically, to calculate properties of transitions states in chemical reactions, thereby allowing estimation of rate constants; to understand intermolecular forces and deal with bonding in solids. Quantum mechanics has many achievements to its credit, but the purpose here is to restrict attention to those aspects having direct chemical interest and which do not require advanced mathematical knowledge for their appreciation. Despite undeniable achievements, quantum chemical models of molecular structures have the following fundamental insufficiencies [6]:

1. Lack of a sufficiently strong binding force: as it is well known, the average of all coulomb forces among the atoms constituting a molecule is identically null at the semi classical level, thus resulting in the absence of any attractive force at all. Quantum mechanics cannot characterize an attractive force among neutral atoms of a Hydrogen molecule.

2. Quantum mechanics cannot explain why the Hydrogen and water molecules admit only two H-atoms and not three or more.

3. Quantum Chemistry has been unable to achieve an exact representation of molecular binding energies and other molecular characteristics via un-adulterated axiomatic principles. Electric and magnetic dipole and multi-pole moments of Hydrogen and other molecules have not been represented accurately by quantum Chemistry.

4. More accurate representation of binding energies violates basic quantum axioms and physical laws. A number of attempts have been conducted, which do indeed achieve a more accurate representation of binding energies, although such representation is reached via a number of mathematical schemes, such as the so-called Gaussian screening of the Coulomb potentials. These schemes imply a necessary violation of quantum axioms and physical laws.

5. Quantum Chemistry cannot provide a meaningful representation of thermodynamic properties. The missing 2% in the representation of binding energies is misleadingly small, because it corresponds to about 1,000 kcal/mole while an ordinary thermo-dynamical reaction implies an average of 20 kcal/mole. No scientific calculation can be conducted when the error factor of the order of 50.

6. Computer usages in quantum chemical calculations require excessively long period of time. This is notoriously due to the slow convergence of conventional quantum series, a feature that persists to this day despite the availability of powerful computers.

7. Quantum Chemistry predicts that all molecules are ferromagnetic. This inconsistence of the most rigorous disciplines of this century,

Quantum electrodynamics, which establishes that, under an external magnetic field, the orbits of valence electrons must be polarized in such a way to offer magnetic polarity opposite to that of the external field (polarization that generally occurs via the transition from space to toroidal distribution of the orbitals).

As it is well known, the individual atoms of a molecule preserve their individuality in the current model of chemical bonds. As a result, quantum electrodynamics predicts that the valence electrons of the individual atoms of a molecular bond must acquire polarized orbits under an external magnetic field. As a result, Quantum Chemistry predicts that the application of an external magnetic field South-North, to hydrogen H–H, water H–O–H and other molecules implies their acquisition of the net total, opposite polarity North-South, $H_{\uparrow}$–$H_{\uparrow}$, $H_{\uparrow}$–$O_{\uparrow}$–$H_{\uparrow}$, etc. However they are dimagnatic which is in dramatic disagreement with this experimental evidence.

A most important insufficiency is the inability to represent deep mutual penetrations of the wave packets of valence electrons in molecular bonds. The latter interactions are known to be:

- *Nonlinear*: i.e. dependent on powers of the wavefunctions grater than one;
- *Non-integral*: i.e. dependent on integrals over the volume of overlapping, which as such, cannot be reduced to a finite set of isolated points; and
- *Nonpotential*: i.e., consisting of "contact" interactions with consequential "zero range" for which the notion of potential energy has no mathematical or physical sense.
- *Non-Hamiltonian*: - i.e. not representable via a Hamiltonian, thus requiring additional terms, and
- *Non-Unitary*: - i.e. the time evolution violates unitary condition $U \times U' = U' \times U = I$.

Notice that the condition of non-unitarity is necessary otherwise one would fall back fully within the basic axioms of quantum chemistry (under the unitary representations). To overcome the above said insufficiency Italian-American scientist Ruggero Maria Santilli first developed new branches of Lie's mathematics. They are now a days called Santilli' iso-, geno-, hyper- and their isodual mathematics. Based on these branches of mathematics he then augmented Newton's, Hamilton's, Lagrange's and quantum mechanics. They are collectively termed as hadronic mechanics. Hadronic mechanics dealing with the chemical valence is called hadronic chemistry. Hadronic chemistry is applicable at distances of about 1 fm (10^{-13}cm) or less. As it is well known that, all fundamental particles with finite mass have wave packets of the order of 1 fm hence the process of molecular binding is a case of interior interactions of these wave packets [6–8].

Most of the environmental pollution is caused by fossil fuel is due to chunks of un-combusted fuel that may be carcinogenic primarily because consisting of incomplete combustion of fuel. Therefore, Santilli proposed and synthesized a new chemical species called as magnecules by applying a very strong magnetic field [7]. Santilli's magnecules are in gaseous, liquid and solid states and consist of stable clusters composed of conventional molecule or dimers with individuals atoms bonded together by opposing magnetic polarities of toroidal polarization of the orbit of at least the peripheral atomic electrons when exposed to sufficiently strong external magnetic fields, as well as the polarization of the intrinsic magnetic moment of nuclei and electrons [1, 6–8]. A population of magnecules constitutes a chemical species when essentially pure i.e. when molecules or other species are contained in very small percentages in a directly identifiable form.

In this paper we discuss magnehydrogen of hadronic chemistry. This new chemical species of magnehydrogen consist of individual hydrogen atom bonded together and form stable clusters under a new internal attractive forces originating from the toroidal polarization of orbitals of atomic electrons when placed in strong magnetic fields. These magnecules are used as pollution free fuel and for other applications because there is no cracking involved while using the stored magnetic energy.

2 Isochemical model

Santilli and Shillady [9,10] developed an isochemical model of valence bond considering deep overlapping of the wave packets of the bond forming valence electrons and obviously needed to consider interactions at 1 fm level of distances having the property of nonlocal, non-linear, non-potential, non-Hamiltonion type and hence based on non-unitary transformations. The deep overlapped singlet state of electrons is termed by Santilli as *isoelectronium* because the energetic description of it requires his isomathematics [6,8]. Its pictorial representation for hydrogen molecule is depicted in Figures 1 and 2 below. The branch dealing it is known as hadronic chemistry [7].

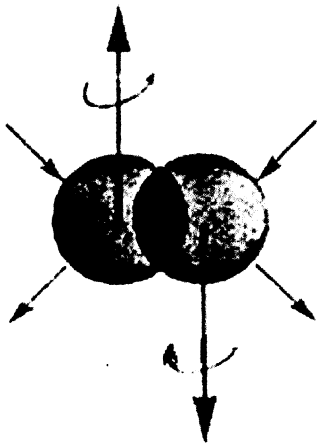

Figure 1: Isoelectronium composed of two valence electrons in singlet coupling.

The main features of the isochemical model are:

1. Exact representation of molecular binding energies from first axiomatic principles without ad hoc adulteration.

2. An explanation for why Hydrogen molecule has only two Hydrogen atoms.

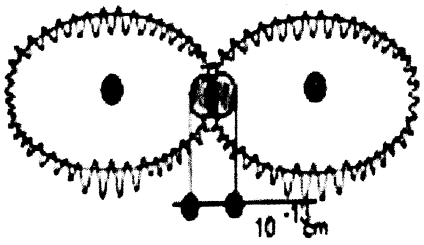

Figure 2: oo-shaped orbit of isoelectronium in hydrogen molecule and dimensions of isoelectronium.

3. Reconstruction of the superposition principle at the isotopic level, thus permitting an axiomatically consistent study of composite systems under non-linear, non-local and non-Hamiltonian interactions. This is achieved by embedding of all non-linear terms in the isotopic element.

4. Reduction of computer time by at least 1000-fold. This is permitted by the fact that the absolute value of the isounit used to compute isoelectronium energy is much bigger than one and, consequently, the isotopic element is much smaller than one, this then turns all slow convergent series into a strong (fast) convergent form [1, 6–8, 11].

This model as shown in Figures 1 and 2 represents motion of isoelectronium in an oo-shaped orbit and this fact lucidly helps in describing the magnecular bonding discussed in next Section.

3 The new novel chemical species of Santilli magnecules

The electromagnecules are clusters generally composed of individual atoms, parts of conventional molecules (radicals) and ordinary molecules under a new internal bond originating from the electric and magnetic polarizations of the orbits of at least some peripheral atomic electrons. Due to dominance of magnetic over electric polarizations as described below electromagnecules

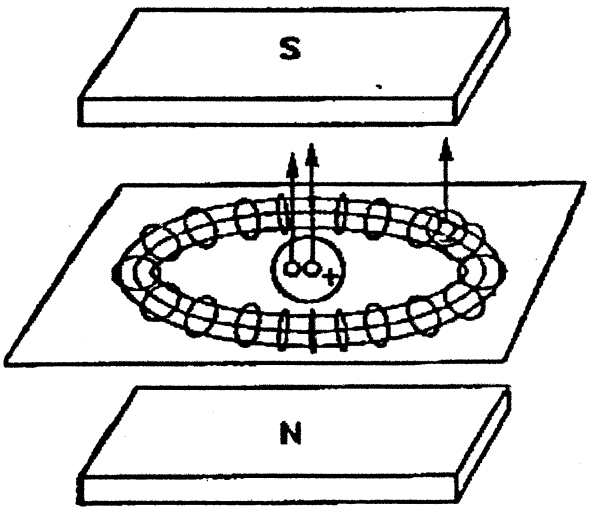

Figure 3: A schematic view of the toroidal polarization of the orbits of peripheral atomic electrons when subjected to a sufficiently strong external magnetic field. Note the additional polarization of the intrinsic magnetic moments of nuclei and of peripheral atomic electron, thus resulting in the availability of three parallel magnetic moments all suitable to create a new bond.

are generally called santilli magnecules. The basic idea underlying the fact is a familiar concept of atomic physics that when an atom is sufficiently strong acquire a toroidal distribution with consequential creation of a new magnetic dipole moment N-S caused by rotation of electron charges by toroidal polarization. Such a dipole gets aligned along the symmetry axes of the toroidal distribution so as to possess the magnetic properties opposite to the external ones shown in Figure 3.

Atoms, radicals or molecules with toroidal polarization of their atomic orbits then bond to each other in chains of opposing polarities N-S-N-S- .resulting in the formation of magnecules shown in Figure 4. Toroidal polarization of atomic orbits creates a magnetic field which is not detectable in the conventional space distribution of the same orbits. Simple calculations

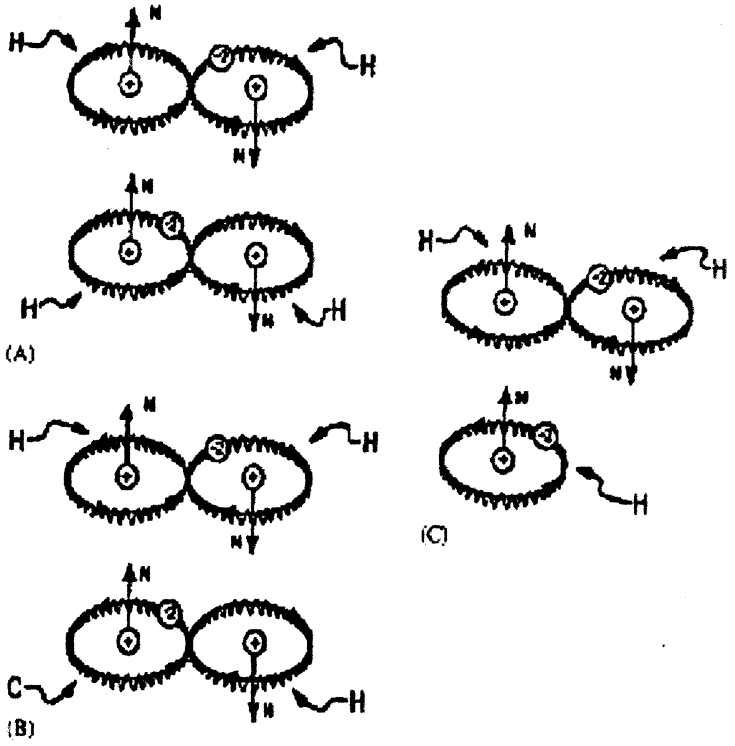

Figure 4: A schematic view of elementary magnecules composed of a diatomic molecule bonded to an individual atom or to another diatomic molecule via opposing magnetic polarities of the toroidal polarization of the orbit of the orbit of individual atoms

show that such a field is strong and 1415 times stronger than the intrinsic magnetic field of the nucleus of hydrogen. Thus toroidal polarization of orbits of peripheral atomic electrons creates a new field sufficiently strong to originate a new chemical species.

An important feature of magnecules is that the magnetic polarization occurs in each individual atom rather than a molecule as a whole. This implies that the new chemical species of magnecules can be formed for all possible gases irrespective of whether they are diamagnetic or paramagnetic.

Thus the primary technological objective of the industrial and scientific production of substances with magnecular structure depends on the control of the space distributions of the orbits of individual atoms, rather than molecules. The new chemical species of magnecules most investigated till date is Santilli magnegas produced by recyclers called hadronic reactors of molecular type. This particular gas is produced by flowing a liquid feedstock (such as fresh water or salt water, antifreeze and oil waste, city and farm sewage, crude oil, etc) through a submerged electric arc between carbon base consumable electrodes.

4 Magnehydrogen

The new species is generically denoted as MH and its individual clusters are denoted MH_n, $n = 2, 3, 4, \cdots$ to specify the number of hydrogen atoms per cluster. Most of the environmental pollution as stated above is caused by fossil fuel is due to chunks of uncombusted fuel that may be carcinogenic primarily because consisting of incomplete combustion of fuel. A population of magnecules constitutes a chemical species when essentially pure i.e. when molecules or other species are contained in very small percentages in a directly identifiable form. To our best understanding, the most plausible interpretation of the new species of MH is that originally presented by Santilli in Ref. [12], namely, a multiple of the specific weight under a high Hydrogen percentage is the evidence of a new clustering of H-atoms which cannot possibly be of valence type due to the evident absence of the valence electrons necessary for a quantitative representation of the clustering of many different atoms. Therefore, Santilli presented the new species of MH as an additional evidence on the existence of the new species of magnecules for Santilli's original presentations (and Ref. [12] for recent experimental confirmations as well as to update the rapidly growing literature in the field). In essence, the new chemical species of magnecules can be defined as clusters of individual atoms (H, O, C, etc.), free radical molecules (HO, CH, etc.) and ordinary molecules (H_2, CO, H_2O, etc.) bonded together by attractive forces between opposing magnetic polarities of toroidal polarizations of atomic orbitals, as well as the polarization of the magnetic

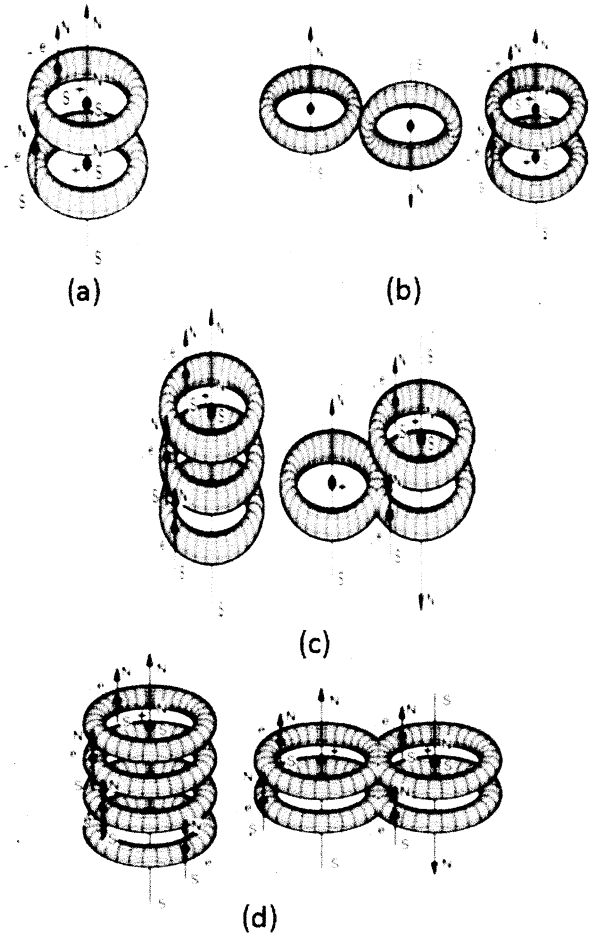

Figure 5: Conceptual rendering of Santilli's magnecules. (a) Magnehydgrogen (MH), two hydrogen atoms forming a magnecule $MH_2(H\times H)$, (b) A cluster MH_2 in MH composed of H–H and H×H molecules, (c) A cluster MH_3 in MH composed of the magnecular species H–H×H and H×H×H, (d) A cluster of MH_4 in MH composed of the magnecular species H×H×H×H and H–H×H–H (not shown species is H–H×H×H).

moments of nuclei and electrons (see a conceptual rendering of MH_n in Fig-

ure 5). Santilli first developed, the so-called PlasmaArcFlow^{TM} Reactor, that converts various liquids into a combustible gaseous fuel known as MagneGas (MG). The gasification is achieved via a submerged DC electric arc between carbon electrodes that, under sufficient powers (of the order of 300 kW or more) is capable of producing at atomic distances the high values of the magnetic field necessary for the polarization of electron orbitals into toroids (estimated as being of the order of 10^{12} Gauss). The conventional covalent bond is shown by '–' and the magnecular bond by $\times$ between the atomic symbols.

5 Practical advantages of Magnehydrogen^{TM}

The chemical analysis given in attachments establish that there are new chemical species whose empirical specific weights are certain multiples of the conventional H_2 molecule. These species have been identified as MH and are composed of hydrogen say up to 99 percent. These new chemical structures have major industrial implications, such as:

1. *Increased energy content*: By recalling that Natural Gas (NG) has an energy content of about 1000 BTU/scf and that conventional H_2 has 300 BTU/scf, it is evident that a species of MH with a specific weight 3.5 times that of H_2 has the same energy content of NG. This eliminates the need for MH to be stored via liquefaction for a number of uses (such as automotive), since MH can be conventionally compressed within the same range of NG.

2. *Increased liquefaction temperature*: It is known that only pure hydrogen liquefies at essentially near about the absolute zero degree temperature, while all other chemical species liquefy at higher temperatures. It is therefore evident that MH liquefies at a temperature higher than 20 degrees Kelvin in a way that is proportional to the increase of specific weight over that of H_2. The advantages of the increased liquefaction temperature of MH over H_2 are evident whenever liquefaction is needed, e.g., for our space or military programs.

3. *Lack of seepage*: Experimental evidence has established that the new Magnecular bonds occur between the Hydrogen atom and other atoms. This implies the creation of layers of Hydrogen atoms on the interior walls of a container at pressure to such an extent the seepage of conventional hydrogen through container walls is avoided. The H_2 seepage causes a serious environmental problem for conventional hydrogen. In fact, once free in our atmosphere, hydrogen quickly rises to our ozone (O_3) layer where we have one of the fastest known chemical reactions, $H_2 + O_3 \rightarrow H_2O + O_2$.
   Hence, hydrogen seepage is one of the major sources of our current depletion of the ozone layer with serious health problems for mankind.

4. In addition to resolving this environmental problem, MH also establishes for the first time the creation of long term storage of Hydrogen. As a result of these features, MagneHydrogen^{TM} has a distinct relevance for NASA, the DOE, and other governmental branches, e.g., because of the capability for the first time for long term storage of Hydrogen, increased energy output, and other advantages. MH is also quite relevant for the petroleum, fertilizer, and other industries because of its faster reactivity as compared to that of conventional Hydrogen.

6 Hypothesis of Magnehydrogen^{TM}

Professor R. M. Santilli had submitted apparently for the first time, the hypothesis that conventional hydrogen H_2 gas can be turned in to a new species with magnecular structure here called Magnehydrogen^{TM} reperesented by MH. As recalled earlier, H_2 is diamagnetic and cannot acquire a total net magnetic polarity. The opposite magnetic moments of the two H atoms explain the diamagnetic character of the hydrogen molecule. The orbit of each H atom acquires a toroidal polarization under sufficiently strong external magnetic field. Intrinsic magnetic moments of nuclei and electrons of H_2 molecule are also polarized. The important aspect for the hypothesis of MagneH^{TM} is that the toroidal polarization of the orbits of the electrons of the individual H atoms, plus the polarization of the intrinsic magnetic mo-

ments of nuclei and electrons in the H_2 molecule is sufficient for the creation of the desired new chemical species with bigger specific weight, because the new bonds can occur between pairs of individual H atoms. The underlying principle here is similar to the magnetization of a ferromagnet, which is also based on the polarization of the orbits of unbounded electrons. The

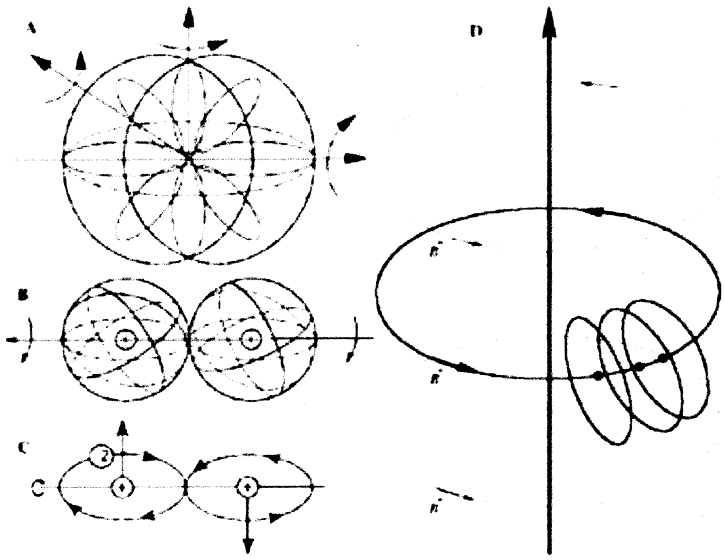

Figure 6: A schematic view of the main mechanism underlying the creation of magnecules, here illustrated for the case of the hydrogen molecule.

main difference is that the creation of MagneH^{TM} requires the application of the same principle to a gaseous, rather than a solid substance. Under the assumption that the original gases are essentially pure, MagneH^{TM} can be schematically represented as below,

$$(H_{\uparrow}\text{–}H_{\downarrow}) \times H,$$
$$(H_{\uparrow}\text{–}H_{\downarrow}) \times (H_{\uparrow}\text{–}H_{\downarrow}),$$
$$(H_{\uparrow}\text{–}H_{\downarrow}) \times (H_{\uparrow}\text{–}H_{\downarrow}) \times H, \quad \text{etc.}$$

It consists in the use of sufficiently strong external magnetic fields which can progressively eliminate all rotations, thus reducing the hydrogen molecule

to a configuration which, at absolute zero degrees temperature, can be assumed to lie in a plane. The planar configuration of the electron orbits then implies the manifestation of their magnetic moment which would be otherwise absent.

The R.H.S of the Figure 6 outlines the geometry of the magnetic field in the immediate vicinity of an electric arc as described in the text for the case of hadronic molecular reactors. The circular configuration of the magnetic field lines around the electric discharge, the tangential nature of the symmetry axis of the magnetic polarization of the hydrogen atoms with respect to said circular magnetic lines, and the consideration of hydrogen atoms at orbital distances from the electric arc 10^{-8}cm, resulting in extremely strong magnetic fields proportional to $(10^{-8})^{-2} \approx 10^{16}$ Gauss, thus being ample sufficient to create the needed polarization. The reason for these results is the intrinsic geometry of the PlasmaArcFlow^{TM} reactor.

7 Industrial production of magnehydrogen

The magnetic polarization of the orbits of peripheral atomic electrons requires extremely strong magnetic fields of the order of billions of Gauss. These values are of simply impossible realization in our laboratories with current technologies, that is, at distances of the order of inches or centimeters. These magnetic fields cannot be realized today even with the best possible superconducting solenoids cooled with the best available cryogenic technology. The only possible, industrially useful method of achieving magnetic fields of the needed very high intensity is that based on direct current (DC) electric arcs with currents of the order of thousands of Amperes (A) when considered at atomic distances, i.e., of the order of 10^{-8}cm. The magnetic field created by a rectilinear conductor with current I at a radial distance r is given by the well known law $B = kI/r$, where $k = 1$ in absolute electromagnetic units.

It then follows that, for currents in the range of 10^3A and distances of the order of the size of atoms $r = 10^{-8}$cm, the intensity of the magnetic field B is of the order of 10^{+13} Oersted, thus being fully sufficient to cause the magnetic polarization of the orbits of peripheral atomic electrons. Atoms

with the toroidal polarization of their orbits find themselves aligned one next to the other with opposing polarities which attract each other, thus forming magnecules. The electric arc decomposes the original molecule, thus permitting the presence of isolated atoms or radicals in the magnecular structure as needed to increase the energy output. In this way, the process transforms the original gas with its conventional molecular structure into a new chemical species consisting of individual atoms, radicals and complete molecules all bonded together by attractive forces among opposite magnetic polarities of the toroidal polarization of the orbits of peripheral atomic electrons.

8 Plasmaarcflow^{TM} reactor

A most efficient industrial production of gas and liquid magnecules or MH is that via the PlasmaArcFlow^{TM} Reactor. This reactor can produce an essentially pure population of gas and liquid Magnecules without appreciable percentages of molecules which is directly detectable in the GC- or LC-MS. Professor Santilli first developed, the so-called PlasmaArcFlow^{TM} Reactor, that converts various liquids into a combustible gaseous fuel known as MagneGas (MG). The gasification is achieved via a submerged DC electric arc between carbon electrodes that, under sufficient powers (of the order of 300 kW or more) is capable of producing at atomic distances the high values of the magnetic field necessary for the polarization of electron orbitals into toroids (estimated as being of the order of 10^{12} Gauss).

The PlasmaArcFlow^{TM} Reactor consists with a submerged DC electric arc between carbon base electrodes to achieve the complete recycled a liquid waste. The arc decomposes the molecules of the liquid into its atomic constituents; ionizes the same; and creates a plasma of mostly ionized H, C and O atoms at about 3500^0K. The flow of the liquid through the arc then continuously removes the plasma from the arc following its formation. Said plasma then cools down in the surrounding liquid, and a number of chemical reactions take place resulting in the formation of magnegas which bubbles to the surface of the liquid where it is collected for industrial or consumer use. Magnecules were directly detectable in the GC- or LC-MS.

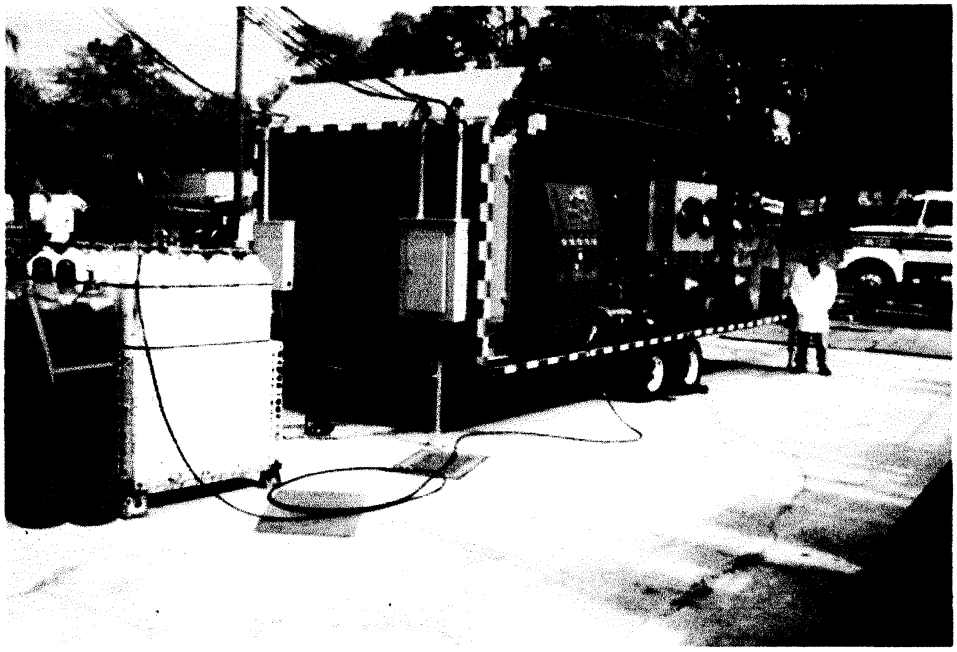

Figure 7: 150 kW Magnegas Refinery producing about 1500 cf of MG per hour with 60% hydrogen content

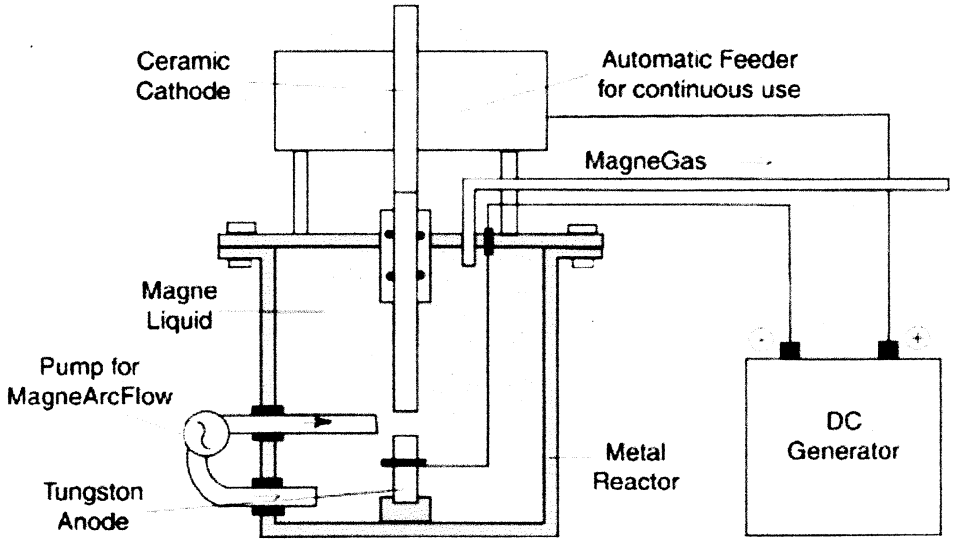

Figure 8: Santilli hadronic refineries, converting liquid waste into a clean burning, cost competitive gaseous fuel with magnecular structure, showing: the pressure metal vessel; the submerged electrodes; the recirculation of the feedstock through the arc; the external AC-DC converter; the external automatic controls of the arc; and the collection of the produced magnecular fuel.

MagneHydrogen is obtained from MG via the use of conventional separation equipment (such as Vacuum Swing Absorption Stations).

9 Energetics of magnecules

The calculation of these polarized magnetic moments at absolute zero degree temperature is elementary [13]. By using rationalized units, the magnetic moment M_{e-orb} of a polarized orbit of one atomic electron is given by the

general quantum mechanical law:

$$M_{e-orb} = \left(\frac{q}{2m}\right) L\,\mu \tag{1}$$

where L is the angular momentum, μ is the rationalized unit of magnetic moment of the electron, $q = -e$ and $m = m_e$. Now on following steps described by Santilli [8] we obtain,

$$\begin{aligned} M_{e-orb} = M_{isoelectronium-orb} &= 1856.959\,\mu, \\ \left(\frac{M_{e-orb}}{M_{p-intr}}\right) &= \frac{1856.959}{1.4107} = 1316.33 \end{aligned} \tag{2}$$

where we have used magnetic moment of proton equal to 1.4107 μ. Thus it shows that the magnetic moment created by the orbiting in a plane of the electron in the hydrogen atom is 1,316 times bigger than the intrinsic magnetic moment of the nucleus, thus being sufficiently strong to create a bond. Say at 10 Tesla of magnetic field the magnecular bond has a strength of about 20-25 kcal/mol [14].

10 Experimental evidence of Magnehydrogen^{TM}

It is important to review the experimental evidence supporting the existence of magnehydrogen. Professor Santilli has very lucidly described problems and their solution in the unambiguous experimental detection of magnecules [13, 15]. Its brief account is given below. The magnegas which was produced by using an antifreeze waste as liquid feedstock was passed through 5Angstrom zeolite filters that essentially consisted of a microporous molecular sieve selecting a gas via molecular size exclusion. The filtered gas was then subjected to the following 3 measurements:

1. The filtered gas was first subjected to analytic measurements by a laboratory via gas chromatography (GC) and other tests confirmed by FTIS. All measurements were normalized, air contamination was removed, and the lower detection limit was identified as being 0.01%.

These GC-MS results are reported in the given Figure 9. From this one can infer that magnehydrogen is composed of 99.2% hydrogen and 0.78% methane, while no carbon monoxide was detected.

2. The average specific weight of this type of MH was measured by two independent laboratories as being 15.06 a.m.u., while conventional pure hydrogen has the specific weight of 2.016 a.m.u., which meant a drastic 7.47 fold increase of the specific weight of conventional hydrogen.

3. The same type of MH that was subjected to the earlier tests was submitted to GC-MS scans via the use of a HP GC 5890 and a HP MS 5972 with operating conditions exclusively set for the detection of magnecules. The GC-MS Scan of a MH Sample is shown in the Figure 9. The results of the third tests are in accordance with the results of GC-FTIS, the GC -MS measurements were expected to show only 2 peaks one for hydrogen at about 2 a.m.u. and that for methane at about 16 a.m.u. but the results confirmed the existence of of a large peak at about 2 a.m.u. for hydrogen ,but no presence of peak at 16a.m.u for methane rather exhibited the presence of a considerable number of additional peaks in considerable percentages accounting to 18 a.m.u. This GC-MS scan established the existence of a magnecular structure for the concerned type of MH studied.

Thus the above mentioned three tests confirm the possibility (and capability) of hydrogen production in multiples of their standard specific weights and consequential increased energy content.

Thus to summarize the the above content with regard to the experimental observations appear to confirm the hypothesis of new forms of hydrogen with magnecular structure capable of producing an industrially significant increase in voltage, power and efficiency of fuel cells.

Professor R. M. Santilli presented [13, 15] theoretical and experimental evidence on the existence of a new species of Hydrogen he called Magne-Hydrogen, which consists of 99% Hydrogen (see Figure 10), yet its specific weight (or, equivalently, molecular weight) is 7.47 times that of conventional Hydrogen.

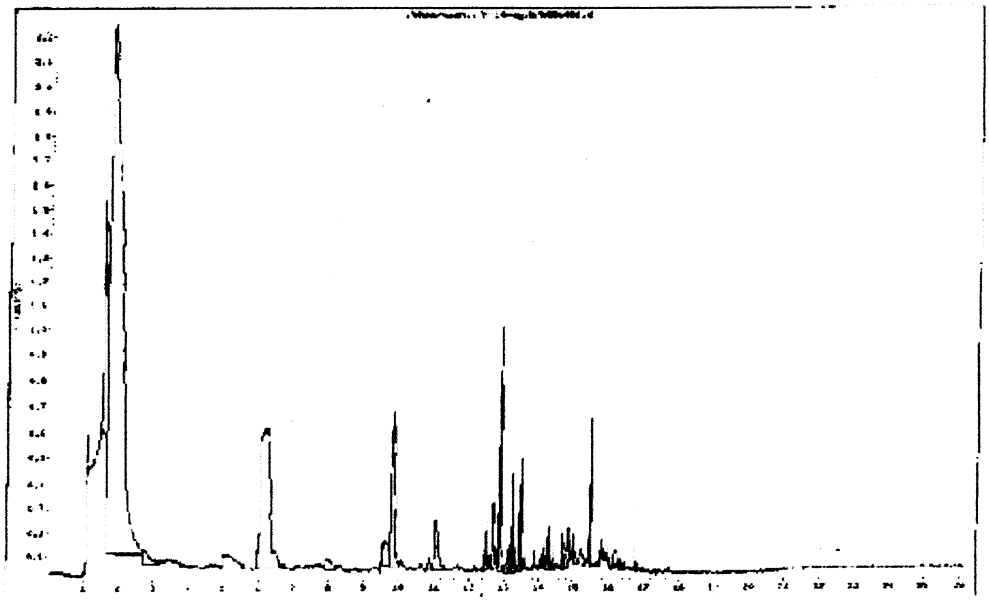

Figure 9: GC-MS Scan of a MH Sample

The second independent certification has also been obtained from the Eprida Laboratories in Atlanta, Georgia, according to which the tested MH has 97.5 percent pure H while its specific weight is 3.8 times that of H_2. Recently Y. Yang and coworkers [16] measured the molecular weight of magnehydrogen using GC-TCD.

The analytical laboratory of MagneGas Corporation is available for independent measurements and verifications by qualified chemists at any mutually agreeable time. Flame temperature of Magnehydrogen is $10{,}500^0$F (see Figure 11), which is more than the double the flame temperature of natural gas or acetylene. This Anomalous flame temperature establishes the high reactivity of the MH contained in MG.

SPECTRALAB
6349 82nd Avenue North
Pinellas Park, Florida 33781
Phone: (727) 545-2297 • Fax (727) 547-8024

Component	Gas
Hydrogen	99.2
Carbon monoxide	None detected
Carbon dioxide	None detected
Methane	0.78
Ethane	None detected
Ethene (ethylene)	None detected
Ethyne (acetylene)	None detected

Figure 10: Elemental analysis of MagneHydrogen

DR. ROBERT R. ALFANO

INSTITUTE
FOR
ULTRAFAST SPECTROSCOPY AND LASERS

THE CITY COLLEGE
OF THE CITY UNIVERSITY OF NEW YORK

March 5, 2012

To: **Magnegas**

From: **Robert R. Alfano**

Subject: **Magnegas project "Temperature of Magnegas Flames" results summary**

The following is a summary of Magnegas flame temperature measurements and it's comparison to Blackbody Distribution
Temperature was calculated using Wien's Law $T=2.9\times10^{6}/\lambda max$

1-**Temperature of Magnegas Flame from crude oil+Oxygen** 3mm from base and fit with Blackbody. The peak wavelength of the flame is $\lambda max=475nm$ The corresponding temperature is **T= 6,132 Kelvin (10,578 Fahrenheit; 5,859 Celsius).**

2-**Temperature of Magnegas Flame from crude oil+Oxygen when cutting metal:** at 3mm above the surface of metal while cutting it (approximately 2mm from base of flame). And fit with Blackbody. The peak wavelength of the flame at $\lambda max=739nm$ The corresponding temperature is **T=3,920 Kelvin (6,597 Fahrenheit; 3,647 Celsius).**

3-**Temperature of Magnegas Flame from antifreeze+ Oxygen** 3mm from base and fit with Blackbody. The peak wavelength of the flame at $\lambda max=476nm$ The corresponding temperature is **T= 6,092 Kelvin (10,506 Fahrenheit; 5,819 Celsius).**

4-**Temperature of Magnegas Flame from antifreeze+ Oxygen when cutting metal:** at 3mm above the surface of metal while cutting it (approximately 2mm from base of flame), and fit with Blackbody. The peak wavelength of the flame at $\lambda max=735nm$ The corresponding temperature is **T= 3,943 Kelvin (6,638 Fahrenheit; 3,670 Celsius).**

The flame spectral intensity distribution has a non Blackbody Distribution form.
Additional details are provided in a separate report.
The measurements were performed by Hani Abumarzouk and Yuri Budansky on February 15th-18th, 2012.

Figure 11: MagneGas Flame Temperature Report

11 Applications of Magnehydrogen^{TM}

The use of MagneHydrogen^{TM} (MH) as fuel for internal combustion engines is significant. Since hydrogen is the fuel with the lowest specific weight, often it has to be liquified to achieve sufficient range, as it is the case for the hydrogen car constructed by the German automaker BMW. In turn, liquefaction of hydrogen, its transportation and maintenance in the liquified state imply additional dramatic costs of the order of hundreds of times the cost of natural gas. For instance, the gasoline gallon equivalent of hydrogen is given by 366 standard cubic foot i.e scf (because one gallon of gasoline has about 110,000 BTU while one scf of hydrogen has 300 BTU). It then follows that the equivalent of 20 gallon of gasoline would require 7,300 scf of hydrogen. At the gaseous state, such a volume would require so much space not to be practical in a car at currently permitted pressures, thus requiring liquefaction. Liquefaction is completely eliminated by MagneHydrogen^{TM} because, due to its specific weight, the equivalent of 20 gallon of gasoline are given by about 1,000 scf of MH, namely, a volume that can be stored in the gaseous state at 3,600 psi in a small tank in the trunk of any car. Another basic feature to be subjected to experimental verifcation is that the combustion of MagneH^{TM} releases more energy than the combustion of conventional H gases. It then follows that the use for internal combustion engines of MagneH^{TM} with a sufficiently high specific weight is expected to eliminate liquefaction, yield essentially the same power as that produced with gasoline, and produce a dramatic decrease of operating costs. Moreover, the use of MagneH^{TM} in fuel cells is expected to yield a significant increase of voltage, power and efficiency and the use of liquified MagneH^{TM} as fuels for rocket propulsion is expected to permit an increase of the payload, or a decrease of the boosters weight with the same payload.

12 Concluding remarks

In preceding Sections, we have described in brief the physical and mathematical background of Santilli's covering of quantum chemistry known as hadronic chemistry. The aspects those covered in brief herein are the iso-

chemical model of valence bond formation, basics of magnecular interactions, some aspects of magnehydrogen and its energetics. The magnecules are pollution free fuels because it provides stored magnetic energy without molecular cracking. Despite of the uneasiness caused by the novelty of Santilli magnecules, the vast experimental evidence supports the following results:

1. The existence of a form of hydrogen with about seven times of the specific weight of hydrogen eliminates the need and the major boulder of liquefaction of molecular hydrogen in automotive uses, without a compromise in the power output essentially similar to gasoline and being cost competitive with respect to fossil fuel when produced in large scale. This new species of hydrogen (MagneH^{TM})is derived by filtering, cryogenic separation nor other means from the new combustible fuel called Santilli MagneGas.

2. The industrial capability of conversion of conventional hydrogen and oxygen into new species with higher atomic weight and energy content for the use in fuel cells with increased voltage, power and efficiency.

3. The existence of a new chemical species whose bonding force is not of valence type, which has been interpreted by this author as being due to the only fields available in a molecular structure, the electric and magnetic fields, and called electromagnecules in general, the name Santilli magnecules being used to denote the dominance of magnetic over electric effects.

4. The existence of a form of hydrogen with about seven times the atomic weight of molecular hydrogen which eliminates the need for liquefaction in automotive use, while having a power output essentially similar to that of gasoline, and being cost competitive with respect to fossil fuel when produced in large scale. This is the new species of hydrogen, called by this author MagneH^{TM}.

5. The existence of new forms of liquid hydrogen and oxygen for rocket propulsion with increased trust, and consequential increased payload or decreased boosters weight with the same payload.

6. The experimental evidence of dramatic departures from quantum chemistry in support of the covering hadronic chemistry.

Acknowledgments

The authors are grateful to Professor R. M. Santilli, Professor C. Corda and Professor R. Anderson for all encouragements to pursue this work. Thanks are due to honourable anonymous referee for constructive suggestions. Authors also acknowledge discussions and help of Dr. V. M. Tangde and Dr. S. S. Dhondge. The authors express their gratitude for the financial support to The R. M. Santilli Foundation.

References

[1] I. Gandzha and J. Kadeisvili, *New Sciences for a New Era.* Sankata Printing Press, Kathmandu, Nepal, 2011.

[2] H. Eyring, J. Walter, and G. E. Kimball, *Quantum Chemistry.* New York: John Wiley, first ed., 1944.

[3] W. Kauzmann, *Quantum Chemistry. An Introduction.* New York: Academic Press, first ed., 1957.

[4] R. K. Prasad, *Quantum Chemistry.* New Delhi: New Age International, 2006.

[5] I. N. Levine, *Quantum Chemistry.* New Jersey: Prentice Hall, sixth ed., August 2008.

[6] R. M. Santilli, *Foundations of Hadronic Chemistry. With Applications to New Clean Energies and Fuels.* P. O. Box 17, 3300 AA Dordrecht, The Netherlands: Kluwer Academic Publishers, Dordrecht/Boston/London, 2001.

[7] R. M. Santilli, *Hadronic Mathematics, Mechanics and Chemistry. Vol. V: Experimental Verifications, Theoretical Advances and Industrial Applications in Chemistry.* Palm Harbor, FL 34682, U.S.A.: International Academic Press, 2008.

[8] R. M. Santilli, *Hadronic Mathematics, Mechanics and Chemistry. Vol. III: Iso-, Geno-, Hyper-Formulations for Matter and Their Isoduals for Antimatter.* Palm Harbor, FL 34682, U.S.A.: International Academic Press, 2008.

[9] R. M. Santilli and D. D. Shillady, "A new isochemical model of the hydrogen molecule," *Intern. J. Hydrogen Energy*, vol. 24, pp. 943 – 956, 1999.

[10] R. M. Santilli and D. D. Shillady, "A new isochemical model of the water molecule," *Intern. J. Hydrogen Energy*, vol. 25, pp. 173 – 183, 2000.

[11] V. M. Tangde, "Advances in hadronic chemistry and its applications," *CACAA*, vol. 2, pp. 365 – 391, December 2013.

[12] Y. Yang, J. Kadeisvili, and S. Marton, "Experimental confirmations of the new chemical species of santilli magnehydrogen," *Int. J. Hydrogen Energy*, vol. 38, pp. 5003 – 5008, 2013.

[13] R. M. Santilli, "Theoretical prediction and experimental verifications of the new chemical species of magnecules," *Hadronic J.*, vol. 21, pp. 789 – 894, 1998.

[14] R. M. Santilli and A. Aringazin, "Structure and combustion of magnegases^{TM}," *Hadronic J.*, vol. 27, pp. 299 – 330, 2004.

[15] R. M. Santilli, *The New Fuels With Magnecular Structure.* Palm Harbor, USA: International Academic Press, first ed., January 2005.

[16] Y. Yang, J. V. Kadeisvilli, and S. Marton, "Experimental confirmation of the new chemical species of santilli magnehydrogen," *Intern. J. Hydrogen Energy*, vol. 38, pp. 5003 – 5008, 2013.

HADRONIC JOURNAL 36, 593 - 623 (2013)

INTRODUCTION TO THE NEW SPECIES OF THE MAGNECULES OF HADRONIC CHEMISTRY[1]

Chandrashekhar P. Pandhurnekar
Department of Applied Chemistry
Ramdeobaba College of Engineering and Management
Nagpur – 440 013, India
pandhurnekarcp@rkned.edu

Received February 28, 2014

Abstract

In memoir [1] of the Italian-American physicist, R. M. Santilli presented for the first time, the theoretical and experimental evidence on the existence of the new chemical species of magnecules defined as clusters of individual atoms (H; O; C; etc.), diatomic free radicals (HO; CH; etc.) and ordinary molecules (H_2; CO; H_2O; etc.) bonded together by attractive forces. This new chemical species is based on a bond much weaker than that of valance bond so as to permit full combustion. Santilli in 2001 released monograph [2], wherein the details of the first industrial realization of the new species of magnecules consisting of the gaseous fuel produced and sold worldwide under the trade name of MagneGas^{TM} (MG) by the U. S. publicly traded company Magnegas Corporation were presented. In monograph [3] of 2005, R. M. Santilli presented an update on the first industrial application of the new species of magnecules via the combustible gas MagneGas indicated earlier, as well as an update of the additional industrial applications for MH, MO, and HHO. In present communication, different topics with particular reference to: origin and adverse effects of increasingly cataclysmic climatic events happening on our planet, hypothesis of Santilli's Magnecules, Numerical value of Magnecular bond and its verification by M. G. Kucherenko, A. K. Aringazin and Yang *et al.*, and unambiguous detection and experimental verification of magnecular structure, have been summarized.

Keywords: Magnecule, Hadronic Chemistry, Cataclysmic Climatic Events.

[1]This work was presented at the 2013 International Workshop on Hadronic Chemistry, Mathematics and Physics held at the Department of Chemistry, R. T. M. Nagpur University, Nagpur, India during October 21-26, 2013.

Copyright © 2013 by Hadronic Press, Inc., Palm Harbor, FL 34684, USA

1 Origin and Adverse Effects of the Increasing Cataclysmic Events

According to official data by recent U.S. Department of Energy (DOE) release [4], about 74 millions barrels of fossil oil, corresponding to about four billions gallons of gasoline, are consumed in our planet per day in an estimated number of half a billion cars, one million trucks, one hundred thousand planes, plus industrial, agricultural, and military uses.

The extremely serious environmental problems caused by the disproportionate combustion of fossil fuels is as follows: [3, 5]

1. The combustion of fossil fuels releases in our atmosphere about sixty millions metric of tons carbon dioxide CO_2 per day that are responsible for the first large environmental problem known as "global warning" or "green house effect." Of these only 30 millions metric tons are estimated to be recycled by our ever decreasing forests.

2. The combustion of fossil fuels causes the permanent removal from our atmosphere of about 21 millions metric tons of breathable oxygen per day, a second, extremely serious environmental problem known as "oxygen depletion".

3. The combustion of fossil fuels releases in our atmosphere about fifteen millions metric tons of carcinogenic and toxic substances per day. This third, equally serious environmental problems is "atmospheric pollution", while in reality it refers to the primary source of the widespread increase of cancer in our societies.

Increasingly cataclysmic climactic events are occurring in the almost every part of the world. Increasingly cataclysmic climactic events are expected in the years ahead also. If we deeply look at the environmental issues which are adversely affecting our planet is not due to fossil fuel but prohibition to achieve complete combustion due to strong valance bond structure of molecules [3]. Thus, indeed this is basic need for clean fuel for the survival of mankind.

Whenever facing the ever increasing cataclysmic climactic events caused by fossil fuel combustion, a rather widespread belief is that the solution

already exists and it is given by hydrogen for the large scale fuel uses of the future because hydrogen is believed to be "the cleanest fuel available to mankind". Hydrogen is indeed an environmentally acceptable fuel, but only when Hydrogen is produced via the electrolytic separation of water; The electricity used for electrolysis originates from clean and renewable energy sources, such as those of hydric, solar or wind nature; and the oxygen produced by the electrolytic process is freely released in the environment so that the subsequent hydrogen combustion leaves unchanged the existing oxygen content of our atmosphere. However, the reality in the production and use of hydrogen is dramatically different than the above ideal conditions. In fact, hydrogen is today produced in its greatest percentage via reformation processes of fossil fuels such as methane CH_4, via the use of highly polluting electric power plants, and no oxygen is released in the atmosphere during production. Santilli explained via simple calculations that the current methods of hydrogen production, transportation and use release in the atmosphere carcinogenic substances, green house gases and other contaminants that are at least twenty times bigger than the contaminants releases by the gasoline production and combustion in contemporary cars with efficient catalytic converters [6].

Further widespread misrepresentations exist for ethanol, natural gas, biogases, and other conventional fuels, that is, fuels possessing the conventional molecular structure, because generally presented as cleaner than gasoline. In effect, ethanol combustion exhaust is the most carcinogenic among all fuels, the pollution caused by biogases is truly alarming, and the same occur for all remaining available conventional fuels. In addition, ethanol, biogases and other fuels of agricultural origin leave large carbon deposits on spark plugs, piston rings and other component, by decreasing considerably the life of the engines. Renewable sources of electricity, even though manifestly valuable, are so minute with respect to the enormity of the demand for fuel that cannot be taken into serious consideration. Nuclear power plants also cannot be taken into serious consideration until governments finally provide serious financial support for basic research on the stimulated decay of radioactive nuclear waste by nuclear power plants themselves, rather than the currently preferred "storage" of nuclear waste in depositories nobody wants to have near-by.

The most basic need for the very survival of our contemporary societies is as summarized below: [7]

1. Develop "new" processes for the nonpolluting, large scale production of electricity, that is, processes beyond the now exhausted predictive capacities of conventional doctrines.

2. Build a large number of large reactors for the large scale removal and recycling of the excess CO_2 in our atmosphere.

3. Develop "new" fuels that are not derivable from crude oil and are capable of achieving full combustion, that is, fuels structurally different than all known fuels due to their highly polluting character.

2 Magnecules: Introduction

The origin of the alarming environmental problems increasingly afflicting our planet are not due to fossil fuels per se, but rather to the strength of their conventional valence bond, since that strength has prohibited the achievement of full combustion during the past one hundred years of efforts. In view of the above occurrence, this author proposed in Ref. [1] of 1998 a new chemical species that, by central assumption, is based on a bond much weaker than that of valence bonds so as to permit full combustion. The name of magnecules is in order to distinguish the species from the conventional "molecules" and the new species is known today as Santilli's "magnecules". In 1998, R. M. Santilli submitted in paper [1] (and then studied in details in monograph [2]) the hypothesis of a new type of stable clusters composed of molecules, dimers and atoms under a new, clearly identified, attractive internal bond which permits their industrial and practical use. The new clusters were called magnecules (patented and International patents pending [8]) because of the dominance of magnetic effects in their formation, as well as for pragmatic needs of differentiations with the ordinary molecules.

Magnecules are also called:

1. elementary when only composed of two molecules; If the conventional valence bond is denoted with the symbol "–" and the new magnetic

bond with the symbol "×", examples of elementary magnecules in gases and liquids are respectively given by

$$\{\text{H–H}\} \times \{\text{H–H}\}, \{\text{O–O}\} \times \{\text{O–C–O}\}, \ etc \tag{1}$$

$$\{\text{C}_{15}\text{–H}_{20}\text{–O}\} \times \{\text{C}_{15}\text{–H}_{20}\text{–O}\}, \ etc \tag{2}$$

2. magneplexes when entirely composed of several identical molecules; examples of magneplexes in gases and liquids are respectively given by

$$\{\text{H–H}\} \times \{\text{H–H}\} \times \{\text{H–H}\}....., \ etc \tag{3}$$

$$\{\text{H–O–H}\} \times \{\text{H–O–H}\} \times \{\text{H–O–H}\}....., \ etc \tag{4}$$

3. magneclusters when composed of several different molecules and examples of magneclusters are given by

$$\{\text{H–H}\} \times \{\text{C–O}\} \times \{\text{O–C–O}\} \times \{\text{C=O}\}....., \ etc \tag{5}$$

$$\{\text{C}_{13}\text{–H}_{18}\text{–O}\} \times \{\text{C}_{14}\text{–H}_{12}\text{–O}_3\} \times \{\text{C}_{15}\text{–H}_{20}\text{–O}\}....., \ etc \tag{6}$$

A generic representation of a gas magnecules requires the presence of individual atoms and dimers, such as:

$$\{\text{H–H}\} \times \{\text{C–O}\} \times \{\text{C=O}\} \times \{\text{H–O–H}\} \times \{\text{C}\}....., \ etc \tag{7}$$

One of the most important features of magnecules is their anomalous release of energy in thermochemical reactions, in view of its evident importance for the industrial development of new clean fuels such as magnegas. This feature is crucially dependent on the existence within the magnecules of individual atoms, such as H, C and O, and/or individual diatomic free radicals, such as H–O and H–C. In fact, at the breakdown of the magnecules due to combustion, these individual atoms and diatomic free radicals couple themselves into conventional molecules via known exothermic reactions such as

$$\begin{aligned} \text{H} + \text{H} &\longrightarrow \text{H}_2 + 105 \text{ kcal/mol}, \\ \text{C} + \text{O} &\longrightarrow \text{CO} + 255 \text{ kcal/mol}, \\ \text{H–O} + \text{H} &\longrightarrow \text{H}_2\text{O} + 28 \text{ kcal/mol, etc.}, \end{aligned} \tag{8}$$

with consequential release during combustion of a large amount of energy that does not exist in fuels with a conventional molecular structure. Finally, magnecules are called:

1. *isomagnecules* when having all single-valued characteristics and being reversible in time, namely, when they are characterized by *isochemistry*;

2. *genomagnecules* when having all single-valued characteristics and being irreversible in time, namely, when they are characterized by *genochemistry*; and

3. *hypermagnecules* when having at least one multi-valued characteristic and being irreversible in time, namely, when they are characterized by *hyperchemistry.*

3 Production and Hypothesis of Magnegases

The primary origin of pollutants contained in fossil fuel exhaust is the valence bond that is so strong as to prevent full combustion. Consequently, Santilli set his research goal to search for a new way of bonding together into stable clusters the same atoms composing fossil fuels under the following:

- CONDITION 1: The new bond should be weaker than the valence bond as a necessary condition to decrease pollutants;

- CONDITION 2: The new weaker bond should allow the formation of clusters that are stable at industrially used storage values of temperature and pressure, e.g., those for methane; and

- CONDITION 3: The new, weaker and stable bond should decompose itself at the combustion temperature to optimize the energy released by the combustion.

In memoir [1] of 1998, the Italian-American physicist R. M. Santilli presented theoretical and experimental evidence on the existence of the new chemical species of "magnecules" defined as clusters of individual atoms (H;

O; C, etc.), diatomic free radicals (HO; CH; etc.) and ordinary molecules (H_2; CO; H_2O, etc.) bonded together by attractive forces between opposing magnetic polarities of toroidal polarizations of atomic orbitals, as well as the polarization of the magnetic moments of nuclei and electrons (see Fig.1). Santilli's hypothesis of a new type of stable clusters under a new, clearly identified, attractive internal bond which permits their industrial and practical use.

To understand the difficulties facing the conception and production of a new chemical species, one should recall that atoms have a spherical distribution of their orbitals, thus normally exhibiting the sole possibility of a valence bond. Hence, *Santilli had to create a new force field in atoms as a condition to achieve a new chemical species.*

The answer originated from Condition 3 that suggested the use of magnetic forces since all magnetic effect disappear at a given temperature (called the Curie Temperature). Therefore, Santilli argued that, in the event a new bond could be based on magnetic fields, all Conditions 1, 2, 3 would be verified because:

- magnetic bonds are known to be weaker than valence bonds;
- they are expected to be stable under ambient conditions;
- and they are expected to decompose themselves at the combustion temperature that was assumed as being the Curie temperature of the new bond.

Santilli argued that the possible control of the distribution of atomic orbitals, from their conventional spherical form to a toroidal form would indeed create a magnetic dipole North-South along the symmetry axis, thus creating the needed new field in atoms that normally have none.

A huge difficulty then emerged because it is known in the technical literature that the control of the orbitals of atomic electrons requires extremely strong magnetic fields of the order of 10^{10} Gauss or more, namely, magnetic fields at least 1000 times stronger then the biggest magnetic field available at the U. S. Large Magnet Laboratory in Tallahassee, Florida.

By again proceeding in his analytic way, Santilli conducted a systematic search of engineering means for exposing atomic orbitals to the needed very

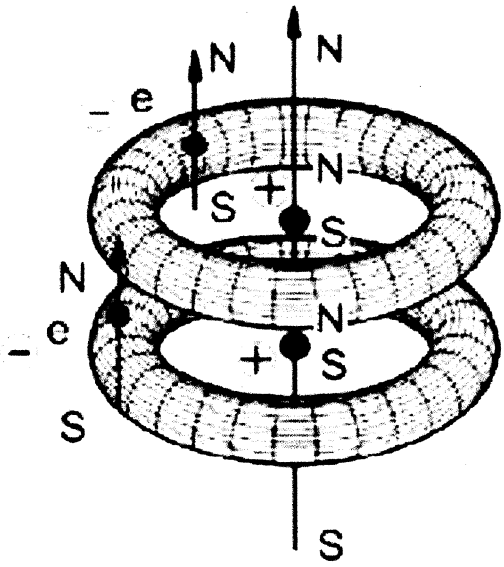

Figure 1: Conceptual rendering of Santilli's magnecules, here referred to the species H×H assumed at absolute zero degree temperature. Note that: the toroidal polarization of the electron orbitals creates a new magnetic field not existing for spherical distributions; all magnetic forces between said toroids as well as between the magnetic polarities of nuclei and electrons are attractive; and the repulsive forces between nuclear and electron charges can be averaged to zero in first approximation since the atoms are individually neutral, thus resulting in the dominance of a new non-valence bond Santilli calls "magnecular". Note that the new bond can be also called "axial" (or "perpendicular") in the sense that the magnetic force exists along the symmetry axis of the toroid (or the magnetic force is perpendicular to the symmetry plane of the toroid).

strong magnetic fields, and concluded his studies with the selection of DC electric arcs sub-merged within a fluid (a gas or a liquid). In fact, in this case, the magnetic field M follows the known law (eq. 9)

$$M = \frac{ka}{r}, \tag{9}$$

where A represents the number of Amperes of the arc, r the distance from the arc and k a constant depending of the selected units whose value is here irrelevant. Therefore, at atomic distances from the arc, that are of the order of 10^{-8} cm, and for currents of the order of 10^3 A, the magnetic field M is indeed of the desired order of 10^{10} Gauss (See Fig.2). In his memoir [1], Santilli also provided entirely new concept i.e. Plasma ArcFlow Reactor^{TM} (Patented and International Patent Pending), for the generation of this new gaseous species with the magnecular chemical structure. Santilli suggested the use of a DC electric arc between graphite electrodes submerged within a liquid (such as distilled water). As it is well known, the arc decomposes the liquid molecules into mostly ionized atoms by creating between the tip of the electrodes a plasma composed of H; C, and O individual atoms, CH and OH diatomic free radicals, and ordinary molecules such as CO, H_2O and others [2].

Magnecules are characterized by, or can be identified via the following main features [3, 9]:

1. Magnecules preliminary exist at large atomic weights;

2. Magnecules are characterized by large peaks in macroscopic percentage in mass spectroscopy;

3. Said peaks do not show detectable infrared signature for gases and no ultraviolet signature for liquids;

4. Magnecules can be formed by molecules of liquids which are necessarily solvable in each other;

5. A gas with magnecular structure does not follow the perfect gas laws;

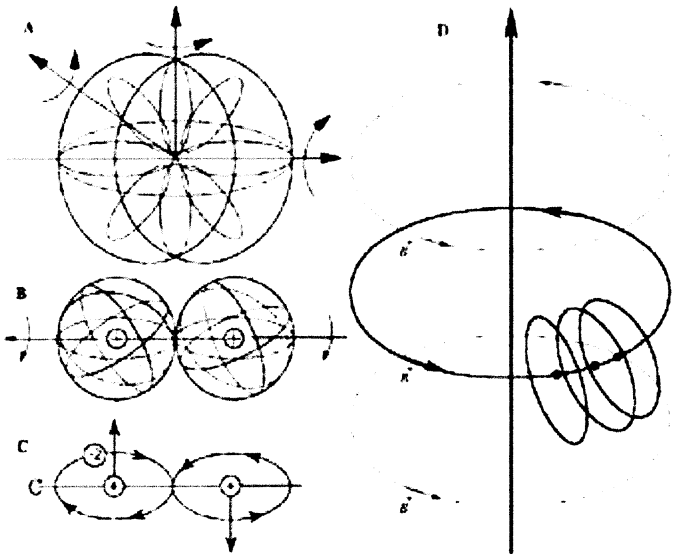

Figure 2: A schematic view of the main mechanism underlying the creation of magnecules, here illustrated for the case of the hydrogen molecule. It consists in the use of sufficiently strong external magnetic fields which can progressively eliminate all rotations, thus reducing the hydrogen molecule to a configuration which, at absolute zero degrees temperature, can be assumed to lie in a plane. The planar configuration of the electron orbits then implies the manifestation of their magnetic moment which would be otherwise absent. The r.h.s. of the above picture outlines the geometry of the magnetic field in the immediate vicinity of an electric arc as described in the text for the case of hadronic molecular reactors. Note the circular configuration of the magnetic field lines around the electric discharge, the tangential nature of the symmetry axis of the magnetic polarization of the hydrogen atoms with respect to said circular magnetic lines, and the consideration of hydrogen atoms at orbital distances from the electric arc 10^{-8} cm, resulting in extremely strong magnetic fields proportional to $(10^{-8})^{-2}$ $= 10^{16}$ Gauss, thus being ample sufficient to create the needed polarization.

6. Substances with magnecular structure have anamolous physical characteristics, such as anamolous specific density, viscosity, surface tension, etc.

7. Magnecules release in thermochemical more energy than that released by the same reactions among unpolarized molecular constituents;

8. All the above characteristics disappear when the Magnecules are brought to a sufficiently high temperature, which varies from species to species, called Curie Magnecular Temperature.

4 Numerical Value of Magnecular Bonds

In the previous section, it has been noted that if sufficiently strong external magnetic field is applied, it polarizes the orbits of peripheral atomic electrons which does not exist in a conventional spherical distribution. It is evident that the polarized magnetic moments at ordinary temperature are smaller than those at absolute zero degrees temperature. This can be explained as, at room temperature, orbit in a plane is not perfectly polarized. But in the case of magnecular structure, polarization occurs in a toroid, as shown in Fig.3, whose sectional area depend upon the intensity of the external field [10].

As an illustrative example, under an external magnetic field of 10 Tesla, an isolated hydrogen atom has a total magnetic field of the following order of magnitude:

$$M_{H-tot} = M_{p-int} + M_{e-int} + M_{e-orb} \approx 3000\mu, \tag{10}$$

while the same hydrogen atom under the same conditions, when a component of a hydrogen molecule has the smaller value

$$M_{H-tot} = M_{p-int} + M_{e-int} \approx 1500\mu, \tag{11}$$

This is very important for the study of Magnecules and their utilization in various industrial applications. An accurate verification of the above calculations was conducted by M. G. Kucherenko and A. K. Aringazin [11,

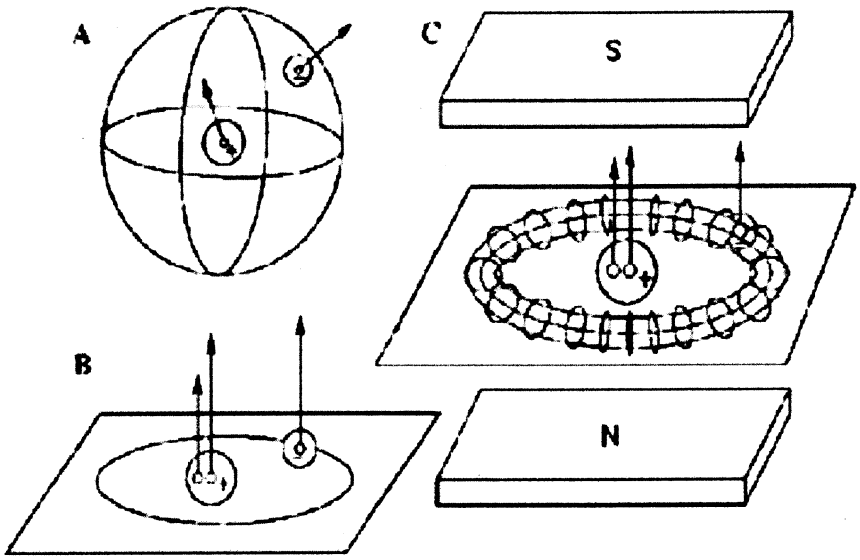

Figure 3: A schematic view of the force fields existing in the hydrogen atom. Fig.3.A depicts an isolated hydrogen atom in its conventional spherical configuration when at absolute zero degree temperature, in which the sole force fields are given by the electric charges of the electron and of the proton, as well as by the intrinsic magnetic moments of the same particles. Fig.3.B depicts the same hydrogen atom in which the orbit of the peripheral electron is polarized into a plane. In this case there is the emergence of a fifth field, the magnetic dipole moment caused by the rotation of the electron in its planar orbit. Fig.3.C depicts the same hydrogen atom under an external magnetic field which causes the transition from the spherical distribution of the peripheral electron as in Fig.3.A to a new distribution with the same cylindrical symmetry as that of the external field, and such to offer magnetic polarities opposite to the external ones. In the latter case, the polarization generally occurs within a toroid, and reaches the perfectly planar configuration of Fig.3.B only at absolute zero degree temperature or under extremely strong magnetic fields.

12], who obtained via the use of alternative models, $M_{e-orb}/\ M_{e-intr}$ equal to 1,315. Recently, A. K. Aringazin study confirms the toroidal configuration of the electron orbit.

It was concluded that under an external, strong, homogeneous, and constant magnetic fields of the order of 10^{13} Gauss $= 10^7$ Tesla, the solutions of Schrodinger equation of the type,

$$\left((p-(e/c)\,A)^2/2m+V\right)|\psi'\rangle = E'|\psi'\rangle \tag{12}$$

imply the restriction of the electron orbits within a single, small size toroidal configuration, while an excited states represented by the double spitted toroidal configuration due to parity. Thus, the binding energy of the ground state of the H atom is much higher that in the absence of an external magnetic field, hence permit new means of storing energy within conventional molecules and atoms.

5 Experimental Verification of Magnecular Structure

Current technologies offer an impressive variety of analytic instruments Gas Chromatography (GC), Liquid Chromatography (LC), Capillary Electrophoresis Chromatography (CEC), Supercritical Chromatography (SCC), Ion Chromatography (IC), Infrared Spectroscopy (IR), Raman Spectroscopy (RS), Nuclear Magnetic Resonance Spectroscopy (NMRS), X-Ray Spectroscopy (XRS), Atomic Absorption Spectroscopy (AAS), Mass Spectrometry (MS), Laser Mass Spectrometry (LMS), Flame Ionization Spectrometry (FIS), and others. Prof. Santilli [1, 3] observed that only some of these instruments are suitable for the detection of magnecules and, when applicable, their set-up and use are considerably different than those routinely used with great success for molecules. Among all available chromatographic equipment, that suitable for the detection of gas magnecules is the GC with column having ID of at least 0.32 mm operated according to certain criteria as mentioned earlier by Santilli [1, 3]. It has been found that among all available spectroscopic equipment, that preferable is the IR, with the understanding that such an instrument is used in a negative way, that is,

to verify that the magnecule considered has no IR signature. The RS may also result in being preferable in various cases, while other instruments, such as the NMRS do not appear to be capable of detecting magnecules despite their magnetic nature. In regard to spectrometric equipment, the most recommendable one is the low ionization MS due to the fact that other instruments seemingly destroy magnecules at the time of their detection.

Santilli [loc. cit.] located a GC-MS equipped with IRD suitable to measure magnecules at the McClellan Air Force Base in North Highland, near Sacramento, California. On June 19, 1998, Santilli visited the analytic laboratory of National Technical Systems (NTS) located at said McClellan Air Force Base and using instruments belonging to that base. The measurements on magnegas were conducted by analysts Louis A. Dee, Branch Manager, and Norman Wade who operated an HP GC model 5890, an HP MS model 5972, equipped with an HP IRD model 5965. In his monograph [1, 3], he has given numorous experimental evidences which clearly prove the existence of new fuel with entirely new structure i.e. magnecular structure, bonded together with new bond of magnetic type, which are different than conventional fuel molecules. Some of these have been reproduced below in this section.

Measurements on the same sample of magnegas tested at NTS were repeated on July 25, 1998, via a GC-MS/IRD located at the Pinellas County Forensic Laboratory (PCFL) of Largo, Florida, with support from Toups Technologies Licensing, Inc. The equipment consisted of a HP GC model 5890 Series II, an HP MS model 5970 and an HP IRD model 5965B. Even though similar to the equipment used at NTS, the PCFL equipment was significantly different inasmuch as the temperature had to be increased from 10^0C to 55^0C and the ramp time reduced from 26 to 1 minute. The latter reduction implied the cramping of all peaks of Fig.4 into one single large peak, a feature confirmed by all subsequent GC-MS tests with short ramp time. Despite these differences, the test at PCFL, confirmed all features of magnecules first detected at NTS. In addition, the tests provided the experimental evidence of additional features.

In early 1998 Santilli [1] obtained a number of samples of fragrance oils from Givaudan-Roure Corporation (GR) with headquarters in Teaneck, New Jersey. About 50 cc of various samples of perfectly transparent fra-

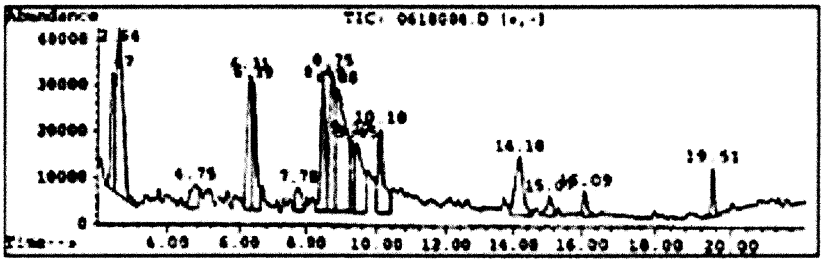

Information from Data File:
File : C:\HPCHEM\1\DATA\0618C04.D
Operator : NAM
Acquired : 18 Jun 98 3:01 pm using AcqMethod VOC_1RMS
Sample Name: TOUP'S TECH
Misc Info : INJ. LOOP; 10C @ ULTRA COLUMN
Vial Number: 1
CurrentMeth: C:\HPCHEM\1\METHODS\DEFAULT.M

Retention Time	Area	Area %	Ratio %
Total Ion Chromatogram			
2.474	1793306	5.386	32.726
2.644	5091514	15.641	95.030
4.754	641536	1.971	11.974
6.307	2737749	8.411	51.098
6.399	2211258	6.793	41.272
7.793	592472	1.820	11.058
8.498	2357396	7.242	43.999
8.756	2784029	8.555	51.977
8.882	5357012	16.460	100.000
9.265	1123809	3.452	20.975
9.440	2421234	7.438	45.191
10.098	1946292	5.979	36.326
14.177	2129791	6.541	39.751
15.073	435208	1.337	8.123
16.085	389822	1.198	7.276
19.569	577433	1.774	10.777

Figure 4: A reproduction of the MS peaks providing the first experimental evidence of the existence of magnecules identified on June 19, 1998, by analysts Louis A. Dee and Norman Wade of the branch of National Technical; Systems (NTS) located at the McClellan Air Force Base in North Highland, near Sacramento, California, with support from Toups Technologies Licensing, Inc. (TTL) of Largo, Florida. The scan is restricted from 40 a.m.u to 500 a.m.u. The peaks refer to magnegas produced via an electric arc between consumable carbon electrodes within ordinary tap water with conventional chemical composition (8.20). Therefore, only the CO_2 peak was expected to appear in the scan with any macroscopic percentage, while no CO_2 was detected at all in the MS scan.

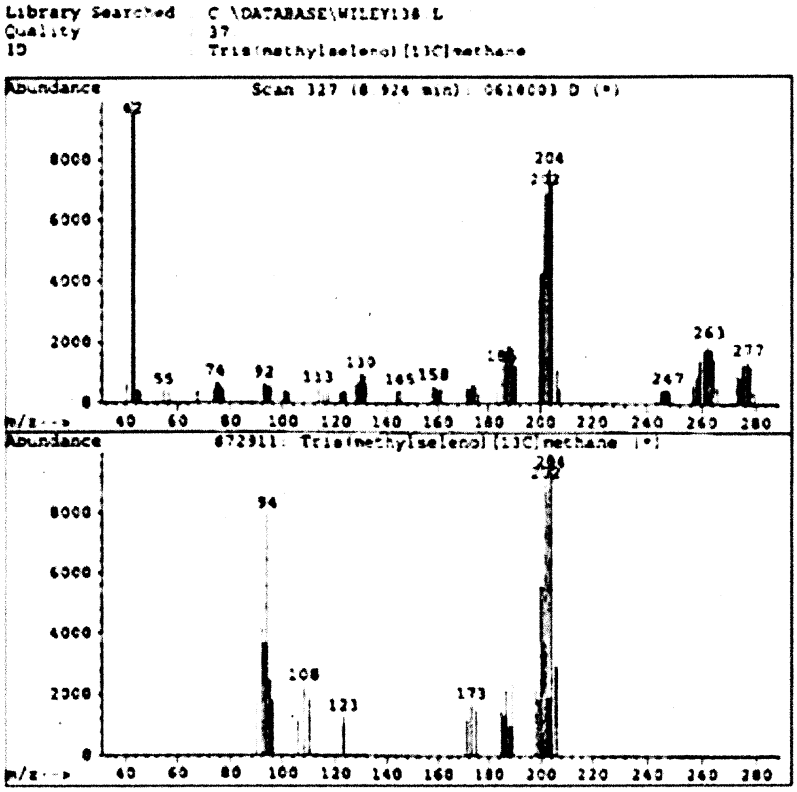

Figure 5: A representation of the first experimental evidence at NTS that the peaks of Fig.4 are "unknown." The peak at the top is at 8.924 minutes, and that at the bottom shows the lack of its identification by the computer search. Note that the best fit identified by the computer does not match the peak considered. Moreover, the identified substance (methylseleno) cannot possibly exist in magnegas because of the impossible presence of the necessary elements. The same situation occurred for all remaining fifteen peaks of Fig.4.

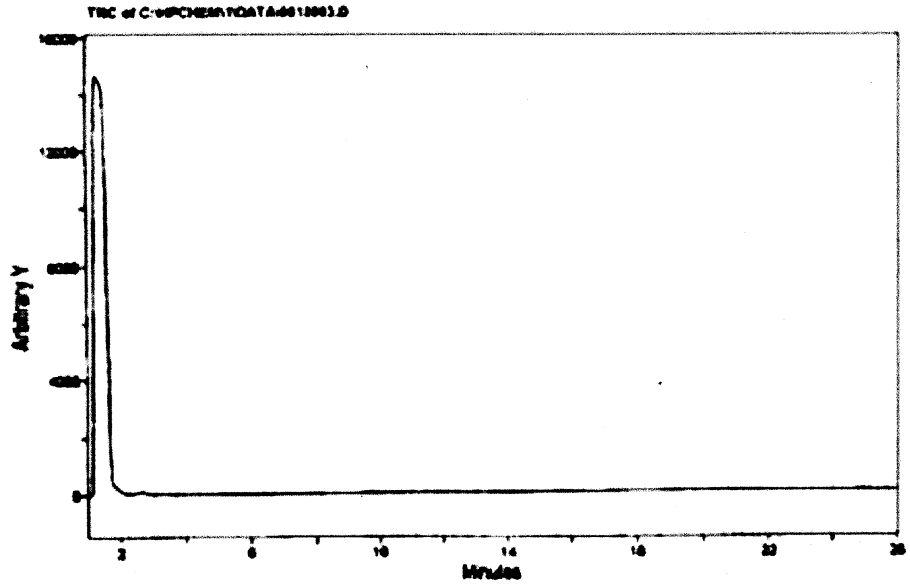

Figure 6: The first experimental evidence at NTS of the lack of IR signature of MS peaks. The evidence establishes the existence of large peaks in the MS that have no IR signature at all. The only identified IR signature that for CO_2, refers to the constituents of the peaks of Fig.4. In the above figure only the IR signature of CO_2 appears because the scan was from 40 a.m.u. to 500 a.m.u. and, as such, could not include the IR signatures of other molecules such as O_2 and CO (H_2 has no IR signature).

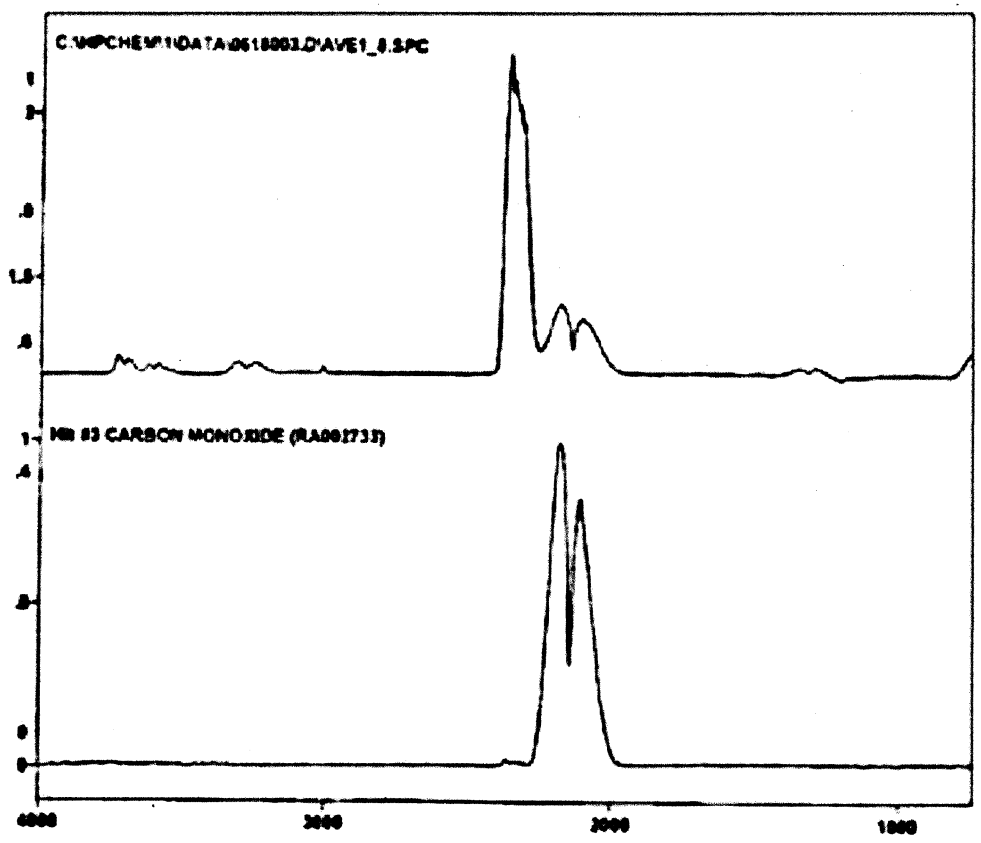

Figure 7: The first experimental evidence at NTS on the mutation of the IR signature of magnetically polarized conventional molecules, here referring to the CO_2 (top) compared to the result of the computer search (bottom). Note that the known, double-lobe peak of CO_2 persists in the detected peak with the correct energy, and only with decreased intensity. Jointly, there is the appearance of two new peaks, which are evidence of new internal bonds within the conventional CO_2 molecule. This evidently implies an increased energy content, thus establishing experimental foundations for the new technology of magnetically polarized fuels such as magnegas [2]. Note that the computer interprets the IR signature as that of CO, which is erroneous since CO is out of the selected range of detection.

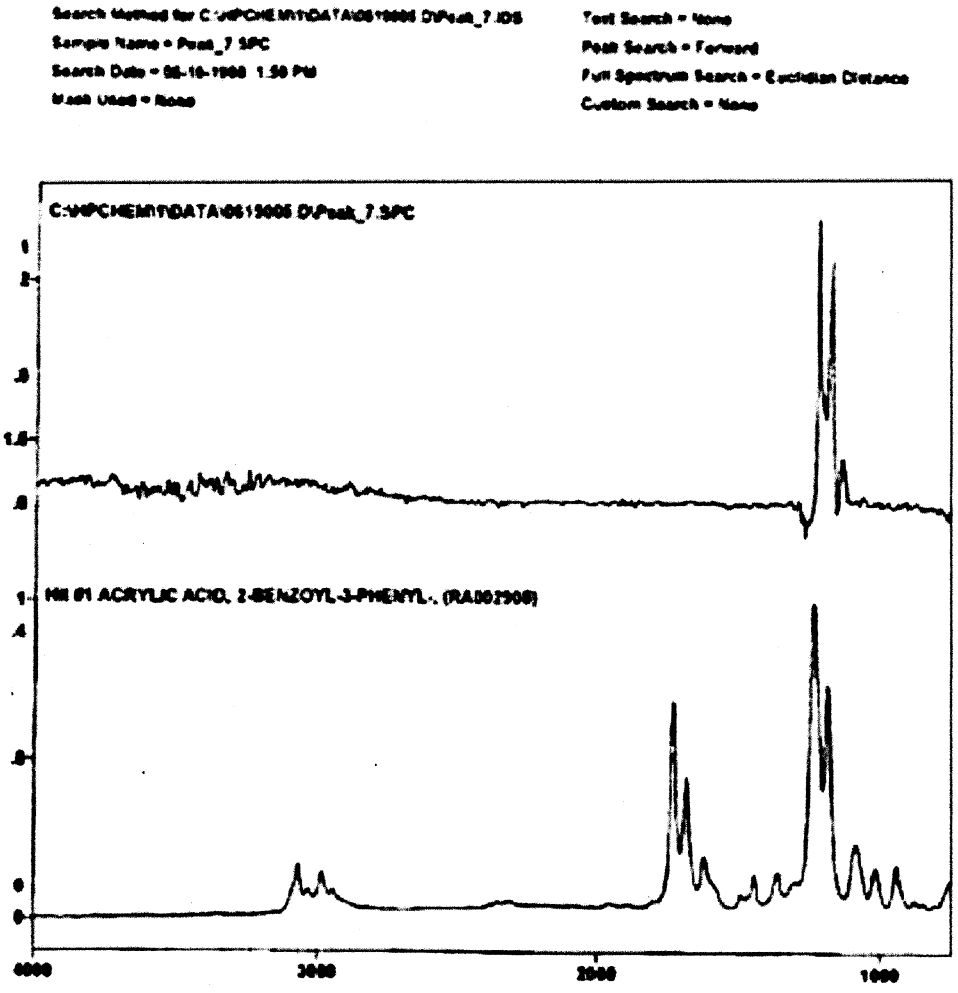

Figure 8: A reproduction of the lack of identification in the computer search of small peaks in the IR scan, which can therefore be additional magnecules, or IR signatures of the magnecules appearing in the MS scan.

grance oils were placed in individual glass containers. One polarity of an alnico permanent magnet with 12,000 G and dimension 1/2"×1"×2" was immersed within said oils. Starting with a perfect transparency, after a few days a darkening of the oils became visible, jointly with a visible increase of the viscosity, with changes evidently varying from oil to oil. Subsequently, there was the appearance of granules of dark complexes in the interior of the oil which were visible to the naked eye. Both the darkening and the viscosity increased progressively in subsequent days, to reach in certain cases a dark brown color completely opaque to light. The viscosity increased to such an extent that the oil lost all its fluidity. After the immersion of the permanent magnets, all samples were left undisturbed at ordinary room conditions. The indicated effects remain unchanged to this day, thus showing that the changes were stable at ordinary conditions of temperature and pressure.

Prof. Santilli has provided the photographic evidences of magnecular structure in liquids i.e. fragrance oil, in his monograph. Alteration of the structure of fragrance oils was confirmed by photographs taken by the GR Research Laboratory in Dubendorf, Switzerland, via a microscope with minimal magnification, as illustrated in the pictures of Figs.9 and 10.

It has been pointed that the above visible effects are of pure magnetic origin because of the lack of any other contribution, e.g., the complete absence of any additives. After the immersion of the permanent magnets, all samples were left undisturbed at ordinary room conditions. The indicated effects remain unchanged to this day, thus showing that the changes were stable at ordinary conditions of temperature and pressure. Santilli's [1] main hypothesis on the darkening of the oils is that their molecules acquire a magnetic polarization in the orbits of at least some of their atomic electrons (called in chemistry *cyclotron resonance orbits*), by therefore bonding to each other according to Definition in a way similar to the corresponding occurrence for gases. It should also be indicate that the immersion of one polarity of a permanent magnet in fragrance oils is, evidently, a rudimentary way to create magnecules in detectable percentage although not an essentially pure population of magnecules as requested for a new chemical species.

Yang *et al.* [13] in their paper presented the experimental verification

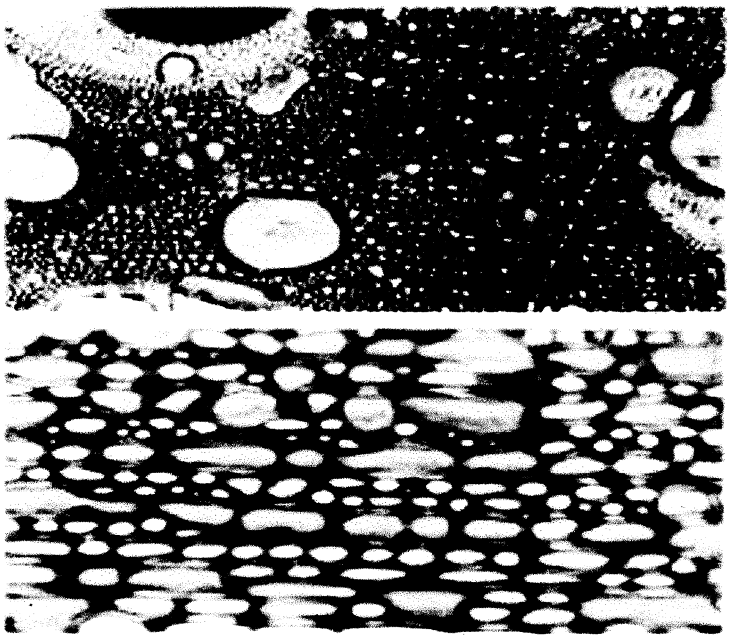

Figure 9: A photographic evidence of magnecules in liquids obtained at the Givaudan-Roure Research Laboratory in Dubendorf, Switzerland, in the GR fragrance oil "ING258IN Test 2" under magnifications 10X and 100X [1].

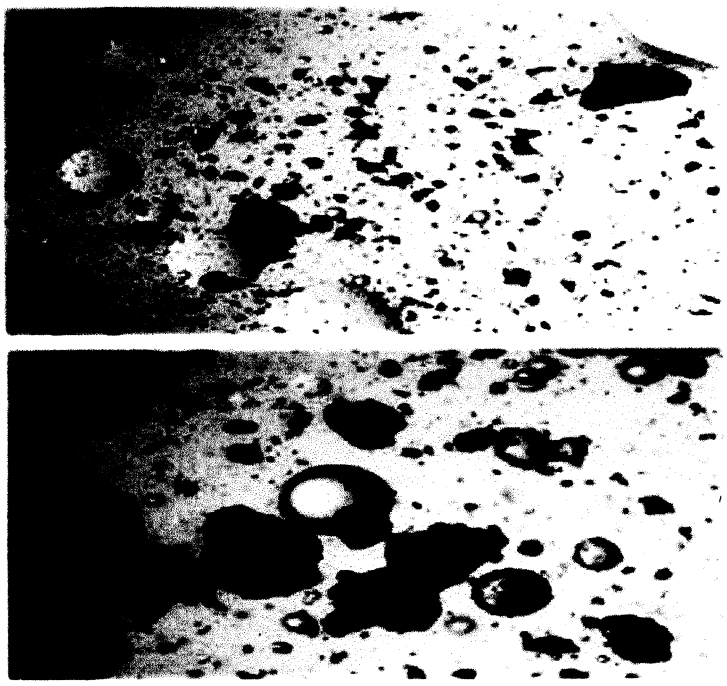

Figure 10: Confirmation of magnecules in GR fragrance oil "Mixture 2" under 10X and 100X obtained at the University of South Florida in St. Petersburg. Note the difference in sizes of the magnecules and their difference with those of Fig.9 [1].

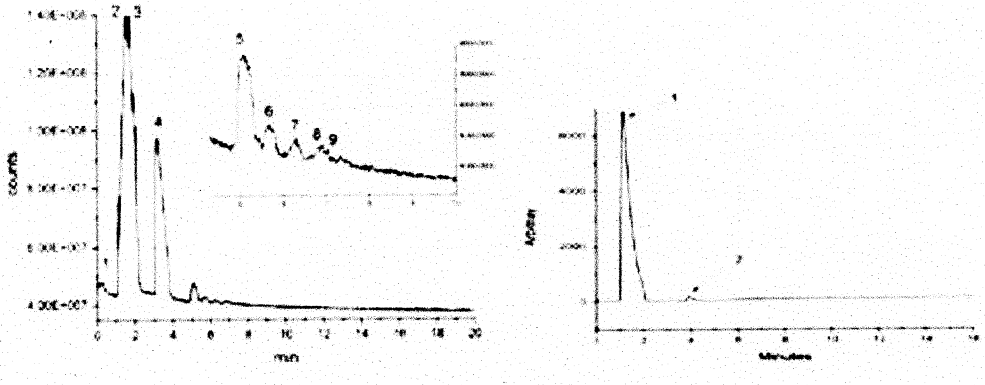

Figure 11: Representative scans achieved by Yang *et al.* on November 8, 2012, via the GC- MS/IRD described in the test. The top view presents a GC-MS scan from 1 a.m.u. to 500 a.m.u. with the column operated at 10^0C and the use of 22 minutes elusion time. The tests were conducted on filtered and compressed MagneGas synthesized from ethylene glycol. The bottom view, is the IRD of the same gas and the same injection which provides experimental confirmation for the presence in MagneGas of clusters without an IR signature, thus confirming the main claim of memoir [1], namely, the existence in nature of bonds other than those based on valence.

of new chemical species using GC-MS/IRD technique which is one of the best spectroscopic techniques to identify the magnecular structure. It has been explained that the principle of jointly testing the same gas with two different equipment is that the GC-MS is useful for the identification of the clusters composing the species, and the IRD for the verification as to whether the bond responsible for the clusters is of valence type or not.

The experimental results have been as mentioned above clearly support the Santilli's claims regarding anomalous properties of magnecules.
Out of a large variety of tests with different magnecular gases, different equipment and different procedures, main results obtained by Yang *et al.* [13] are presented in the representative scans of in (Figs.11 to 16), and can be summarized as follows:

1. Characterization of magnecules by weakly bonded individual atoms,

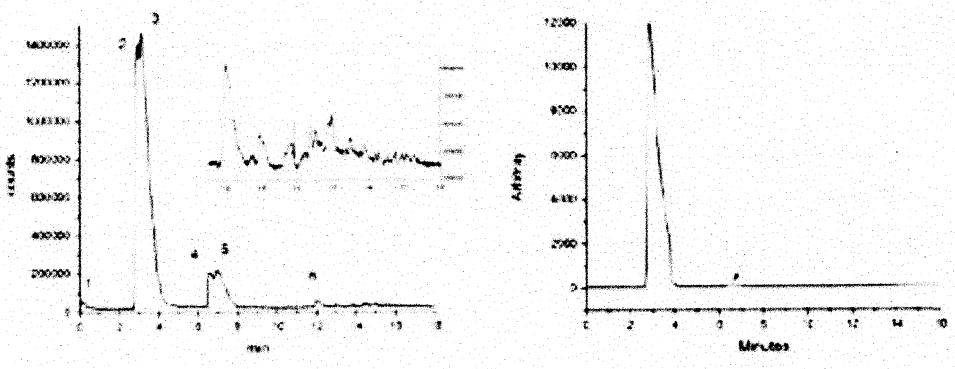

Figure 12: Scans obtained via the same GC-MS/IRD, the same 22 minutes elusion time, and the same magnecular gas as those for (Fig.4), but with the column operated at 40^0C. In the top view, we present a GC-MS scan showing a decrease of the magnecular species of (Fig.11) due to the increased temperature of the column, thus confirming the dependence of the detection of magnecules from the column temperature first identified by Santilli [1]. In the lower view, we present an IRD scan of the same setting as in the top view confirming the absence of IR signature by magnecular clusters also identified in Ref. [1].

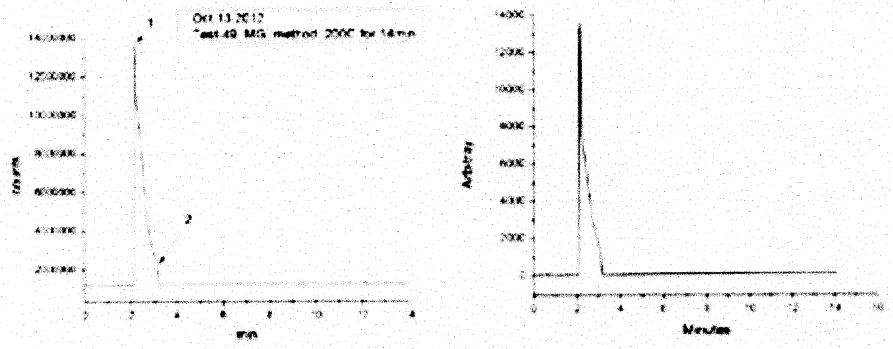

Figure 13: Scans obtained via the same GC-MS/IRD, the same 22 minutes elusion time, and the same magnecular gas as those for (Fig.11), but with the column operated at 200^0C. The top view presents a GC-MS scan showing the disappearance of magnecules, thus confirming Santilli's claim [1] that magnecular clusters admit a temperature (*the Curie temperature*) at which magnetic bonds disappear. The lower view presents the corresponding IRD scan confirming the absence of IR signatures for magnecular species [1].

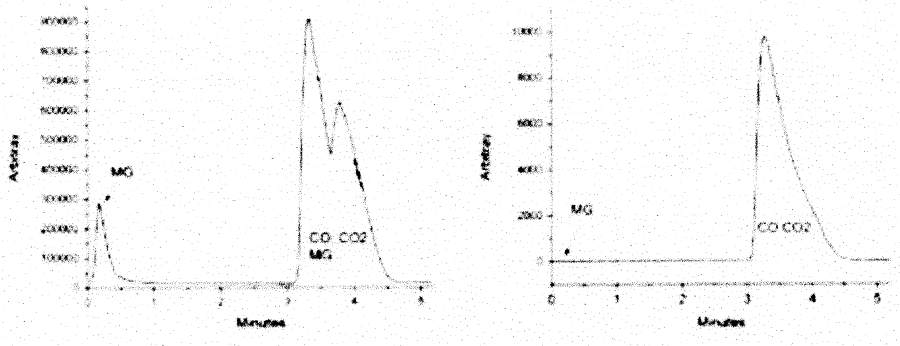

Figure 14: Scans obtained via the same GC-MS/IRD, and the same magnecular gas as those for (Fig.11), but with the elusion time reduced from 22 to 5 minutes and the column temperature increased from 10^0C to 55^0C. The top view confirms Santilli's mutation of magnecular clusters [1], namely, their clear change with the change of procedures in the same instrument. The bottom view presents an IRD scan that also shows deviations from the corresponding scan of (Fig.4).

dimers, and conventional molecules;

2. Stability of magnecules at ambient temperature;

3. Progressive reduction of magnecules with the increase of the temperature;

4. Termination of magnecules at a suitable Curie temperature;

5. Detection of magnecular clusters under a suitably selected and operated GC-MS;

6. Transparency of magnecules to infrared detectors for the a.m.u. of the clusters (and not at a smaller a.m.u. characterizing constituents);

7. Dependence of detected magnecules from the elusion time;

8. Anomalous mutation of magneculer clusters in time and under different detection procedures or equipment;

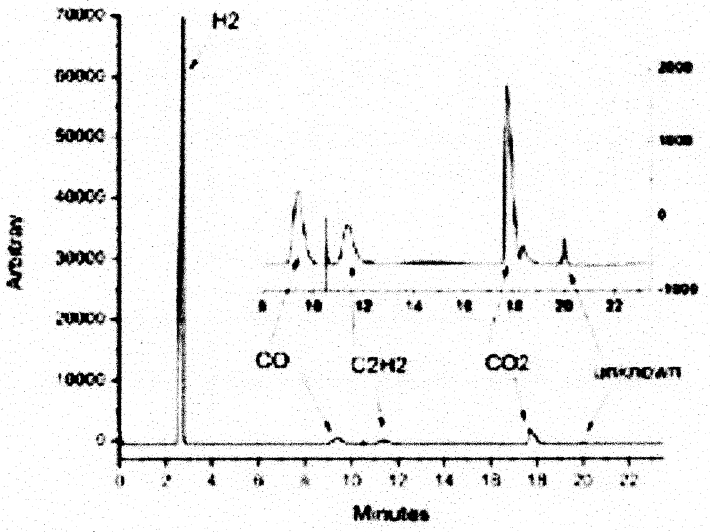

Figure 15: Scan of MagneGas of (Fig.11) with the GC-TCD identified in the text and operated from 40^0C to 200^0C showing the conventional molecular constituents of MagneGas without any appreciable magnecules. This confirms Santilli's claim [1] that GC-TCD operated at temperatures normal for molecular species destroys, rather than detects, magnecular species.

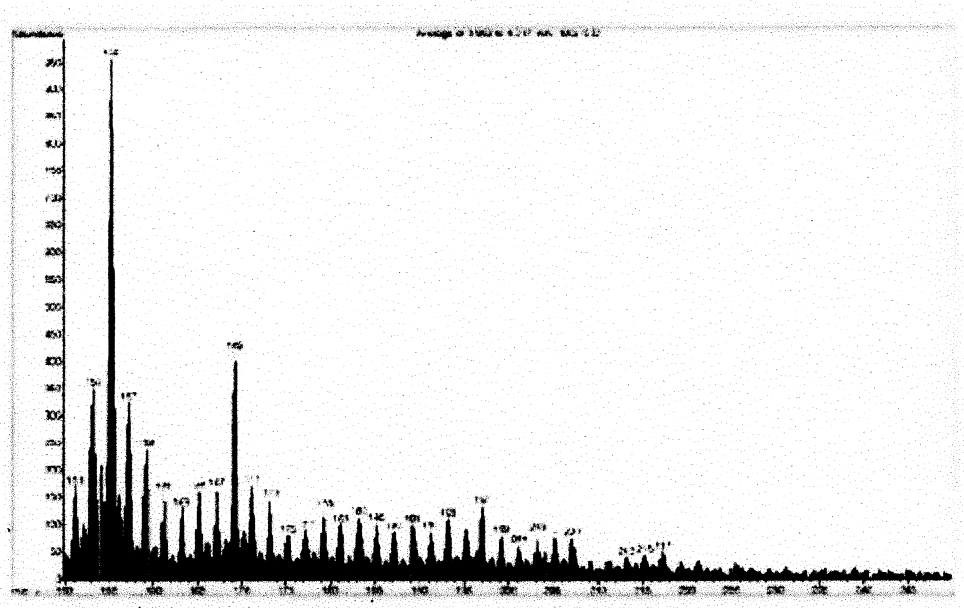

Figure 16: One of numerous scans from the GC-MS operated at low temperature and with the longest possible elusion time confirming Santilli's anomalous accretion by a magnecular cluster of one individual Hydrogen atom that can be observed from 2 a.m.u. to hundreds of a.m.u.

9. Anomalous accretion of magnecular clusters by individual atoms; and other features.

6 Concluding Remarks

Despite the known uneasiness created by novelty, the rather vast experimental evidence, only partially reproduced in this paper to avoid a prohibitive length, supports the following results:

1. The existence in nature of a new chemical species whose bonding force is not of valence type.

2. Scientific measurements of new species of magnecules are intriguing inasmuch as they reminds us that the available analytical tools and techniques are just insufficient for true measurement of magnecules beyond the levels of personal beliefs, because magnecules are not as stable as molecules and they can experience decomposition as well as mutations triggered by the available detection means.

The author solicits the independent verification carried out by Yang *et al.* of all results presented in this paper without which no real scientific advance is possible.

Acknowledgments

The author would like to thank Professor R. M. Santilli, Professor C. Corda, Professor Anderson and Professor A. A. Bhalekar for initiating me in this subject, helping me to understand this new subject and constant encouragement without which this paper would not have seen the light of the day. Special thanks are due to the Dr. S. S. Dhondge for penetrating criticisms that have been crucial to achieve a better maturity of presentation. Additional thanks are due to Dr. V. M. Tangde for countless consultations and in depth suggestions. The last but not the least the financial support of the R. M. Santilli Foundation is gratefully acknowledged.

References

[1] R. M. Santilli, Hadronic J., 21, 789-894 (1998).

[2] R. M. Santilli, Foundations of Hadronic Chemistry with Applications to New Clean Energies and Fuels, Kluwer Academic Publishers, Dordrecht, The Netherlands, 2001.

[3] R. M. Santilli, The New Fuels with Magnecular Structure, International Academic Press, Palm Harbor, Florida, U. S. A., 2005.

[4] See, e.g., the website
`http://www.eia.doe.gov/emeu/international/energy.html`.

[5] See for details the website
`http://www.magnegas.com/technology/part6.html`.

[6] R. M. Santilli, Alarming oxygen depletion caused by oxygen produced from regenerating methods, Contributed paper, International Hydrogen Energy Forum 2000, Munich, Germany, September 11-15, 2000,
`http://www.magnegas.com/technology/part4.html`.

[7] R. M. Santilli, Hadronic Mathematics, Mechanics and Chemistry, Volume V: Experimental Verifications, Theoretical Advances and Industrial Applications in Chemistry, International Academic Press, Palm Harbor, Florida, U. S. A., 2008.

[8] R. M. Santilli, U.S. patents numbers 6, 926, 872; 6, 673, 322; 6, 663, 752; 6, 540, 966; and 6, 183, 604.
Magnegas website `http://www.magnegas.com`.

[9] R. M. Santilli, J. New Energy, 4, 5-314 (1999); R. M. Santilli and D. D. Shillady, Intern. J. Hydrogen Energy, 24, 943-956 (1999); 25, 173-183 (2000).

[10] R. M. Santilli, Int. J. Hydrogen Chem., 28, 177-196 (2003).

[11] M. G. Kucherenko and A. K. Aringazin, Hadronic J., 21, 895-902 (1998).

[12] A. K. Aringazin, Y. Yayli and E. Soyturk, Hadronic J., 24, 395-433 (2001).

[13] Y. Yang, J. V. Kadeisvili and S. Morton, Intern. J. Hydrogen Energy, 38, 5003-5008 (2013).